



UNIVERSITÀ  
DEGLI STUDI  
FIRENZE

DOTTORATO DI RICERCA IN  
SCIENZE CHIMICHE

CICLO XXVII

COORDINATORE Prof. Andrea Goti

Gold Compounds as Anticancer Agents:  
A Systematic Study of Gold-Protein Metalation

Settore Scientifico Disciplinare CHIM/03

**Dottorando**

Dott. Massai Lara

**Tutore**

Prof. Messori Luigi

**Coordinatore**

Prof. Goti Andrea

Anni 2012/2014

Jump!  
And you will find out  
How to unfold your wings as you fall

(Ray Bradbury)

## TABLE OF CONTENTS

### Outlook

### Chapter 1 – Metals in medicine: An overview

1. Metals in medicine	10
2. Metal complexes as anticancer agents	11
2.1 Platinum-based anticancer drugs	12
2.1.1 Cisplatin mode of action	12
2.1.2 Second and Third generation of platinum compounds	15
2.2 Ruthenium background	19
2.2.1 Ruthenium properties suited to biological	20
3. Gold: the main project	21
3.1 Chemistry of Gold	22
3.2 Gold (I)	23
3.3 Gold(III)	24
4. Biomolecules as target	26
4.1 Tioredoxin Reductase System	27
4.2 Targeting Mitochondria for anticancer gold compounds	28
5. Basic aspect of Gold/Protein interactions	29
6. DNA-Quadruplex as target	30
References	31

### Chapter 2 – Protein Metalation by Cytotoxic Gold Compounds

#### Section A - Gold (III) Compounds

1. Introduction	38
2. Results	40
2.1 Solution behavior of the three gold(III) compounds	40
2.2 Reactions of gold compounds with model proteins: spectrophotometric analysis	42
2.3 ESI MS spectra of metallodrug-protein samples	44
2.3.1 Auoxo6 and Au <sub>2</sub> phen	44
2.3.2 Aubipyc	46
2.3.3 Auranofin	46
2.4 Reactions of gold compounds with model proteins in the presence of reducing agents	47
3. Discussion	48
4. Experimental section	50

References	52
Section B - Gold (I) Compounds	
1. Introduction	55
2. Results	57
2.1 Synthesis and structural characterization	57
2.2 Solution chemistry	60
2.3 Cellular studies/antiproliferative properties	61
2.4 Reactions with Cytochrome c and Lysozyme	62
3. Discussion	63
4. Experimental section	65
References	69
Chapter 3 – Cytotoxic Gold Compounds bind Copper Chaperone Atox-1: Biological and Pharmacological Implications	
1. Introduction	74
2. Results	76
2.1 Interaction with gold compounds and Atox1	76
2.2 Interactions with NHC gold(I) complexes and Atox1	79
2.3 Characterisation of gold binding in Aubipic/Atox1	80
2.4 Metal Binding Properties of Atox1 versus other soft metals	81
2.5 Metal Competition Studies	82
3. Discussion	83
4. Experimental section	84
References	86
Chapter 4 - Interactions of Gold-Based Drugs with proteins: a structural perspective	
1. Introduction	90
2. Results	91
2.1 Gold-Based Drugs and Lysozyme	91
2.2 Gold-Based Drugs and RNase A	94
3. Discussion	97
4. Experimental section	99
References	102
Chapter 5 – Interactions of Selected Gold(III) Complexes with DNA G Quadruplexes	
1. Introduction	108

2. Results	110
2.1 The DNA thermal stabilization promoted by gold(III) complexes is a function of their structure and of nucleic acid folding	110
2.2 Auoxo6 forms conserved complexes with telomeric G-quadruplex irrespectively of solution conditions	111
2.3 Quantitative analysis of binding affinity of gold(III) complexes for telomeric G-quadruplex	113
2.4 Binding stoichiometry of gold(III) complexes toward telomeric G-quadruplex	114
2.5 Auoxo6 is efficient in inducing G-quadruplex formation	117
3. Discussion	117
4. Experimental section	119
References	122
Chapter 6 - The future: Heterometallic Compounds?	
1. Heterometallic compounds	126
2. Uv-Vis studies	127
3. ESI-MS studies: protein/complexes interaction	128
4. Cellular studies	130
5. Conclusion	132
References	133
Chapter 7 - Conclusion	136
Acknowledgements	139

## OUTLOOK

The main goal of the present work has been to elucidate the modes of action of cytotoxic gold compounds which are still poorly understood. Accordingly, a small panel of representative cytotoxic gold compounds have been extensively characterised from the chemical point of view. Particular attention has been paid to the description of their solution behaviour and of their stability under experimental conditions similar to those of the biological tests. Afterward, a systemic investigation has been carried out to describe the reactivity of gold compounds with likely protein targets; in particular, their reactions with a few model proteins have been assayed through ESI MS experiments. Remarkably, the peculiar coordination properties of the gold(III) center allow the obtainment of metal complexes showing an almost co-planar localization of extended aromatic surfaces, that seem highly suitable for a particular nucleic acid targeting: DNA G-quadruplex.

The whole work is organized into six distinct chapter as detailed below.

Chapter 1 : A general review on the use of metals as anticancer agents from past years to present days focusing the attention on gold compounds.

Chapter 2: Protein metalation by cytotoxic gold(I)/(III) compounds (Auoxo<sub>6</sub>, Aubipyc, Au<sub>2</sub>phen, Au(NHC), Au(NHC)<sub>2</sub>) and one comparative gold complex (Auranofin) with two representative proteins, i.e. lysozyme and cytochrome c explored through UV-visible absorption spectroscopy and ESI MS in order to characterise the inherent protein metalation processes; the applied investigational approach provides detailed insight into formation of metallodrug-protein derivatives.

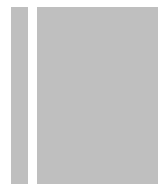
Chapter 3: The cytotoxic gold compounds of this study (previously mentioned) produce stable adducts upon reaction with the copper chaperone Atox-1; notably, such adducts contain gold in the oxidation state +1. These findings are of interest to understand the intracellular metabolism of medicinal gold species and to develop new potent inhibitors of the copper trafficking system.

Chapter 4: The interactions between Auoxo<sub>6</sub> /Au<sub>2</sub>phen/Ausac<sub>2</sub> and hen egg white lysozyme(HEWL)/Ribonuclease A (RNase A) were studied by X-ray crystallography. High resolution crystal structures solved for three metallodrug-protein adducts provide valuable insight into the molecular mechanism of these promising metal compounds and the inherent protein metalation processes.

Chapter 5: The interactions of Auoxo6, Aubipyc and [Aubipyc]<sub>2</sub> compounds with short DNA G quadruplexes were analysed through a variety of biophysical methods including DNA melting, circular dichroism, SPR and ESI MS; remarkably, the dinuclear gold(III) complex Auoxo6 turned out very effective in binding/stabilising the G quadruplex DNA conformation with a high selectivity: implications of these results are discussed.

Chapter 6: An introduction on a supplementary subject which could be an upgrade of the investigated gold compounds. Preliminary results on heterometallic compounds which contain a gold center are described.

Chapter 7: A summary of the obtained results.



# **Chapter 1**

## **Metals in medicine: An overview**





## 1. Metals in medicine

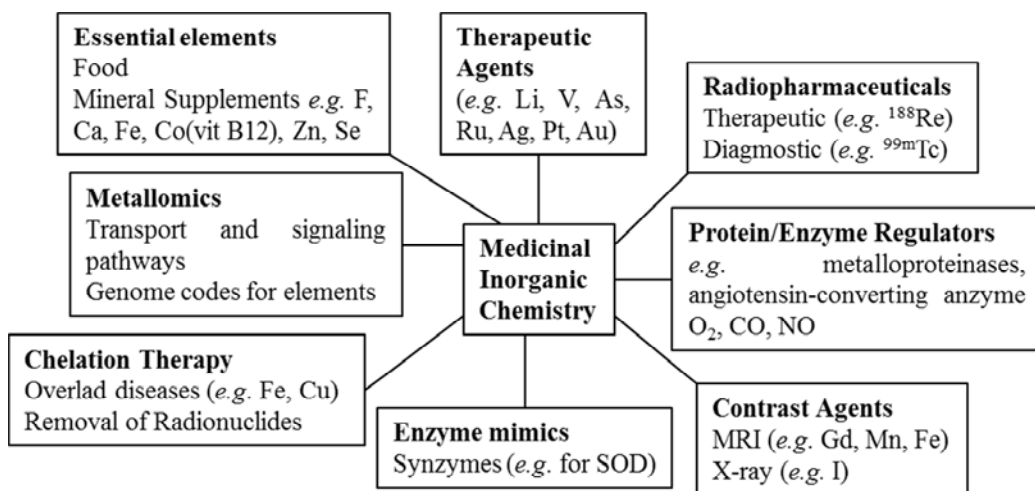
*“Inorganic chemistry is an essential part of life.*

*It is not just the chemistry of dead or inanimate things.*

*It was probably even inorganic chemistry that started it all off”.*

By Enzo Alessio - Bionorganic Medicinal Chemistry - John Wiley & Sons, Inc.

There is currently emerging interest in the medicinal chemistry of metal. Activity is done not just to the metal but is also related to the ligand and to the type of complex. Whilst a given metal does exhibit recurring features peculiar to itself (e.g., preference for particular oxidation states and ligand geometries) the ligand environment can have a marked effect on the overall reactivity of the complex. Furthermore, the behavior of a metal complex is dependent on both its composition and the environment in which it finds itself. Predicting and controlling that behavior is one of the challenges for advancing the rational design of inorganic pharmaceuticals. The use of metals in medicine is varied [1– 5] (figure 1.1). Fundamental wide-reaching medical problems such as bacterial, viral (particularly HIV), and parasitic infections such as malaria are being addressed by research on metal-based medicines. There are also promising developments for tackling the main diseases affecting an affluent, aging western population: cardiovascular, age-related inflammatory diseases, neurological diseases (e.g., Parkinson’s, Alzheimer’s), cancer [6–8], diabetes, and arthritis. Metal-based diagnostic agents for MRI and X-ray are in routine clinical use; for example, gadolinium MRI contrast agents have now been administered to ~ 50 million patients worldwide.



Medicinal Inorganic Chemistry (figure 1)

Medicinal inorganic chemistry is a relatively young, interdisciplinary research area that has grown primarily due to the success of cisplatin, a Pt-based anticancer drug developed in the late 1960s. In addition to metal-centered therapies, metals may also be used to enhance the efficacy of organic drugs and as small-molecule delivery vehicles (e.g., for NO, CO). Organic compounds used in medicine may be activated by metal ions or metalloenzymes, and others can have a direct or indirect effect on metal ion metabolism.

The rational design of metal-based drugs is a relatively new concept; in general a metal complex that is administered is likely to be a “prodrug” that undergoes a transformation in vivo before reaching its target site. Most importantly, the biological properties of metal complexes depend not only on the metal and its oxidation state but also on the ligands. Ligands can render either the whole complex inert to ligand substitution reactions or can activate other coordination positions stereospecifically. Besides the metal itself, the ligands can also be the centers of redox reactions, or hydrolytic and other reactions.

The rational design of metal complexes as drugs requires a greater understanding of their effect on cell signaling pathways. An interaction of the metal complex with a constituent (e.g., protein) in one pathway may have consequences for a seemingly unrelated target for which the metal has little affinity. Drugs based on the essential elements need to take into account the pathways programmed by genomes for the uptake, transport, and excretion of those elements (homeostasis).

We need to make use of metallomics in therapy: corrective procedures are needed when there are metals in the wrong place at the wrong time, or indeed are not present in the right place at the right time.

## 2. Metal complexes as anticancer agents

Cancer is caused when genetic damage to the cells prevents them from being responsive to normal tissue controls. The cancer spreads when affected cells multiply rapidly, forming tumors of varying degrees. Different therapies can be used, depending on how far the cancer has spread. In the case of cancer, a chemotherapeutic agent is one that kills the rapidly dividing cells, thus slowing and stopping the cancer from spreading.

The modern era of metal-based anticancer drugs began with the discovery of the platinum(II) complex cisplatin by Barnett Rosenberg in the 1960s [9]. Stimulated by the success of cisplatin, also other coordination compounds based on ruthenium, gold, titanium, copper, rhodium, vanadium, and cobalt were tested for their anticancer activity and several promising candidates are currently in (pre)clinical evaluation [10-16].

Developing metal complexes as drugs, however, is not an easy task. Accumulation of metal ions in the body can lead to deleterious effects. Thus biodistribution and clearance of the metal complexes as well as its pharmacological specificity are to be

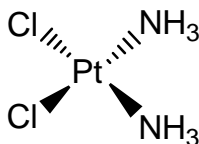
considered. Favorable physiological responses of candidate drugs need to be demonstrated by *in vitro* study with targeted biomolecules and tissues as well as *in vivo* investigation before they enter clinical trials. A mechanistic understanding of how metal complexes achieve their activities is crucial to their clinical success, as well as to the rational design of new compounds with improved potency.

Of particular interest is the elucidation of the mechanism of action of the various non-platinum metal complexes and the investigation of the final target and the corresponding molecular lesion. Indeed, while several data are now available regarding the mechanism of platinum(II) compounds, little work has been done on the mechanism of action of non-platinum metal complexes which exhibit encouraging cytotoxicity and antitumor activity profiles.

### 2.1 Platinum-based anticancer drugs

Since the discover of cisplatin(Cis-diamminodichloroplatinum(II); (cis-(NH<sub>3</sub>)<sub>2</sub>PtCl<sub>2</sub>; cis-DDP) a lot of platinum-based drugs have been developed to obtain a good candidate as anticancer agents and to overcome the side effect, so derivatives as carboplatin and oxaliplatin have entered in clinical practice.

Cisplatin is highly successful against a number of cancer types, chiefly testicular, ovarian, cervical, head and neck, oesophageal and small cell lung cancers [17], but reacts with a wide range of biomolecules other than its chemotherapeutic target, DNA. Despite its clinical success there are several disadvantages associated with cisplatin, such as low solubility [18], significant toxicity, which limits patient doses [18], severe side effects such as nausea, nephrotoxicity, neurotoxicity [19], and intrinsic or acquired resistance in some cancer types [20,21]. Many analogous platinum complexes have been developed in an attempt to overcome these limitations, but in many cases these compounds have similar mechanisms of action and resistance profiles.



Cisplatin(figure 2)

#### 2.1.1 Cisplatin Mode of action

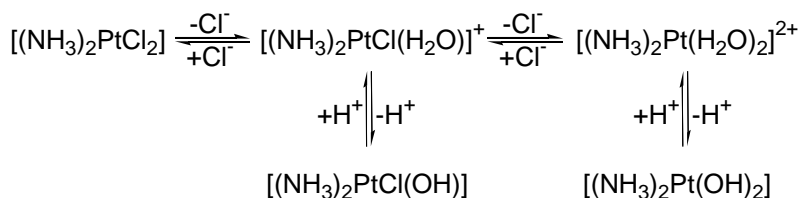
It is generally accepted the DNA is the principal target for cisplatin in cells and that DNA replication and transcription are the major functions impaired by this drug in the tumor cells; in fact, the ability of cisplatin adducts on DNA to stop the processive

action of DNA polymerase translates into inhibition of cell division and, hence, antitumor activity [22,23]. It is also believed that cisplatin coordination to DNA not only inhibits replication and transcription of DNA, but also leads to programmed cell death (apoptosis)[24].

The structural features of all the platinum(II)-based drugs showing antitumor activity are interpreted in relationship to the possibility to form platinum(II)-DNA adducts. Strictly, these features (all present in cisplatin itself) are summarized as follows:

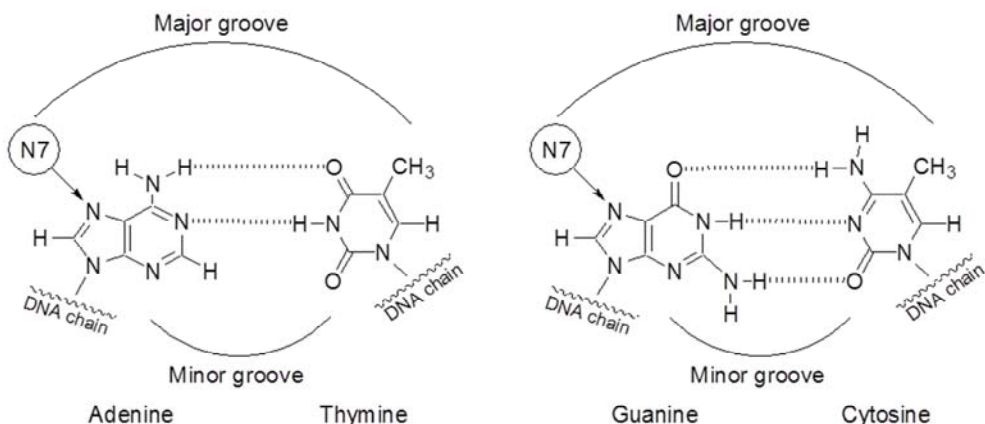
- 1) platinum(II) complexes must contain two labile leaving groups and two inert ligands (that is, chloride ions and ammonia molecules respectively in cisplatin);
- 2) both labile and inert ligands must be in reciprocal cis position.

The neutral compound then enters the cell by either passive diffusion or active uptake by the cell itself. During this process the neutral cisplatin molecule undergoes hydrolysis in which a chloride ligand is replaced by one molecule of water, thus generating a positively charged species (Scheme 1)[25]. It is this hydrolyzed form that does react with DNA; in fact, it has been proved that the formation of Pt(II)-DNA adducts and the first cisplatin hydrolysis reaction occur with similar rates, so the mono-aqua species  $[(\text{NH}_3)_2\text{PtCl}(\text{H}_2\text{O})]^+$ , is predominant in cytoplasm[25].



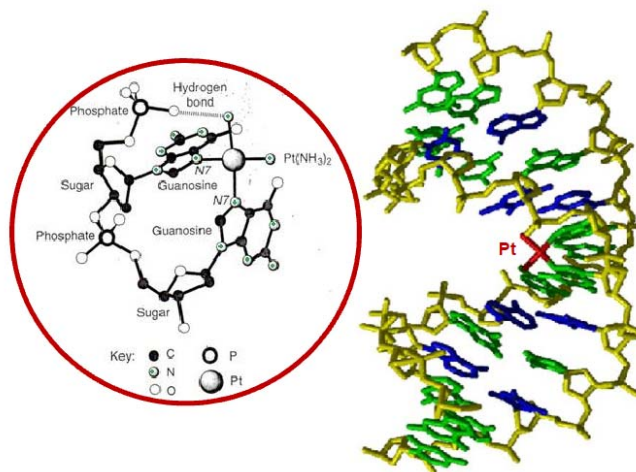
#### Hydrolysis reactions of CDDP (Scheme 1)

The major site of platination in double-stranded DNA (65%) derives from intrastrand cross-links between two neighboring deoxyguanosines, d(GpG). About 20% of the DNA platination derives from intrastrand cross-links at an d(ApG) sequence, but no adducts were detected when these two nucleosides, adenosine and guanosine, were in the opposite order (i.e., d(GpA)). Another 9% of the platination derives from cross-links between two deoxyguanosines separated by a third nucleoside (d(GpNpG), where N is any nucleoside). All of these modifications occur through the N(7) position on the purine ring because it does not form hydrogen bonds with any other DNA base; these nitrogen atoms are located in the DNA major groove, so they are more exposed to platination (Scheme 2)[26].



The DNA base pairs; cisplatin coordinates to the N(7) atoms of the guanine and adenine purine rings (scheme 2)

In 1995 Lippard and coworkers published the single crystal x-ray analysis of cisplatin bound to a 12-mer DNA duplex with the sequence CCTCTGGTCTCC/GGAGACCAGAGG, with the binding site of the  $[\text{Pt}(\text{NH}_3)_2]^{2+}$  unit indicated in boldface type in the sequence. The platinated DNA duplex was made by reacting the diaqua form of cisplatin, with the C-rich oligonucleotide DNA strand, which, after purification, was hybridized to the G-rich complementary strand. This ensured that the  $[\text{Pt}(\text{NH}_3)_2]^{2+}$  unit was attached to only one site; that is, the central GG sequence of the duplex DNA. The structure shows that the platinum ion is bound to N-7 of both guanines located in the major groove and that it significantly distorts the axis of the double helix, bending it toward the major groove, which opens the 'face' of the minor groove of DNA on the opposite side, (figure 3)



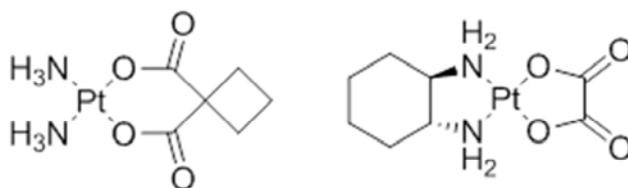
Crystal structure of cisplatin bound to the DNA 12-mer duplex, CCTCTGGTCTCC/GGAGACCAGAGG, with the site of binding, GG, of the  $[\text{Pt}(\text{NH}_3)_2]^{2+}$  unit indicated in boldface type. (a) The binding of the  $[\text{Pt}(\text{NH}_3)_2]^{2+}$  unit to the GG sequence on one strand bends the helix axis of the double-stranded DNA toward the major groove of DNA by  $\sim 40^\circ$ . (b) View showing the  $[\text{Pt}(\text{NH}_3)_2]^{2+}$  unit bound to N-7 of the guanine bases in the GG sequence. The two cis ammonia molecules are black circles above and below the platinum ion. Reprinted by permission from Macmillan Publishers Ltd: P.M. Takahara et al., Crystal Structure of Double Stranded DNA Containing the Major Adduct of the Anticancer Drug Cisplatin, *Nature*, 377, 649–52. Copyright 1995 (figure 3)

A major problem with cisplatin therapy is that repeated exposure to the drug causes the cancer being treated to become resistant to it, which ultimately forces termination of therapy. While it would seem reasonable to simply increase the dose of the cisplatin given to the patient, the drug has a relatively narrow therapeutic window, which means that the difference between the dose required for an anticancer effect and a dose that is toxic to the patient is small. When cells become resistant to the cisplatin by repeated exposure to the drug it is noticed that they bind much less platinum than normal or sensitive cells that have not been repeatedly exposed to it. From the molecular standpoint, resistance to cisplatin can be caused by cells becoming more efficient at blocking platinum from entering them, effectively moving it back across the membrane (sometimes in a chemically modified form), or if it has made its way to an important target such as DNA, removing it from the DNA via a DNA repair process.

### 2.1.2 Second and Third generation of Platinum compounds

Besides cisplatin, the second-generation drug, carboplatin (diamine[1,1-cyclobutanedicarboxylato(2-)]-O,O'-platinum(II)) (figure 4) has been introduced into oncotherapy. The observed pharmacokinetic differences between cisplatin and

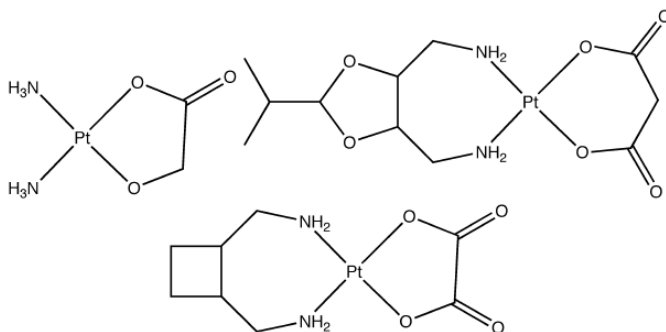
carboplatin depend primarily on the slower rate of conversion of carboplatin to reactive species. Studies on the interaction of carboplatin with DNA indicate that the reaction proceeds via ring-opening in carboplatin and subsequent binding with DNA constituents. Replacement of the chloride groups in the cisplatin molecule by cyclobutanedicarboxylate ligands significantly diminished the nephrotoxic effects of the formed carboplatin, without affecting its antitumor potency. Due to the reduced spectrum of adverse side effects, carboplatin is better tolerated by patients and can be used at several-fold higher doses than cisplatin. It should be noted that among more than thirty platinum antineoplastic agents studied in clinical trials, only carboplatin has been accepted worldwide [27,28]. Thus, further investigations are carried out to synthesize “the second generation platinum drugs” with improved toxicological profiles and “third generation drugs” overcoming cisplatin resistance.



Other platinum drug approved for worldwide clinical use: Carboplatin and Oxaliplatin (figure 4)

Very recently (2004), a further platinum drug, oxaliplatin (eloxatin; Sanofi-Aventis) has become the third to achieve worldwide clinical acceptance. The clinical advantage of oxaliplatin is that it has a different spectrum of activity: in particular, it is effective against colorectal cancer, a disease not treatable using cisplatin or carboplatin [29]. Moreover, oxaliplatin is active against some cisplatin-resistant cancers. The predominant DNA adducts formed by oxaliplatin are 1,2 intrastrand GG adducts analogous to those formed by cisplatin. However, in oxaliplatin the amines are incorporated into a 1,2-diaminocyclohexane (dach) framework and the adducts are thus not {cis-Pt(NH<sub>3</sub>)<sub>2</sub>} adducts but {Pt(dach)} DNA adducts. The precise biological reasons for the difference in spectrum of activity and the ability of this agent to circumvent some cisplatin resistance mechanisms remain to be fully elucidated, but seems to hinge on the dach ligand: the alternate diamine ligands used in heptaplatin and lobaplatin do not confer these same effects.

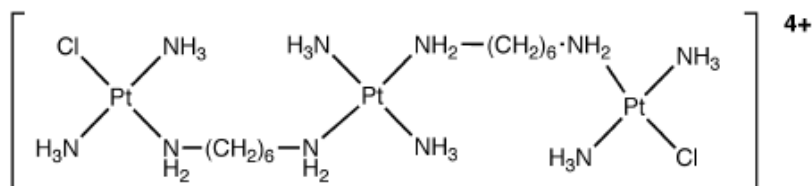




Platinum drugs approved for regional clinical use: (top left) Nedaplatin (Japan); (right top) Heptaplatin (South Korea); (bottom) Lobaplatin (China). (figure 5)

Early on in the studies of cisplatin it was recognized that the trans-isomer (transplatin) was inactive [30], and thereafter the need for a cis geometry at platinum rapidly became a dogma. However, this dogma (as the other design rules) has more recently been shown to be invalid and three distinct classes of trans compounds shown to possess anticancer activity [31]: Trans compounds containing pyridine ligands (developed by Farrell) [32], trans compounds containing an alkylamine and an isopropylamine (developed by Navarro-Ranninger) [33], and trans compounds containing iminoether ligands (developed by Natile and Coluccia) [34].

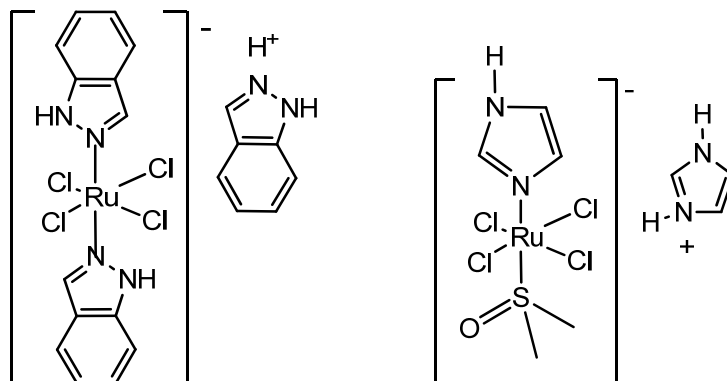
The most dramatic example of platinum(II) agents that break the traditional design rules are Farrell's di- and tri-nuclear platinum compounds (figure 6) in which the metal centers are linked by flexible diamine chains [35]. These compounds are not only multinuclear but also polycationic. Moreover, they do not contain platinum centers with cis leaving groups. The reward for creating a design which breaks all the rules is that these agents are much more potent anticancer drugs than cisplatin itself and exhibit activity against a broad spectrum of tumors, including cisplatin-resistant tumors.



BBR3464; an example of Farrell's active multinuclear cationic trans-platinum(II) compounds (figure 6)

## 2.2 Ruthenium: background

Ruthenium is particularly attractive as the ligand exchange kinetics in its complexes can be similar to those of platinum complexes. Two ruthenium-based anticancer agents (figure 7) are currently in clinical trials.



KP1019 and NAMI A (figure 7)

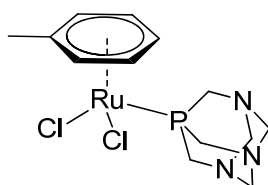
The first ruthenium agent to enter clinical trials was NAMI-A [36,37], imidazolium trans-[tetrachloro( dimethylsulfoxide)(imidazole)ruthenate(III)]. The drug, developed by Alessio and Sava, is an anionic complex which contains an octahedral ruthenium(III) center bound to one imidazole ligand, with a S-coordinated dmsoligand trans to the imidazole and four chlorides completing the coordination sphere. Despite its lack of activity against primary tumors, the drug is, however, a potent agent against metastasis tumors. This is potentially very important because although great leaps have been made in treating primary cancers (including surgery, chemotherapy, and radiotherapy) secondary metastases represent a major clinical challenge. While NAMI-A can bind to DNA, this is not believed to be the source of its biological action. The mechanism of metastasis control seems to be attributable to the combined effects of anti-angiogenic and anti-invasive properties of NAMI-A on cancer cells and on blood vessels.

The second of the ruthenium agents currently in clinical trials is indazolium trans-[tetrachlorobis( 1H-indazole)ruthenate(III)] (KP1019 or FFC14A) developed by Keppler [38,39]. Despite its structural similarity to NAMI-A, this agent is a cytotoxin which is active against primary tumors, and is being investigated for activity against colorectal cancers. The agent causes apoptosis via the mitochondrial pathway and is believed to act as a pro-drug with the actual active species as yet not identified. Under physiological conditions, at least one of the chlorides is exchanged for aqua (or hydroxy) ligands.

Once inside the cell, the agent can bind to DNA with a preference shown for G and A residues: indeed, it is observed to bind to DNA in tumor cells and causes some (though

not many) strand breaks. However, the DNA adducts are not very effective at terminating transcription. Although DNA might be the biomolecular target through which the drug's cytotoxic activity is revealed, the demonstrated and effective binding to protein histidine residues means that action via other biomolecules cannot be excluded. A substantial body of information has already been assembled regarding the effect of this compound on cells and their components and to drug resistance pathways. The continuing studies into its action seem likely to provide valuable information to guide others in the metallo-drug field and may reveal new potential intracellular targets.

More recently, another class of ruthenium anticancer agents have been developed, centered around ruthenium arene compounds (figure 8).



RAPTA agent of Dyson (figure 8)

The ruthenium arene 1,3,5-triaza-7-phosphaadamantane (RAPTA) agents developed by Dyson which are similar aryl ruthenium piano-stool complexes, but in which the three remaining coordination sites are occupied by two chlorides and a monodentate 1,3,5-triaza-7-phosphatrimethyldecane [40]. The compounds developed out of studies to create pH-dependent DNA-binding agents, but were shown to be of only very low toxicity toward cancer cell lines. Like NAMI-A, these agents are inactive against primary tumors but found *in vivo* to have activity against metastases. The RAPTA complexes are slightly less potent antimetastatic agents than NAMI-A, but (in mice) less toxic and thus can be administered in higher doses. As NAMI-A, the indications are that proteins, rather than DNA, are the biomolecular targets for action of the drug. Enhanced activity against lung metastases on coadministration of cisplatin has been demonstrated. Given the structural differences between the RAPTA and NAMI-A complexes, they might be expected to act differently with proteins, perhaps selecting different biomolecular targets or pathways. Ultimately, cocktails of different antimetastatic metallo-drugs which target different proteins might be envisaged.

### 2.2.1 Ruthenium properties suited to biological application

There are three main properties that make ruthenium compounds well suited to medicinal application [41]:

- (i) rate of ligand exchange

Many ruthenium complexes have been evaluated for clinical applications, particularly in the treatment of cancer, due in part, to Ru(II) and Ru(III) complexes having similar ligand exchange kinetics to those of Pt(II) complexes. Ligand exchange is an important determinant of biological activity, as very few metal drugs reach the biological target without being modified. Most undergo interactions with macromolecules, such as proteins, or small S-donor compounds and/or water.

- (ii) the range of accessible oxidation states

Ruthenium is unique amongst the platinum group in that the oxidation states Ru(II) and Ru(III) are all accessible under physiological conditions. The redox potential of ruthenium compounds can be exploited to improve the effectiveness of drugs in the clinic. For example, the drug can be administered as relatively inert Ru(III) complexes, which are activated by reduction in diseased tissues. In many cases the altered metabolism associated with cancer results in a lower oxygen concentration in these tissues, compared to healthy ones, and this promotes a reductive environment.

- (iii) the ability of ruthenium to mimic iron in binding to certain biological molecules.

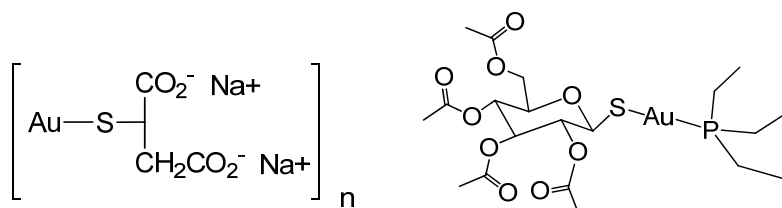
The low toxicity of ruthenium drugs is also believed to be due to the ability of ruthenium to mimic iron in binding to many biomolecules, including serum transferrin and albumin.

Ruthenium drugs are particularly important in the clinic due to their low toxicity. This is in part due to the ability of ruthenium to mimic the binding of iron to biomolecules, exploiting the mechanisms that the body has evolved for nontoxic transport of iron. In addition, the redox potential between the different accessible oxidation states occupied by ruthenium enables the body to catalyse oxidation and reduction reactions, depending on the physiological environment. As demonstrated for cancer tissues, but also true in other diseased states, the biochemical changes that accompany disease alter the physiological environment, enabling ruthenium compounds to be selectively activated in diseased tissues. These two features combine to give ruthenium drugs a remarkably low toxicity compared to other platinum group metal compounds and therefore make ruthenium compounds promising in the clinic.

### 3. Gold: the main project

Gold compounds have a long and important tradition in medicine (also known as Chrysotherapy), which dates back to the ancient Egyptians and especially flourished during the late Middle Age and the Renaissance. Gold compounds were widely used in early times of modern pharmacology, for the treatment of several diseases, especially as anti-infective and antitubercular agents.

Nowadays, gold compounds have found rather limited medical application, and some of them, namely gold(I) complexes with thiolate and phosphine ligands (figure 9), are presently used only for the treatment of severe rheumatoid arthritis, [42] although also proved to possess anticancer properties.



Aurothiomalate and Auranofin (figure 9)

Gold compounds constitute a variegated family of very promising experimental agents for cancer treatment. Indeed, several gold(I) and gold(III) complexes were shown to manifest outstanding antiproliferative properties *in vitro* against selected human tumor cell lines, and some of them performed remarkably well even in tumor models *in vivo*. [43,44] As previously mentioned, investigations on the cytotoxicity scores of gold complexes have been initially focused mainly on auranofin (1-thio- $\beta$ -D-glucopyranose-2,3,4,6-tetraacetato-S)(triethylphosphine) gold(I), and its analogues, which present linear gold phosphane thiolate structures. [45]. More recently, a variety of gold derivatives have also been tested as potential antitumor agents, including organogold derivatives, complexes with polydentate nitrogen donor ligands, gold porphyrins, gold dithiocarbamates, and gold N-heterocyclic carbene (NHC) carbenes. [46-50].

### 3.1 Chemistry of Gold

The chemistry of gold contains some unique aspects that are most likely the consequence of important unique electronic properties of the gold center. For instance, gold has a great propensity to form strong gold-gold bonds (the so-called ‘‘aurophilic interactions’’)[51]. A rich redox chemistry is associated with the three main oxidation states of gold. In turn, redox changes are strictly linked to changes in the coordination sphere with a frequent switch from square planar gold(III) complexes to linear dicoordinated gold(I) complexes[52]. All these aspects may be exploited to build up a variety of gold-based pharmacologically active compounds.

The most important oxidation states for gold are the following: Au(0), Au(I), and Au(III). The elemental forms of gold, principally metallic and colloidal gold, are stable; however, in the presence of relatively strong ligands, elemental gold can undergo rather facile oxidation. The chemistry of gold complexes in the oxidation states +1 and +3 has been investigated in depth as well as their behavior in solution and reactivity with biomolecules [52-54] A relatively easy interchange between the

oxidation states +1 and +3 even under physiological conditions is possible[55]. This specific property may be pharmacologically relevant.

### 3.2 Gold (I)

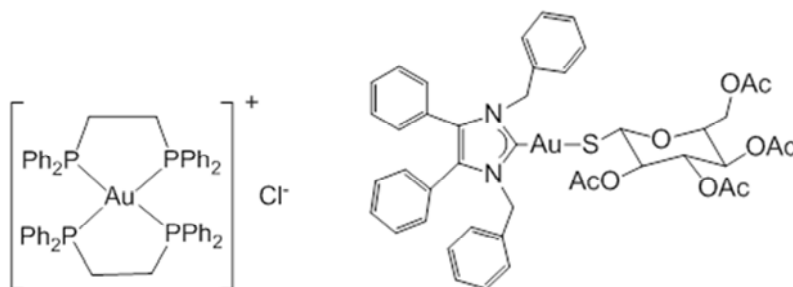
Gold(I) has a  $d^{10}$  closed-shell configuration, which is the basis for three principal coordination environments: linear two-coordination, by far the most important, but also trigonal three-coordination and tetrahedral four-coordination. Gold(I) is a soft cation with a preference for soft ligands.

Gold (I) anticancer compounds are divided into two classes : (i) neutral, linear, two-coordinate complexes, such as auranofin and aurothiomalate and (ii) lipophilic cationic complexes such as  $[\text{Au}(\text{dppe})_2]^+$  and dinuclear Au(I) NHC complexes. For both classes tumor cell mitochondria are likely targets [56], with apoptosis induced by alteration of the thiol redox balance [57].

Auranofin exists as a monomeric species, while the other compounds have been isolated in solid state in oligomeric forms. The aqueous solution chemistry of these compounds has been intensely investigated [54,58] and indicates that thiolate ligands are usually more labile than phosphine ligands and undergo rapid aquation. The resulting cationic species usually show a strong reactivity with biomolecules. Analogously, phosphine ligands may undergo aquation but these reactions are generally far slower.

The cytotoxic activity of auranofin against HeLa cancer cells was first reported in 1979 by Lorber and coworkers [59], and subsequent studies showed that auranofin increased the survival times of mice with P388 leukemia [60]. The recent work of Bindoli and coworkers [61] has shed light on the mechanism and it is proposed that apoptosis induction occurs due to alteration of the thiol redox balance in cells, as a result of TrxR inhibition. Moreover, aurothiomalate – in contrast to auranofin – is poorly effective in inhibiting TrxR and inducing apoptosis in Jurkat T cells [62]. A recent study, however, has shown that both aurothiomalate and aurothioglucose exhibit potent antitumor effects in *in vitro* and *in vivo* pre-clinical models of non-small cell lung cancer [63].

The high reactivity toward protein thiols (a characteristic feature of linear two-coordinate Au(I) complexes) limits its antitumor activity *in vivo*. While a range of auranofin analogs have shown promising cytotoxic activity *in vitro*, similar reactions are likely to limit their application as anticancer agents. It was this aim of reducing the high thiol reactivity that led to early investigations of Au(I) complexes with chelated diphosphines, and to the development of  $[\text{Au}(\text{dppe})_2]\text{Cl}$  (figure 11), shown to exhibit significant antitumor activity against a range of tumor models in mice [64]. *In vitro*,  $[\text{Au}(\text{dppe})_2]\text{Cl}$  was also very cytotoxic to isolated dog and rat hepatocytes (Hoke *et al.*, 1988; Smith *et al.*, 1989). Pre-clinical development of  $[\text{Au}(\text{dppe})_2]\text{Cl}$  was abandoned because of the severe hepatotoxicity *in dogs*. The hepatotoxicity was attributed to alterations in mitochondrial function.  $[\text{Au}(\text{dppe})_2]\text{Cl}$  is very lipophilic and consequently targets the mitochondria in all cells. (Berners-Price *et al.*, 1999).

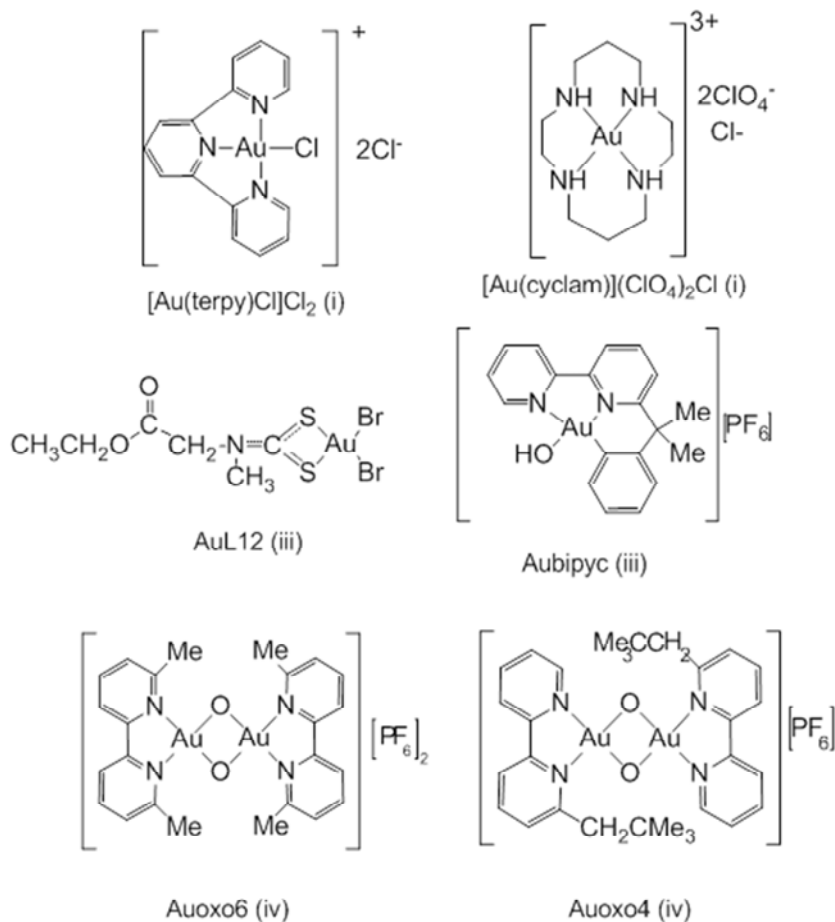


$[\text{Au}(\text{dppe})_2]\text{Cl}$  and NHC-gold(I)- (2',3',4',6'-tetra-*O*-acetyl- $\beta$ -D-glucopyranosyl-1-thiolate) (figure 10).

Many studies have shown that N-heterocyclic carbenes (NHCs) have similar properties to phosphines in the way they interact with metals, including gold (figure 10). For example, Ott et al. reported the synthesis and biological evaluation of a series of benzimidazol-2-ylidene-gold(I) complexes and found strong antiproliferative effects against MCF-7, HT-29 (cancerous), and HEK-293 (noncancerous) cells as well as TrxR inhibition for the NHC-Au-PPh<sub>3</sub> complexes [65].

### 3.3 Gold (III)

Gold(III) has a  $d^8$  closed-shell configuration, which originates metal complexes that are isoelectronic and isostructural to platinum(II) complexes; accordingly, the dominant coordination geometry for gold(III) complexes is square planar tetra-coordination. The bond lengths are shorter than the corresponding gold(I) bond lengths although differences are not very large. The reactivity behavior of the gold(III) cation is borderline, showing a preference not only for soft ligands but also for nitrogen donors. The oxidation state +3 is strongly oxidizing unless the gold(III) cation is stabilized by an appropriate set of nitrogen or soft donors. A vast array of gold(III) complexes showing rather variegated structural chemistry have been considered as potential anticancer drugs [53]. The gold(III) compounds of interest may be grouped into the four following classes: (i) classical mononuclear gold(III) complexes; (ii) gold(III) porphyrins; (iii) organogold(III) compounds; (iv) dinuclear gold(III) complexes (figure 11).



Gold(III) Compounds (figure 11).

Classical Mononuclear Gold(III) are square planar gold(III) compounds mostly with nitrogen or halide ligands (i.e AuCl<sub>4</sub> , [Au(dien)Cl]Cl<sub>2</sub> , [Au(cyclam)](ClO<sub>4</sub>)<sub>2</sub>Cl [Au(phen)Cl<sub>2</sub>]Cl ) [66] As nitrogen ligands are stronger and less labile than chloride ligands, it follows that chloride ligands undergo far more facile aquation reactions that lead to complex activation. In turn, nitrogen ligands induce significant stabilization of the oxidation state +3. Notably, other compounds belonging to this group are gold(III) dithiocarbamate complexes. The compounds containing N,N-dimethyldithiocarbamate and ethylsarcosinedithiocarbamate ligands, developed in Padua, have been intensely studied as possible anticancer agents (figure 11-AuL12)[67].



In the Gold(III) porphyrins, the porphyrin ligand greatly stabilizes the gold(III) center and drastically reduces its redox reactivity and oxidizing character[68]. It has been hypothesized that the primary target for gold(III) porphyrins is DNA following intercalation; however, recent studies reveal that gold(III) porphyrins may greatly affect mitochondrial functions as well[69].

Organogold(III) Compounds are characterized by the presence of at least one direct carbon–gold(III) bond; this latter feature is very important for the stabilization of gold oxidation state +3. Organogold(III) compounds are generally stable under physiological conditions and have a scarce tendency to be reduced to gold(I). They are significantly cytotoxic to human tumor cell lines [70].

Dinuclear Gold(III) complexes are structurally related with an oxo-bridged dinuclear gold(III).  $[\text{Au}_2(\mu\text{-O})_2(\text{N}^{\wedge}\text{N})_2](\text{PF}_6)_2$ , where  $\text{N}^{\wedge}\text{N}$  is 2,2'-bipyridine or a substituted 2,2'-bipyridine, have recently been shown to exhibit appreciable stability under physiological-like conditions and to manifest important antiproliferative effects toward selected human tumor cell lines. All these compounds contain a common structural motif consisting of an  $\text{Au}_2\text{O}_2$  “diamond core” linked in a roughly planar arrangement [auoxo6]

#### 4. Biomolecules as target

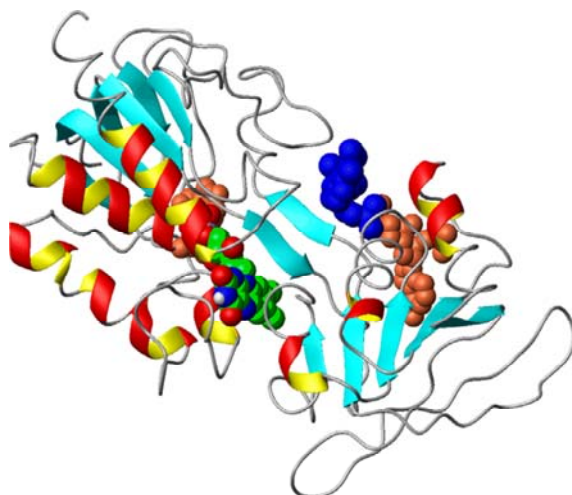
Anticancer metallodrug development has for a long time been characterised by the similarity of new drug candidates to cisplatin and DNA as the primary target. Recent advances in bioanalytical techniques with high sensitivity and selectivity have revealed that metal-based drugs can undergo a wide range of biomolecular interactions beyond DNA and have generated interest in proteins as possible targets for metallodrugs. In fact, implementation of metallomics approaches that are able to reveal the fate of the compounds in biological systems can help to move drug development towards more targeted and rational design of novel metallodrugs.

Overall, from a detailed analysis of the mechanistic studies carried out so far on the biological reactions of gold compounds, it is possible to define three major classes according to their mode of action with biological targets.

- (1) Gold compounds are prodrugs capable of coordinating tightly to biomolecules' side chains, e.g. thiols, imidazole, and selenols, after activation (usually through the release of a labile ligand), e.g. auranofin. This behavior involves an alkylation mechanism similar to that of the platinum compounds.
- (2) Gold complexes are big cations capable of crossing membranes and of binding noncovalently but strongly to biomolecules (proteins, enzyme, DNA) (coordination compounds that target biomolecules) e.g. gold-based DNA intercalators, gold(III) porphyrins
- (3) Gold compounds that react with biomolecules mainly through redox chemistry causing oxidative damage e.g. Auoxo6

## 4.1 Thioredoxin Reductase System

The action of gold compounds on the enzyme thioredoxin reductase, might explain the relevant alterations observed in mitochondrial functions (e.g. permeability transition) after gold treatment.[71,72] The thioredoxin redox system comprises thioredoxin reductase (TrxR), a homodimeric selenium containing flavoprotein, and thioredoxin (Trx), a ubiquitously expressed small protein with a conserved Cys-Gly-Pro-Cys redox catalytic site capable of reducing a variety of substrates [73]. Both Trx and TrxR in mammals are expressed as dedicated isoforms for either predominantly cytosolic (Trx1 and TrxR1), shown in figure12, or mitochondrial (Trx2 and TrxR2) localization [74]. Thioredoxin plays multiple functions in the cell that include the providing of reducing equivalents for DNA synthesis through ribonucleotide reductase (RR) enzyme and for reactive oxygen species (ROS) scavenging through the peroxiredoxins (Prxs). In addition, thioredoxin is found to reduce, and thus activate, a number of transcription factors that are all involved in the regulation of various aspects of cell growth and cell survival, including NF-kB,66 AP-1,67 SP-1, and p53 [75].



Schematic representation of the molecular structure of mammalian TrxR1 visualised with the Swiss-Pdb Viewer software (figure 12)

In addition, thioredoxins are vital in the regulation of redox signalling pathways via thiol redox control and a growing number of transcription factors have been identified that require thioredoxin reduction for DNA binding. [76]. The up-regulation of thioredoxins in malignant diseases is well established, with the growth-promoting effects of thioredoxin outweighing the beneficial anti-oxidant properties. Elevated expression of thioredoxin is associated with increased proliferation of tumour cells, inhibition of apoptosis, aggressive tumour growth and decreased patient survival. In addition, high concentrations of thioredoxin reductase can support tumour cell drug resistance [77].

Both gold(I) and gold(III) compounds are found to interact strongly with the thioredoxin system.

The ability of gold(I) compounds, in particular auranofin, to inhibit TrxR and induce apoptosis has been recently investigated in cisplatin-resistant human ovarian cancer cells [78]. The treatment with auranofin of cisplatin-sensitive and -resistant ovarian cancer cells causes a consistent release of cytochrome c in both cell lines while cisplatin is effective only in the sensitive cells. Apoptosis is accompanied by the increased production of ROS. In resistant cells, hydrogen peroxide production is counteracted by a large overexpression of TrxR. Thus, these authors suggest that auranofin, acting as a potent inhibitor of TrxR, determines an alteration of the redox state of the cell, leading to increased production of hydrogen peroxide and to oxidation of the components of the thioredoxin system, which creates the conditions for augmented apoptosis.

Similarly to gold(I) compounds, gold(III) compounds are known to target, rather strongly and selectively, thiol and imidazole groups of proteins (as well as selenol groups) [79]. Some gold(III) compounds developed by Cinellu et al. [80, 81] are shown to inhibit mitochondrial TrxR2 and to greatly perturb mitochondrial functions [82]. The presumed site of interaction is the selenol moiety present in the active site of the carboxy terminus of the enzyme as well as other cysteine and histidine residues.

#### 4.2 Targeting Mitochondria for anticancer gold compounds

Over 70 years ago, Warburg [83] observed that cancer cells frequently exhibit increased glycolysis and depend largely on this metabolic pathway for generation of ATP to meet their energy needs. He attributed this metabolic alteration to mitochondrial “respiration injury” and considered this as the most fundamental metabolic alteration in malignant transformation or “the origin of cancer cells” [84]. During the past several decades, the Warburg effect has been consistently observed in a wide spectrum of human cancers, although the underlying biochemical and molecular mechanisms are extremely complex and remain to be defined. Among the possible mechanisms, mitochondrial malfunction and hypoxia in the tumor microenvironment are considered two major factors contributing to the Warburg effect. Consistent with these structural changes, mitochondrial dysfunction have been observed in various types of cancer cells, evident by a compromised capacity in mitochondrial ATP generation and an abnormal increase in ROS generation, Chen 2007.

The Warburg effect may involve a series of metabolic defects including unregulated, supernormal glucose uptake with up-regulation of the rate-limiting steps of glycolysis (for instance driven by constitutive activation of the Akt pathway), Elstrom et al., 2004, as well as defects in mitochondrial respiration, as they manifest in cancer cells.

Several different classes of gold-based compounds (in both Au(I) and Au(III) oxidation states) have attracted interest as potential antitumour agents and there is evidence that many act by mechanisms involving mitochondrial cell death pathways

## 5. Basic aspect of Gold/Protein interactions

Most of the gold compounds are known to behave as pro-drugs, in other words an activation step is required before they can react with biomolecular targets and cause their specific biological effects. Usually, this step consists of the release of a weak ligand (the so called “leaving group”) from the first coordination sphere of the metal and of its replacement by a water molecule. The resulting “aqua species” usually manifest a high propensity to react with protein side-chains, showing a pronounced preference for histidine, cysteine and methionine residues, but also for carboxylate groups. Alternatively, metallodrug activation may occur through a redox process, for instance metal reduction, as mentioned before. In most cases, the reaction of activated metallodrugs with protein side chains leads to formation of relatively tight metallo-drug–protein complexes or adducts in which metallic fragments are covalently bound to proteins. These adducts usually manifest an appreciable stability. However, a further reactivity may be expected: (i) if the metallic fragments still bears reactive sites; (ii) if the adduct is reacted with other biomolecules showing a higher affinity for the metal itself; (iii) if the protein possesses stronger, but kinetically disfavoured, binding sites for the metallic fragment. Of course, this residual reactivity may be very important in order to assess whether the formed species will keep some biological activity.

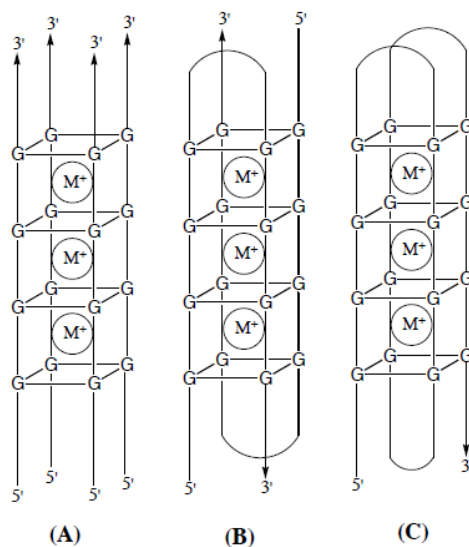
Nowadays there is strong concern within the anticancer research community regarding improvement of the arsenal of the analytical techniques in use. This led in particular to a growing number of metallo-protein investigation performed using techniques superior as ESI and MALDI MS, to characterize metal-protein adduct at molecular level and X-ray diffractions to provide detailed structural information of such adducts. Conversely the rapid development of proteomic technologies and the use of advanced methods, hold promise for successful analysis of complex mixtures of metallated proteins and for identification of those proteins that act as primary “metallodrug receptors” and/or “metallodrug targets”. Thus, these latter techniques open the way to the investigation of far more complicated systems such as metallodrug/treated cell populations and/or cell homogenates, that reflect more closely the reality of metallic species in the cell world.

Some example of proteins that are suitable models to test reactivity with metallodrugs are the following: hen egg white lysozyme (HEWL), horse heart cytochrome c (cyt c), ribonuclease A (RNase A). Schematic drawings for some of these proteins are shown in figure 13. For all these proteins high resolution crystal structures are available. Notably, these proteins are of moderate to small size with MW ranging from 14000 (HEWL) to 12000 (cyt c) Da. Moreover, all these proteins are commercially available,

manifest a high stability in solution under physiological- like conditions, are relatively cheap and water soluble. In most cases, they exhibit a basic pI and are thus appropriate for ESI MS detection in the positive mode. All these features render experimental work on these model systems rather comfortable

## 6. DNA Quadruplex as target

In 1994 it was reported that the vast majority (approx. 85%) of tumour cells exhibit elevated levels of telomerase activity [85]. The maintenance of telomeres plays a key role in the “immortalisation” of cancer cells by preventing chromosomes from shortening during cell division. In contrast, in most normal human cells, there is a significant loss of telomere DNA every time a cell divides, which ultimately results in the cells undergoing apoptosis. Human telomeric DNA occurs at the ends of chromosomes and consists of single stranded DNA (ssDNA) that is rich in guanine residues. There is now considerable evidence from both solid state and solution techniques that guanine rich sequences such as these can fold in ways that result in structures known as DNA quadruplexes. Since the natural substrate of telomerase is ssDNA, it is believed that the formation and/or stabilisation of quadruplex DNA (qDNA) is very likely to prevent the enzyme from performing its normal function. This has raised the prospect of designing small molecules that can stabilize qDNA, or even induce ssDNA present in telomeres to form qDNA, thereby inhibiting telomerase and rendering cancer cells more susceptible to normal apoptotic pathways. mind.



Schematic illustration of a selection of different quadruplex DNA topologies. (A) Intermolecular parallel qDNA formed from four DNA strands. (B) Intermolecular antiparallel

qDNA formed from two DNA strands. (C) Intramolecular antiparallelqDNA formed from one DNA strand. Adapted from S.M. Nelson et al., *Cell and Chromosome* 2004, 3, 1-26.(figure 13)

Metal complexes have a very broad range of structural and electronic properties that can be successfully exploited when designing quadruplex DNA binders. A metal center can be envisaged as a structural locus that organizes ligands in specific geometries and relative orientations for optimal quadruplex binding. Variation can be introduced by modifying the ligands (but retaining the geometry around the metal center) or by changing the metal center (which can then furnish compounds of different geometries). In addition to their structural features, the electron-withdrawing properties of metal centers can reduce the electron density on coordinated aromatic ligands. This affords electron-poor systems, which are expected to display stronger  $\pi$  interactions with G-quartets. Also, the electropositive metal can, in principle, be positioned at the center of a G-quartet, thereby increasing the electrostatic stabilization by substituting the cationic charge of the alkali metal cation that would normally occupy this site. The current strategy when designing quadruplex DNA binders is to use planar molecules, which possess the ability to interact through  $\pi$  stacking with G-quartets. Some Gold(III) complexes have been reported as potential quadruplex DNA inhibitors[86].

## References

- [1] L. Ronconi, P.J. Sadler, *Coord. Chem. Rev.*, 2007, 2007 251, 1633–1648.
- [2] Z. Guo, P.J. Sadler, *Adv. Inorg. Chem.*, 2000, 49, 183–306.
- [3] C. Orvig, M.J. Abrams, *Chem. Rev.*, 1999, 99, 2201–2203.
- [4] Z. Guo, P.J. Sadler, *Angew. Chem. Int. Ed.*, 1999, 38, 1512–1531.
- [5] A. Mukherjee, P.J. Sadler, *Metals in medicine: therapeutic agents*, in *Wiley Encyclopedia of Chemical Biology*, Wiley-Blackwell, 2009, 3, 80–126.
- [6] P.C.A. Bruijninx, P.J. Sadler, *Curr. Opin. Chem. Biol.*, 2008, 12, 197–206.
- [7] B. Desoize, *Anticancer Res.*, 2004, 24, 1529–1544.
- [8] A.M. Pizarro, P.J. Sadler, *Biochimie*, 2009, 91, 1198–1211.
- [9] B. Rosenberg, L. VanCamp, J.E. Trosko, V.H. Mansour, *Nature*, 1969, 222, 385–386.
- [10] M.J. Clarke, F. Zhu, D.R. Frasca, *Chem Rev.*, 1999, 99, 2511–2533.
- [11] A.M. Evangelou, *Crit Rev Oncol Hematol.*, 2002, 42, 249–265.
- [12] C.G. Hartinger, S. Zorbas-Seifried, M.A. Jakupec, B. Kynast, H. Zorbas, B.K. Keppler, *J. Inorg Biochem.*, 2006, 100, 891–904.
- [13] N. Katsaros, A. Anagnostopoulou, *Crit Rev Oncol Hematol.*, 2002, 42, 297–308.
- [14] I. Kostova, *Med Chem.*, 2006, 6, 19–32.
- [15] I. Kostova, *Med Chem.*, 2009, 9, 827–842.
- [16] I. Ott, R. Gust, *Arch Pharm (Weinheim)*, 2007, 340, 117–126.
- [17] G. Giaccone, *Drugs Exp. Clin. Res.*, 2000, 59 (Suppl. 4), 9-17.
- [18] B.A. Chabner, C.J. Allegra, G.A. Curt, P. Calabresi, P. In: Goodman and Gilman's *The Pharmacological Basis of Therapeutics*. Hardman, G. J.; Limbird, E. L.; Gilman, G. A. Eds.; McGraw-Hill: New York, 1996.
- [19] P.J. Loehrer, L.H. Einhorn, *Ann. Intern. Med.*, 1984, 100, 704-713.
- [20] E.R. Jamieson, S.J. Lippard, *Chem. Rev.*, 1999, 99, 2467-2498.
- [21] L.R. Kelland, *Drugs Exp. Clin. Res.*, 2000, 59 (Suppl. 4), 1-8.

- [22] J. J. Roberts, A. J. Thompson, *Prog. Nucl. Acids Res. Mol. Biol.*, 1979, 22, 71.
- [23] S. J. Lippard, *Pure Appl. Chem.*, 1987, 59, 731.
- [24] A. Eastman, *Cancer Cells*, 1990, 2, 275.
- [25] M. C. Lim, R. B. Martin, *J. Inorg. Nucl. Chem.*, 1976, 38, 1911.
- [26] A. L. Pinto, S. J. Lippard, in: T. G. Spiro (Ed.), *Metal Ions in Biology 1*, John Wiley & Sons, 1980, 31.
- [27] Jakupec MA, Galanski M, Keppler BK. *Rev Physiol Biochem Pharmacol* 2003; 146: 1–53.
- [28] I. Kostova, *Recent Patents on Anti-Cancer Drug Discovery*, 2006, 1, 1-22 1
- [29] B. Lippert (Ed.). Wiley- VCH, Weinheim (1999).
- [30] B. Rosenberg, L. Van Camp, E. B. Grimley, A. J. Thomson, *J. Biol. Chem.* 1967, 242, 1347- 1352
- [31] G. Natile, M. Coluccia, *Coord. Chem. Rev.*, 2001, 216–217, 383-410.
- [32] N. Farrell, T. T. B. Ha, J.-P. Souchard, F. L. Wimmer, S. Cros, N. P. Johnson. *J. Med. Chem.*, 1989, 32, 2240-2241
- [33] E. I. Montero, S. Diaz, A. M. Gonzalez-Vadillo, J. M. Perez, C. Alonso, C. Navarro-Ranninger. *J. Med. Chem.*, 1999, 42, 4264-4268
- [34] M. Coluccia, A. Nassi, F. Loseto, A. Boccarelli, M. A. Mariggio, D. Giordano, F. P. Intini, P. A. Caputo, G. Natile., *J. Med. Chem.*, 1993, 36, 510-531
- [35] N. Farrell. *Metal Ions Biol. Sys.*, 2004, 41, 252-296.
- [36] G. Sava, E. Alessio, A. Bergamo, G. Mestroni, *Top. Biol. Inorg. Chem.*, 1999, 1, 143-169.
- [37] G. Sava, S. Pacor, G. Mestroni, E. Alessio, *Clin. Exp. Metastasis*, 1992, 10, 273-280.
- [38] M. H. Seelig, M. R. Berger, B. K. Keppler, *J. Cancer Res. Clin. Oncol.*, 1992, 118, 195–200.
- [39] C.G. Hartinger, S. Zorbas-Seifried, M.A. Jakupec, B. Kynast, H. Zorbas, B.K. Keppler, *J. Inorg. Biochem.*, 2006, 100, 891–904.
- [40] W. H. Ang, P. J. Dyson, *Eur. J. Inorg. Chem.*, 2006, 4003-4018 .
- [41] C. S. Allardyce, P. J. Dyson, *Platinum Metal Rev.*, 2001, 45(2), 62-69.
- [42] L. Messori, G. Marcon, *Met Ions Biol Syst*, 2004, 41, 279–304.

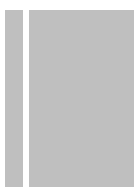


- [43] D. Fregona, L. Ronconi, D. Aldinucci, *Drug Discov. Today*, 2009, 14, 1075–1076.
- [44] C.M. Che, R.W.Y. Sun, W.Y. Yu, C.B. Ko, N.Y. Zhu, H.Z. Sun, *Chem. Commun.*, 2003, 1718–1719.
- [45] E.R. Tiekink, *Bioinorg. Chem. Appl.*, 2003, 1, 53–67.
- [46] S. Nobili, E. Mini, I. Landini, C. Gabbiani, A. Casini, L. Messori, *Med. Res. Rev.*, 2010,30, 550-580
- [47] L. Ronconi, D. Fregona, *Dalton Trans.*, 2009,48, 10670–10680.
- [48] R.W.Y. Sun, C.M. Che, *Coord. Chem. Rev.*, 2009, 253,1682-1691
- [49] I. Ott, *Coord. Chem. Rev.*, 2009, 253, 1670-1681
- [50] A. Bindoli, M.P. Rigobello, G. Scutari, C. Gabbiani, A. Casini, L. Messori, *Coord. Chem. Rev.*, 2009, 253, 1692–1707.
- [51] C. Gabbiani, A. Casini, L. Messori, A. Guerri, M.A. Cinellu, G.Minghetti, M. Corsini, C. Rosani, P. Zanella, M. Arca, *Inorg Chem*, 2008, 47, 2368–2379.
- [52] C.F. Shaw III, *Chem Rev*, 1999, 99, 2589–2600.
- [53] A. Casini, C. Hartinger, C. Gabbiani , E. Mini, P.J. Dyson, B.K. KeppleR, L. Messori, *J Inorg Biochem*, 2008,102, 564–575.
- [54] C.F. Shaw III, *Comments Inorg Chem*, 1989, 8, 233–267.
- [55] E.R. Tiekink, *Crit Rev Oncol Hematol* , 2002, 42, 225–248.
- [56] M.J. McKeage, L. Maharaj, S.J. Berners-Price, *Coord. Chem. Rev.*, 2002, 232, 127–135.
- [57] P.J. Barnard, S.J. Berners-Price, *Coord. Chem. Rev.*, 2007, 251, 1889–1902.
- [58] C.F. Shaw III, *Top Biol Inorg Chem*, 1999, 2, 187.
- [59] T.M. Simon, D.H. Kunishima, G.J. Vibert, A. Lorber, *Cancer*, 1979, 44, 1965–1975.
- [60] T.M. Simon, D.H. Kunishima, G.J. Vibert, A. Lorber, *Cancer Res.*, 1981, 41, 94–97.
- [61] M.P. Rigobello, G. Scutari, R. Boscolo, A. Bindoli, A., *Br. J. Pharmacol*, 2002, 136, 1162–1168.
- [62] M.P. Rigobello, A. Folda, B. Dani, R. Menabo`, G. Scutari, A. Bindoli, *Eur. J. Pharmacol.*, 2008, 582, 26–34.

- [63] M. Stallings-Mann, L. Jamieson, R.P. Regala, C. Weems, N.R., Murray, A.P. Fields, *Cancer Res.*, 2006, 66, 1767–1774.
- [64] S.J. Berners-Price, C.K. Mirabelli, R.K. Johnson, M.R. Mattern, F.L. McCabe, L.F. Faucette, C.M.S. Can, I. Kitanovic, H. Alborzina, M. Stefanopoulou, M. Kokoschka, S. Mönchgesang, W.S. Sheldrick, S. Wölfl, I. Ott, *J. Med. Chem.* 2011, 54 (24), 8646–8657.
- [66] L. Messori, F. Abbate, G. Marcon, P. Orioli, M. Fontani, E. Mini, T. Mazzei, S. Carotti, T. O’Connell, P. Zanello, *J. Med. Chem.*, 2000, 43, 3541–3548.
- [67] L. Ronconi, L. Giovagnini, C. Marzano, F. Betti, R. Graziani, G. Pilloni, D. Fregona, *Inorg. Chem.*, 2005, 44, 1867–1881.
- [68] C.M. Che, R.W. Sun, W.Y. Yu, C.B. Ko, N. Zhu, H. Sun, *Chem. Commun. (Camb)* 2003, 14, 1718–1719.
- [69] Y. Wang, Q.Y. He, R.W. Sun, C.M. Che, J.F. Chiu, *Cancer Res.*, 2005, 65, 11553–11564.
- [70] L. Messori, G. Marcon, M.A. Cinellu, M. Coronello, E. Mini, C. Gabbiani, P. Orioli *Bioorg. Med. Chem.* 2004, 12, 6039–6043.
- [71] M.P. Rigobello, G. Scutari, R. Boscolo, A. Bindoli, *Br. J. Pharmacol.*, 2002, 136, 1162–1168.
- [72] M.P. Rigobello, L. Messori, G. Marcon, M.A. Cinellu, M. Bragadin, A. Folda, G. Scutari, A. Bindoli, *J. Inorg. Biochem.*, 2004, 98, 1634–1641.
- [73] E.S. Arner, A. Holmgren, *Semin. Cancer Biol.*, 2006, 6, 420–426.
- [74] A. Holmgren, *Thioredoxin. Annu. Rev. Biochem.*, 1985, 54, 237–271.
- [75] M. Ueno, H. Masutani, R.J. Arai, A. Yamauchi, K. Hirota, T. Sakai, T. Inamoto, Y. Yamaoka, J. Yodoi, T. Nikaido, *J. Biol. Chem.*, 1999, 274, 35809–35815.
- [76] S. Gromer, S. Urig, K. Becker, *Med. Res. Rev.*, 2004, 24, 40–89.
- [77] A. Burke-Gaffney, M.E.J. Callister, H. Nakamura, *Trends Pharmacol. Sci.*, 2005, 26, 398–404
- [78] C. Marzano, V. Gandin, A. Folda, G. Scutari, A. Bindoli, M.P. Rigobello, *Free Radic. Biol. Med.* 2007, 42, 872–881.
- [79] A. Casini, C. Hartinger, C. Gabbiani, E. Mini, P.J. Dyson, B.K. Keppler, L. Messori, *J. Inorg. Biochem.*, 2008, 102, 564–575.

- [80] M.A. Cinellu, A. Zucca, S. Stoccoro, G. Minghetti, M. Manassero, M. Sansoni, J. Chem. Soc. Dalton. Trans., 1996, 22, 4217–4225.
- [81] M.A. Cinellu, G. Minghetti, M.V. Pinna, S. Stoccoro, A. Zucca, M. Manassero, Eur. J. Inorg. Chem., 2003, 12, 2304–2310.
- [82] M.P. Rigobello, L. Messori, G. Marcon, M.A. Agostina Cinellu, M. Bragadin, A. Folda, G. Scutari, A. Bindoli, J. Inorg. Biochem. 2004, 98, 1634–1641.
- [83] O. Warburg, London Constable Co. Ltd.; 1930.
- [84] O. Warburg, Science, 1956, 123, 309–314.
- [85] N.W. Kim, M.A. Piatyszczek, K.R. Prowse, C.B. Harley, M.D. West, P.L.C. Ho, G.M. Coviello, W.E. Wright, S.L. Weinrich, J.W. Shay, Science, 1994, 266, 2011–2015.
- [86] K. Suntharalingam, D. Gupta, P.J. Sanz Miguel, B. Lippert, R. Vilar, Chem. Eur. J., 2010, 16(12), 3613–3616.





## **Chapter 2**

### **Protein Metalation by Cytotoxic Gold Compounds \***

\* The results presented in this chapter have been published in “Protein metalation by metal-based drugs: reactions of cytotoxic gold compounds with cytochrome c and lysozyme” C. Gabbiani, L. Massai, F. Scaletti, E. Michelucci, L. Maiore, M. A. Cinellu, L. Messori; *J. Biol. Inorg. Chem.*; (2012) 17, 1293-1302. And in “Chemistry and Biology of Two Novel Gold(I) Carbene Complexes as Prospective Anticancer Agents”, L. Messori, L. Marchetti; L. Massai, F. Scaletti, A. Guerri, I. Landini, S. Nobili; G. Perrone, E. Mini, P. Leoni, M. Pasquali, C. Gabbiani, *Inorg. Chem.* (2014) 53(5), 2396-2

## SECTION A: Gold(III) compounds

## 1. Introduction

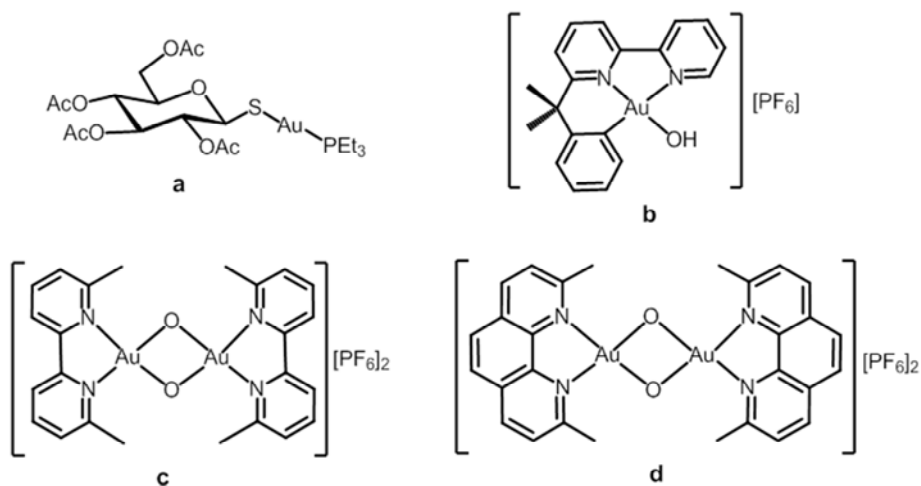
A few recent studies highlighted the importance of gold compounds as a new family of cytotoxic agents with the potential of becoming effective anticancer drug candidates [1,2,3]. Indeed, a variety of gold compounds, either gold(III) or gold(I), bearing different structural motifs, were reported to cause effective cell death *in vitro* [4,5,6,7] in numerous cancer cell lines; for a few gold(III) compounds *i.e.* gold(III) porphyrins and gold(III) dithiocarbamates, preliminary but very promising *in vivo* results were also achieved [1,8].

The modes of action of antiproliferative gold compounds are still largely unknown and a matter of intense research and debate. In any case, they appear to be multifaceted and deeply distinct from those of clinically established platinum compounds. Notably, there is now a growing body of evidence suggesting that some selected protein targets rather than nucleic acids primarily mediate the biological effects of cytotoxic gold compounds [9,10]. A few studies postulated that the cytotoxic effects of gold compounds are driven by specific antimitochondrial mechanisms, ultimately leading to apoptotic cancer cell death [11,12,13]; however, this latter hypothesis still needs conclusive validation.

Notably, over the last 30 years, a number of studies have appeared concerning the interactions of gold compounds with proteins at the molecular level. Some pioneering work was carried out by Frank Shaw and co-workers describing the reactions of *Auranofin* with serum albumin [14]. Other important studies were reported by Peter Sadler and co-workers dealing with serum albumin and with cyclophilin [15,16]. Talib *et al* used MS methods to investigate the binding of various gold(I) compounds to serum albumin [17]. A systematic study conducted in our laboratory a few years ago considered the reaction of various gold compounds with serum albumin and investigated the underlying mechanisms [9,18,19]. Very recent studies, mainly based on ESI MS, analysed the reactions of cytotoxic gold compounds with small proteins such as *cytochrome c* and *lysozyme* and described the resulting adducts [20,21].

During the last few years, we have prepared and characterised three novel gold(III) complexes –namely [(bipy<sup>2Me</sup>)<sub>2</sub>Au<sub>2</sub>(μ-O)<sub>2</sub>][PF<sub>6</sub>]<sub>2</sub> (where bipy<sup>2Me</sup> = 6,6'-dimethyl-2,2'-bipyridine) (*Auoxob*), [(phen<sup>2Me</sup>)<sub>2</sub>Au<sub>2</sub>(μ-O)<sub>2</sub>][PF<sub>6</sub>]<sub>2</sub> (where phen<sup>2Me</sup> = 2,9-dimethyl-1,10-phenanthroline) (*Au<sub>2</sub>phen*) and [(bipy<sup>dmb</sup>-H)Au(OH)][PF<sub>6</sub>] (where bipy<sup>dmb</sup>-H = deprotonated 6-(1,1-dimethylbenzyl)-2,2'-bipyridine) (*Aubipyc*) - that revealed quite promising antiproliferative properties when tested *in vitro* on a variety of cancer cell lines. The three mentioned complexes are shown in Chart 1; the schematic structure of

*Auranofin*, a clinically established gold(I) drug used here for comparison purposes, is also reported.



Auranofin (MW 678.50) (a), Aubipyc (MW 634,32) (b), Auoxo6 (MW 1084.41) (c), Au<sub>2</sub>phen (MW 1132,39) (d) (chart 1)

Auoxo6 and Au<sub>2</sub>phen are dioxo-bridged dinuclear gold(III) complexes with 6,6'-dimethyl-2,2'-bipyridyne and 2,9-dimethyl-1,10-phenanthroline as ancillary ligands, respectively [22,23,24]. Both gold(III) centers, in *Auoxo6* and Au<sub>2</sub>Phen, display a classical square-planar coordination, with slight square-pyramidal distortions. *Aubipyc* is a gold(III) cyclometalated derivative of 6-(1,1-dimethylbenzyl)-2,2'-bipyridine, which features a N,N,C sequence of donor atoms of the terdentate bipyridine ligand and an oxygen atom of a hydroxo ligand coordinated to the gold(III) center in a square planar geometry [25]. *Auranofin*, 2,3,4,6-tetra-O-acetyl-1-thio- $\mu$ -D-pyranosato-S-(triethylphosphine)gold(I) is a linear gold(I) complex of the type R<sub>3</sub>P-Au(I)-SR' where SR' is a sugar thiolate.

The cytotoxic properties of the above gold(III) complexes were evaluated in vitro on a standard 36 cancer cell lines panel available at Oncotest, Germany, according to established procedures [26,27]. The COMPARE algorithm [28,29] applied to the analysis of the obtained growth inhibition data revealed that the profiles of Au<sub>2</sub>phen are very similar to those of Auoxo6; this behaviour reflects the pronounced structural analogy existing between these two compounds [22]. Tentatively, the patterns of antiproliferative activity obtained for Au<sub>2</sub>phen and Auoxo6 were referred to inhibition of histone deacetylase (HDAC) based on bioinformatic analysis. At variance, *Aubipyc*, though being appreciably cytotoxic in the A2780 ovarian cancer cells, turned out to be only moderately effective in the Oncotest panel. *Auranofin* was confirmed to be

highly cytotoxic in the Oncotest panel with a mode of action resembling that of antiproteasomal agents [30]. As mentioned above, correlations in the antiproliferative profiles between the various gold compounds and cisplatin resulted to be very poor implying the occurrence of drastically different modes of action.

On the whole, COMPARE analysis of these compounds as well as of several other cytotoxic gold compounds suggested that a variety of proteins such as HDAC, CDK kinase, Proteasome proteins, mTOR, *etc.* might represent reliable biomolecular targets and thus account for their biological effects; in other words, the biological actions of the investigated gold compounds might be best interpreted in terms of metalation and inactivation of a few crucial intracellular proteins that are effective cancer targets.

The great interest currently existing for the mechanistic aspects of metal based drugs/protein interactions prompted us to carry out a systematic analysis of the reactions taking place between the above gold compounds and two model proteins, namely *lysozyme and cytochrome c*. Notably, these small proteins are very amenable to ESI MS analysis and were specifically chosen for the present investigation.

The main goal of our study is to identify and define, at the molecular level, the modes of *Protein Metalation* produced by the above metallodrugs. *Protein Metalation* is indeed the process through which Proteins are modified upon reaction with metal containing compounds; such reactions typically involve formation of adducts between the protein and a metal species (typically a *molecular fragment* derived from the starting metal compound). The *metallic fragment* may be bound to the protein either by a direct coordinative bond or through a non-covalent interaction. Precise information on the actual metalation mechanisms may be achieved quite realistically through a detailed structural characterisation of metal-protein adducts including adduct quantification with respect to native unmodified proteins, identification of the nature and the number of protein bound metallic fragments; localization of the anchoring sites for metallic fragments. ESI MS appears to be a very appropriate and powerful tool to gain this kind of information; conversely, absorption spectroscopy offers the chance to monitor continuously “*in real time*” the various metallodrug-protein samples.

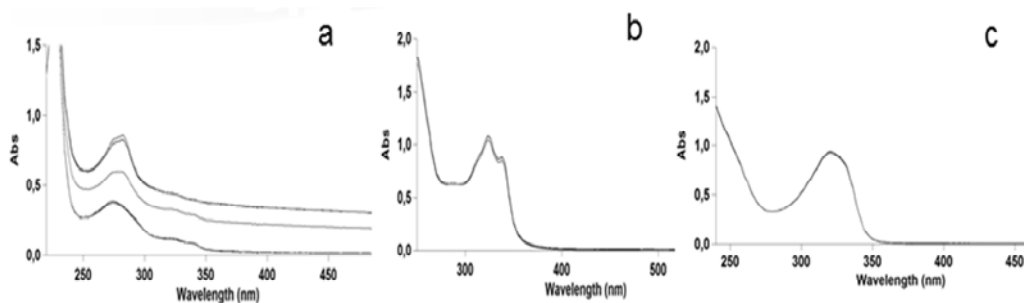
## 2. Results

### 2.1 Solution behavior of the three gold(III) compounds

Before studying their interactions with model proteins, we analysed the solution behaviour of the three investigational gold(III) complexes as such, under well controlled experimental conditions. UV-Visible absorption spectroscopy was selected as the method of choice to monitor continuously the behaviour of their gold(III) chromophores in the reference buffer (10 mM phosphate buffer, pH 7.4). Notably, all

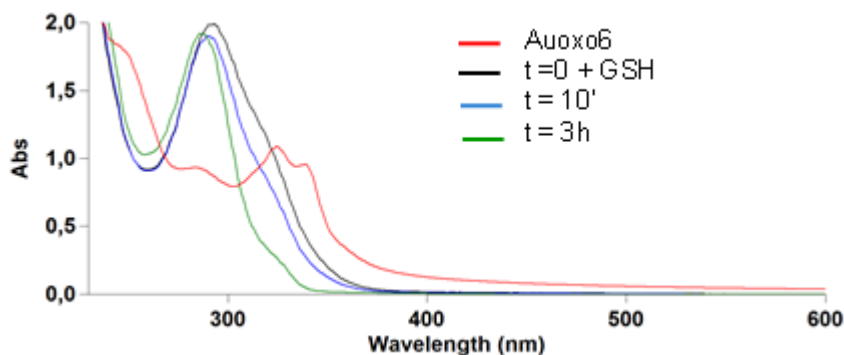


three gold(III) compounds manifested an appreciable stability when monitored over 24 hours, at 20 °C, as documented by the substantial stability of their absorption spectra (figure 1). These observations are in agreement with previous spectrophotometric results obtained for the same compounds under slightly different experimental conditions [6,25]. It is remarkable that the oxidation state +3 is essentially conserved, in all cases, over the whole observation period.



Time course UV-vis spectra of gold compounds. Au<sub>2</sub>phen (a) shows an evident baseline drift during the 24 h due to its low solubility in water; Auoxo6 (b) and Aubipyc (c) are stable over 24 h. (figure 1)

In contrast, important spectral changes were highlighted when these gold(III) complexes were challenged with an excess of two biologically occurring reducing agents i.e. ascorbic acid and glutathione. Notably, Auoxo6 and Au<sub>2</sub>phen were found to undergo quick and facile reduction upon addition of an excess of either reducing agent, which is documented by evident spectral changes. The reaction of Auoxo6 with glutathione is very representative as shown in figure 2; indeed, the LMCT band centered at 325 nm rapidly disappears upon GSH addition. Conversely, in the case of Au<sub>2</sub>phen, we noticed large modifications in the shape and intensity of the composite band centered at 280 nm that are suggestive of gold(III) reduction. Aubipyc turned out to be far more resistant toward reduction: indeed, ascorbic acid failed to reduce it while an excess of GSH was found to induce a progressive -though slow- reduction of the gold(III) center.



UV-vis spectra of AuOxO6. Spectra reported in the figure were recorded before (red line) and after the addition of the reducing agent at 0' (black line), 10' (light blue line), and 3h (green line). (figure 2)

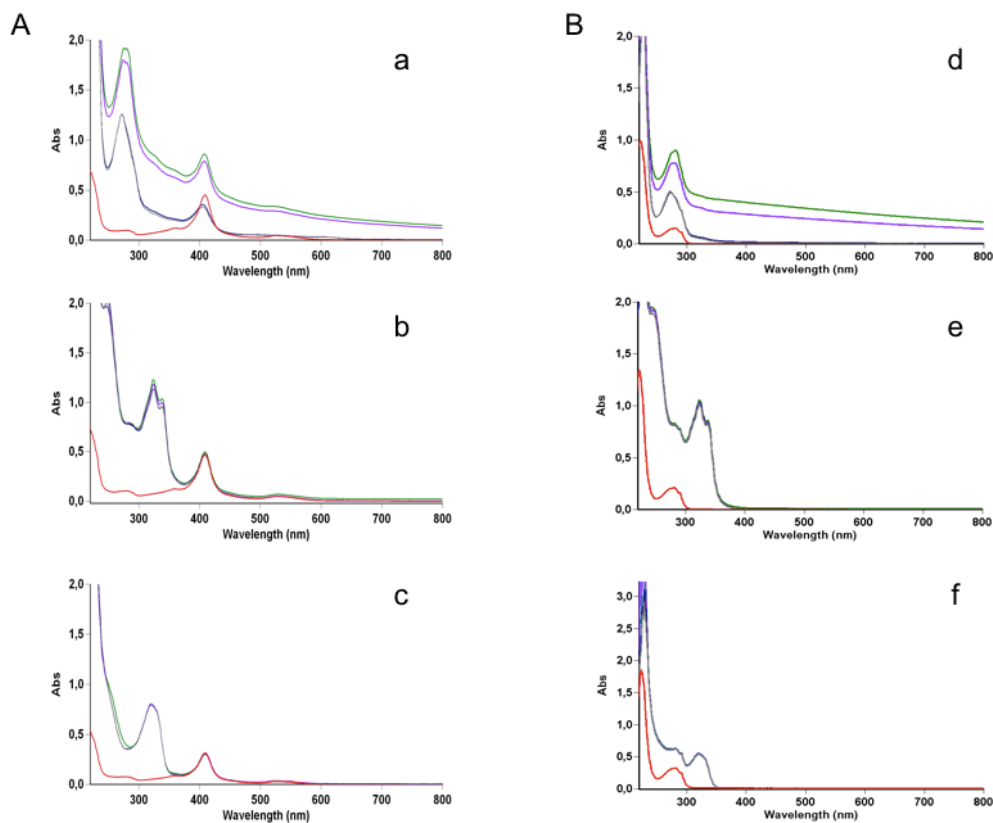
## 2.2 Reactions of gold compounds with model proteins: spectrophotometric analysis

Afterward, the interactions of these gold(III) compounds with the two above mentioned model proteins were explored. Each of the above gold(III) compounds was reacted with cyt c or lysozyme, at a standard metal-to-protein molar ratio of 3:1, according to previously defined experimental procedures and the resulting solutions incubated for 72 hours at 37°C (25 mM tetramethylammonium acetate buffer, TMeAmAc, pH 7.4). Samples were continuously monitored through spectrophotometric analysis. For comparison purposes, similar experiments were carried out using Auranofin as the metalating agent. At the end of the incubation period, samples were analysed by ESI MS as it will be described in the next section.

UV-vis spectrophotometric analysis of metallodrug-protein samples allows the continuous monitoring of the various gold(III) centers in the presence of these model proteins. Remarkably, in the case of cytochrome c (cyt c) -i.e. a metalloprotein characterised by intense transitions in the visible region- it is possible to monitor simultaneously both the metallodrug and the active site of the protein in the course of their interaction.

From spectral inspection, it is apparent that protein addition does not affect importantly the behaviour of the various gold(III) chromophores (figure 3). Yet, modest –but slowly progressive- spectral changes were detected in the case of the reaction of AuOxO6 with cyt c as shown in Figure 2. Some significant changes in the shape of the composite band of Au<sub>2</sub>Phen centered at 280 nm were also detected that are suggestive

of the occurrence of partial gold(III) reduction. Conversely, the spectra of the various metallodrug-cyt c systems reveal that the protein chromophore is substantially stable over 24 hours, with cyt c remaining in its oxidised ferric form.



UV-vis spectra of gold compounds with lysozyme or cytochrome c. Figures on the left side (A) show the spectral features of cytochrome c upon addition of Au<sub>2</sub>Phen (a), Auoxo6 (b) and Aubipyc (c). Figures on the right side (B) show the spectral features of lysozyme upon addition of Au<sub>2</sub>Phen (d) Auoxo6 (e) and Aubipyc (f). All reported spectra were recorded before (red line) and after the addition of the three gold compounds at 0h (green line), 1h (violet line), 12h (blue line) and 24h (grey line). (figure 3)

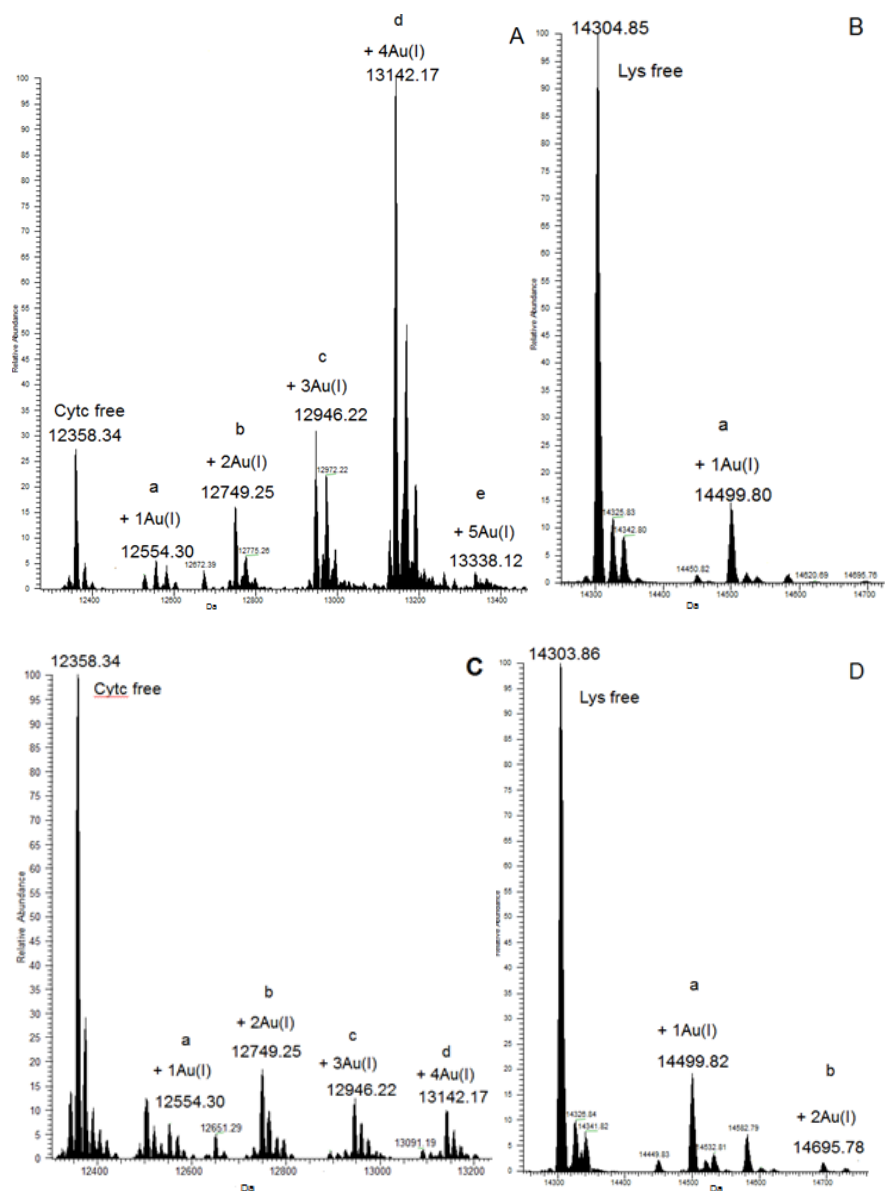
### 2.3 ESI MS spectra of metallodrug-protein samples

ESI MS is a very powerful analytical tool to characterise metallodrug- protein interactions at the molecular level [31,32]. Accordingly, ESI MS analysis of the above described samples allowed us to identify and characterise a number of metal-protein adducts whose presence is hardly documented in the electronic absorption spectra due to the intrinsic limitations of the latter technique. In particular, ESI MS measurements permitted disclosing the nature of protein bound metallic fragments and their binding stoichiometries thus providing indirect mechanistic insight into the respective metalation processes. As a variety of different situations were met in dependence of the nature of the metallodrug and, to a lesser extent, of the protein, the various cases will be illustrated separately, below.

#### 2.3.1 Auoxo6 and Au<sub>2</sub>phen

These two gold complexes are described together as they manifested a rather similar reactivity pattern toward both *lysozyme* and *cyt c*. ESI MS spectra of protein solutions incubated with these two compounds for 72 hours, at a 3:1 metallodrug/protein molar ratio, are comparatively shown in figure 4.

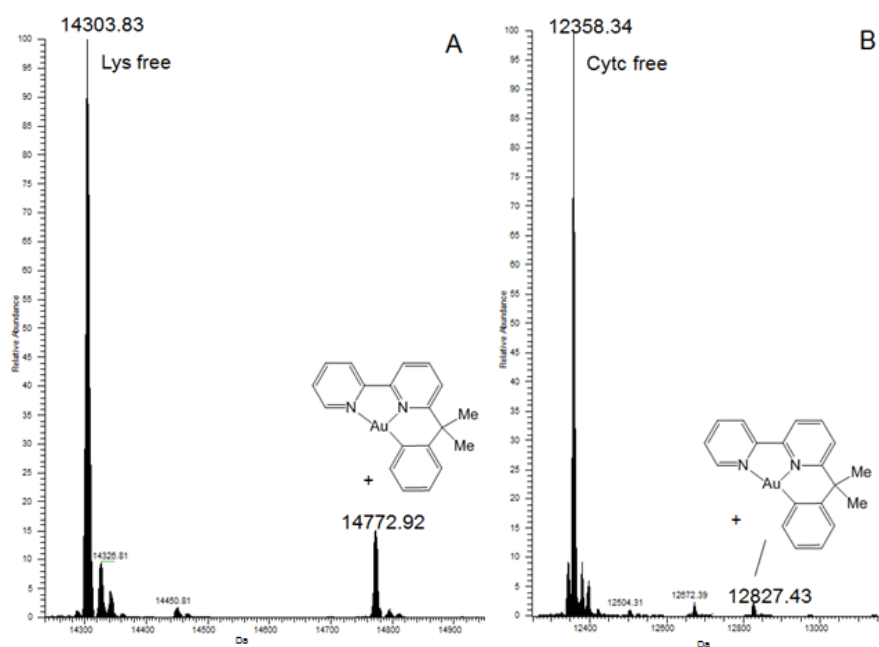
From careful inspection of this figure it is evident that a number of metal-protein adducts are formed in the various cases, though in greatly different amounts, as judged by comparing the relative peak intensities. Remarkably, Au<sub>2</sub>Phen manifests a very high reactivity with *cyt c* which is accompanied by the formation of relatively large amounts of adducts; in the other cases only small amounts of metal-protein adducts are formed. In all cases, the position of the peaks permits to assign these adducts to protein binding of one or more “naked” gold(I) ions; no evidence of “mass shifts” corresponding to the original gold(III) ligands was instead obtained implying that gold(III) reduction and complex disruption always precede protein binding. Very interestingly, *cyt c* favours the formation of a metal protein adduct with a 4:1 stoichiometry (i.e. four gold(I) ions bound to the protein, see the peak with molecular mass of 13142 Da); this observation is in agreement with previous studies on the reaction of *cyt c* with gold saccharinate compounds [20].



LTQ-Orbitrap ESI mass spectra of gold compounds in the presence of the two representative proteins (lysozyme and cytochrome c). Figures on the left side show Au<sub>2</sub>Phen in the presence of cytochrome c (A) or lysozyme (B); figures on the right side show Auoxo6 in the presence of cytochrome c (C) or lysozyme (D). All spectra show the peak of the native protein and of gold(I)-protein adducts, with 1:1 (a), 2:1 (b), 3:1 (c), 4:1 (d) and 5:1 (e) stoichiometry, respectively (figure 4)

## 2.3.2 Aubipyc

When challenged against cyt c and lysozyme, Aubipyc manifested a quite constant behaviour that is different from that of Auoxo6 and Au2phen. Small amounts of metal-protein adducts were formed with both proteins; in both cases the protein bound molecular fragment was the same, corresponding to the [(bipydmb-H)Au] moiety, i.e. the gold(III) center plus the N,N,C, terdentate ligand, as proved by ESI MS analysis (figure 5). The fact that gold, in the Aubipyc-protein adducts, remains in the oxidation state +3 is in agreement with previous results documenting the high redox stability of this organogold(III) compound and its relatively scarce reactivity [25].

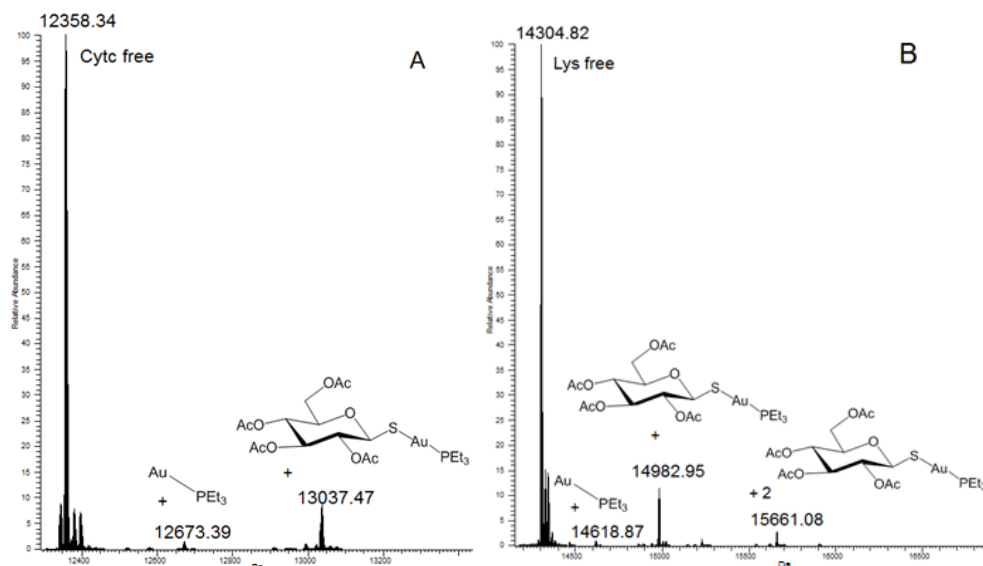


LTQ-Orbitrap ESI mass spectra of *Aubipyc* in the presence of *lysozyme* (A) and *cytochrome c* (B) Both spectra show peaks of the native protein and of [(bipydmb-H)Au] moiety-protein adduct (where bipy<sup>dmb</sup>-H = deprotonated 6-(1,1-dimethylbenzyl)-2,2'-bipyridine ;MW 472.36). (figure 5)

## 2.3.3 Auranofin

The reaction profiles of Auranofin with the two model proteins were also investigated for comparative purposes. ESI MS spectra obtained at 72 hrs for Auranofin-protein adducts are shown in figure 6. ESI MS spectra well document, formation of metallodrug-protein adducts, though in modest amounts. In both cases, the position of

the major peak for metal-protein adducts is consistent with protein binding of the intact Auranofin molecule, probably based on a non-covalent interaction. Quite interestingly, the amount of formed adduct is nearly the same. Also, there is some evidence, in both cases, for the formation of additional adducts where the [(triethyl phosphine) Au(I)] moiety is protein bound.



LTQ-Orbitrap ESI mass spectra of Auranofin in the presence of cytochrome c (A) or lysozyme (B). The two spectra show peaks referred to the native protein (a) and to the formation of [(triethylphosphine)Au(I)] moiety-protein adduct (MW 315)(b), Auranofin-protein adduct respectively with 1:1 (c) and 2:1 stoichiometry (d). (figure 6)

## 2.4 Reactions of gold compounds with model proteins in the presence of reducing agents

Interestingly, the above reported results suggest that gold(III) reduction may play a crucial role in the protein metalation process, especially in the case of Auoxo6 and Au<sub>2</sub>phen. This observation led us to explore the effects of the addition of an excess of “physiological” reducing agents, such as ascorbic acid and glutathione, to the various reaction batches in the assumption that a strongly reducing environment might favour the protein metalation process. Indeed, it is well known that hypoxic cancer tissues exhibit a frankly reducing microenvironment. Studies were restricted to Auoxo6 and Au<sub>2</sub>phen as the gold(III) center in Aubipyc is known to be highly resistant to reduction.

Thus, Auoxo6 and Au<sub>2</sub>phen were dissolved in the buffer, in the presence of either cyt c or lysozyme, at standard 3:1 molar ratios and ascorbic acid or glutathione were added. The concentration of the reducing agent was fixed at 1 mM as this value reflects the typical intracellular concentrations of glutathione. Remarkably, both reducing agents caused quick disappearance of the characteristic LMCT bands of Auoxo6 implying a rapid reduction of the two gold(III) centers while cyt c experienced simultaneous conversion to its reduced form; important spectral changes were also observed for Au<sub>2</sub>phen in line with those previously described for the reduction of Au<sub>2</sub>phen alone in the reference buffer.

The resulting metallodrug-protein samples (Auoxo6 and Au<sub>2</sub>phen reacted with cyt c or lysozyme) were then analysed by ESI MS, after short incubation times. Comparative analysis of the spectra allows stating that addition of ascorbic acid invariably causes formation of far greater amounts of metal-protein adducts. At variance, GSH while accelerating the reduction of the gold(III) centers does not induce greater adduct formation. This fact may be explained by assuming that GSH at high concentrations (1 mM, as it is the case here) is capable of sequestering most gold(I) ions in the form of Au(GSH)<sub>2</sub> complexes.; yet, the presence of small quantities of adducts where gold(I) ions are attached to these two proteins could be demonstrated.

### 3. Discussion

Gold compounds form a new class of promising cytotoxic metallodrugs that are attracting growing attention within the scientific community as potential anticancer agents. The modes of action of cytotoxic gold compounds are still poorly understood. However, a number of observations suggest that cytotoxic gold compounds, at variance with established platinum(II) drugs, are scarcely reactive toward DNA. Accordingly, their biological actions are most probably the result of tight interactions taking place with a number of intracellular protein targets. Inactivation of some crucial proteins might indeed constitute the “decisive event” ultimately triggering apoptotic cell death. In particular, the selenoenzyme thioredoxin reductase seems to be a good candidate protein target for several cytotoxic gold compounds; yet a variety of other protein targets were proposed as well [33,34,35]. Conclusive target validation is still missing. We have analysed –systematically- the interactions of three representative gold(III) compounds with two model proteins- i.e. lysozyme and cyt c - to disclose the molecular details of the inherent metalation processes. Comparative studies have been carried out on Auranofin, a clinically established antiarthritic gold(I) drug. All these gold compounds typically behave as classical prodrugs; upon “chemical activation”, they react with proteins and form stable adducts. Complex activation may simply



consist of a ligand replacement reaction but also of reductive disruption of the gold(III) center and consequent formation of “naked” gold(I) ions.

The metalation processes of the mentioned model proteins were investigated – independently- by absorption spectroscopy and ESI MS methods. Absorption spectroscopy allowed us to monitor continuously the various metallodrug-protein systems over the whole incubation time of 72 hours. Conversely, ESI MS spectra, recorded on metallodrug-protein samples at the end of the incubation period, turned out particularly informative in revealing adduct formation and in determining the final metal to protein stoichiometry and the nature of protein bound metallic fragments. Notably, protein metalation could be documented in most cases, based on the identification of a variety of metal-protein adducts in the ESI MS spectra. The number and the nature of protein bound metallic species was determined. A rough estimate of the amount of protein metalation was achieved by comparing the experimental peak intensities- i.e. the peak of the free protein versus those of its metal adducts. Three main types of metallodrug-protein adducts were identified in our studies. These adducts are formed through one of the following mechanisms: a) gold(III) reduction, complex disruption and coordinative binding of the resulting gold(I) ions to typical protein donors e.g. His, Met or Cys; b) coordinative binding of a redox stable gold(III) fragment to protein donors; c) non coordinative binding of the intact gold complex to the protein. Remarkably, large differences were highlighted in the relative efficiency of the various metalation processes and, accordingly, in the quantities of formed adducts. Differences in protein metalation processes may be very relevant for the actual mechanism of action of gold(III) compounds. Particularly interesting is the case of the reaction of Au<sub>2</sub>phen with cyt c that leads to the formation of large amounts of a tetragold cyt c adduct where four gold(I) ions are tightly associated to the protein. Further studies are under way to better characterise this latter adduct.

Typically, our studies were conducted according to a standard protocol with a long incubation time of 72 hours. However, some additional experiments were carried out on cytochrome c with shorter incubation times (data not shown). Notably, reduction of the incubation time just resulted in a drastic reduction in the amounts of formed adducts with no evident change in the nature of the adducts. Overall, the present investigation stresses the biological and pharmacological relevance of protein metalation processes that seem to play a central role in determining the cellular effects of cytotoxic gold compounds (and more in general of various families of metal based drugs) . It is reasonable to assume that the cytotoxic gold(III) complexes that were selected for the present investigation have the potential of metalating and altering a great number of cellular proteins according to the above described mechanisms; in turn, selective inactivation of some crucial protein (the true targets) may ultimately

cause irreversible cell damage and death. A lot of experimental effort is still needed to elucidate these issues in depth, this being of the major missions of modern metallomics.

The role of reducing agents in the protein metalation processes was also assessed through a few additional experiments. Though it is evident that protein metalation, in two specific cases, requires gold(III) reduction to gold(I), we could establish that the presence of an excess of two distinct biological reducing agents, i.e. glutathione and ascorbic acid, while causing rapid reduction of the gold(III) centers, and also of cyt c, had contrasting effects on the formation of metal-protein adducts. Indeed, ascorbic acid greatly favoured adduct formation in the reactions of Auoxo6 and Au<sub>2</sub>phen with cyt c or lysozyme; in contrast GSH did not sort a similar effect possibly because of extensive gold(I) complexation by GSH itself.

In conclusion, with the present study, we have tried to elucidate at the molecular level the processes of protein metalation that occur when reacting a few representative gold compounds with two model proteins. A variety of situations were encountered depending on the nature of the metal complex and of the protein. Based on the obtained results we can state that the process of adduct formation may follow a number of distinct routes leading to a variety of structurally different adducts. However, prediction of which route will be preferred and what kinds and amounts of metal-protein adducts will be formed for a metallodrug-protein pair remains, at the moment, a very hard task; in fact, the protein metalation processes appear to depend greatly both on the nature of the metal complex and of the protein. We also showed that creating a strongly reducing microenvironment sorted variable effects on the protein metalation processes depending on the nature of the applied reducing agent. It follows that each case of interest is yet to be investigated individually and that specific trends will be hopefully defined only when a far larger mass of experimental data are available .

#### 4. Experimental section

##### *Metal complexes and proteins*

Au<sub>2</sub>phen [21], Auoxo6 [6] and Aubipyc [25] were synthesized and characterised as previously described (see the respective refs). Auranofin was purchased from Vinci-Biochem. Horse heart cytochrome c (C7752) and chicken hen egg white lysozyme (L7651) were purchased from Sigma and used as received.

##### *Physico chemical measurements.*

UV/vis spectra were recorded on a Varian Cary 50 UV-vis spectrophotometer. Mass spectra were recorded in an LTQ-Orbitrap high-resolution mass spectrometer (Thermo, San Jose, CA, USA), equipped with a conventional ESI source.

### *UV-visible spectrophotometric studies*

The electronic spectra were recorded diluting small amounts of freshly prepared concentrated solutions of the individual complexes in DMSO (or EtOH/H<sub>2</sub>O for Auranofin) in the reference buffer (10 mM phosphate, pH 7.4). The concentration of each gold compound in the final sample was 30 μM. The resulting solutions were monitored collecting the electronic spectra over 24 h at room temperature.

### *Interactions with Proteins*

Electronic spectra of the model protein (lysozyme or cytochrome c) at 10 μM were recorded before and after the addition of each gold complexes at a stoichiometric ratio of 3:1 (metal-to-protein) over 24 h at room temperature, in 10 mM phosphate buffer, pH 7.4. Similar spectrophotometric studies were carried out in the presence of reducing agents i.e. glutathione (GSH) or ascorbic acid, added to the various reaction batches to a final concentration of 1 mM.

### *Sample preparation and mass spectrometric analysis*

Metal complex/protein adducts were prepared by mixing equivalent amounts of the three proteins (100 μM) in 25 mM tetramethylammonium acetate buffer (TMeAmAc), pH 7.4. Then the three gold(III) complexes and Auranofin were added (3:1 metal/protein ratio) to the solution and incubated at 37°C for 72h. After a 20-fold dilution with water, ESI-MS spectra were recorded by direct introduction at 5 μl/min flow rate in an Orbitrap high-resolution mass spectrometer (Thermo, San Jose, CA, USA), equipped with a conventional ESI source. The working conditions were the following: spray voltage 3.1 kV, capillary voltage 45 V and capillary temperature 220°C. The sheath and the auxiliary gases were set, respectively, at 17 (arbitrary units) and 1 (arbitrary units). For acquisition, Xcalibur 2.0. software (Thermo) was used and monoisotopic and average deconvoluted masses were obtained by using the integrated Xtract tool. For spectrum acquisition a nominal resolution (at m/z 400) of 100,000 was

### References

- [1] S. Nobili, E. Mini, I. Landini, C. Gabbiani, A. Casini, L. Messori, *Med. Res. Rev.*, 2010, 30, 550–580.
- [2] C. Gabbiani, A. Casini, L. Messori, *Gold Bull.*, 2007, 40, 73–81.
- [3] E.R.T. Tiekink, *Crit. Rev. Oncol. Hematol.*, 2002, 42, 225–248.
- [4] E. Vergara, A. Casini, F. Sorrentino, O. Zava, E. Cerrada, M.P. Rigobello, A. Bindoli, M. Laguna, P.J. Dyson, *Chem.Med.Chem.*, 2010, 5, 96–102.
- [5] M.J. McKeage, L. Maharaj, S.J. Berners-Price, *Coord. Chem. Rev.*, 2002, 232, 127–135.
- [6] A. Casini, M.A. Cinellu, G. Minghetti, C. Gabbiani, M. Coronello, E. Mini, L. Messori, *J. Med. Chem.*, 2006, 49, 5524–5531.
- [7] C.M. Che, R.W.-Y. Sun, W.Y. Yu, C.B. Ko, N.Y. Zhu, H.Z. Sun, *Chem. Commun.*, 2003 1718–1719.
- [8] V. Milacic, D. Chen, L. Ronconi, K.R. Landis-Piwowar, D. Fregona, Q.P. Dou., *Cancer Res.*, 2006, 66, 10478–10486.
- [9] C. Gabbiani, L. Messori, *Anti-Cancer Ag. Med. Chem.*, 2011, 11, 929-939.
- [10] C.K. Mirabelli, C.M. Sung, J.P. Zimmerman, D.T. Hill, S. Mong, S.T. Crooke. *Biochem. Pharmacol.*, 1986, 35, 1427–1433.
- [11] A. Bindoli, M.P. Rigobello, G. Scutari, C. Gabbiani, A. Casini, L. Messori, *Coord. Chem. Rev.*, 2009, 253, 1692–1707.
- [12] R. Rubbiani, I. Kitanovic, H. Alborzina, S. Can, A. Kitanovic, L.A. Onambele, M. Stefanopoulou, Y. Geldmacher, W.S. Sheldrick, G. Wolber, A. Prokop, S. Wöfl, I. Ott, *J. Med. Chem.*, 2010, 53, 8608-18.
- [13] J.L. Hickey, R.A. Ruhayel, P.J. Barnard, M.V. Baker, S.J. Berners-Price, A. Filipovska, *J. Am. Chem. Soc.*, 2008, 130, 12570-1
- [14] J.R. Roberts, J. Xiao, B. Schliesman, D.J. Parsons, C.F. Shaw III, *Inorg. Chem.*, 1996, 35, 424-433.
- [15] J. Christodoulou, P.J. Sadler, A. Tucker, *Eur. J. Biochem.*, 1994, 225, 363-368.
- [16] J. Zou, P. Taylor, J. Dornan, S.P. Robinson, M.D. Walkinshaw, P.J. Sadler, *Angew. Chem. Int.*, 2000, 39, 2931-2934.
- [17] J. Talib, J.L. Beck, S.F. Ralph, *J. Biol. Inorg. Chem.*, 2006, 11, 559-570.

- [18] G. Marcon, L. Messori, P. Orioli, M.A. Cinellu, G. Minghetti, *Eur. J. Biochem.*, 2003, 270, 4655-4661.
- [19] L. Messori, A. Balerna, I. Ascone, C. Castellano, C. Gabbiani, A. Casini, C. Marchioni, G. Jaouen, A. Congiu Castellano, *J. Biol. Inorg. Chem.*, 2011, 16, 491-499.
- [20] L. Maiore, M.A. Cinellu, E. Michelucci, G. Moneti, S. Nobili, I. Landini, E. Mini, A. Guerri, C. Gabbiani, L. Messori, *J. Inorg. Biochem.*, 2011, 105, 348-355.
- [21] C. Gabbiani, A. Casini, G. Kelter, F. Cocco, M.A. Cinellu, H.H. Fiebig, L. Messori, *Metallomics*, 2011, 3, 1318-1323.
- [22] M.A. Cinellu, L. Maiore, M. Manassero, A. Casini, M. Arca, H.H. Fiebig, G. Kelter, E. Michelucci, G. Pieraccini, C. Gabbiani, L. Messori, *ACS Med. Chem. Lett.*, 2010, 1, 336-339.
- [23] C. Gabbiani, A. Casini, L. Messori, A. Guerri, M.A. Cinellu, G. Minghetti, M. Corsini, C. Rosani, P. Zanello, M. Arca, *Inorg. Chem.*, 2008, 47, 2368-2379.
- [24] M. A. Cinellu, G. Minghetti, M. V. Pinna, S. Stoccoro, A. Zucca, M. Manassero, M. Sansoni, *J. Chem. Soc., Dalton Trans.*, 1998, 1735-1741.
- [25] G. Marcon, S. Carotti, M. Coronello, L. Messori, E. Mini, P. Orioli, T. Mazzei, M.A. Cinellu, G. Minghetti, *J. Med. Chem.*, 2002, 45, 1672-1677
- [26] A. Casini, G. Kelter, C. Gabbiani, M.A. Cinellu, G. Minghetti, D.s Fregona, H.H. Fiebig, L. Messori, *J. Biol. Inorg. Chem.*, 2009, 14, 1139-1149.
- [27] <http://www.oncotest.de/>
- [28] K.D. Paull, R.H. Shoemaker, L. Hodes, A. Monks, D.A. Scudiero, L. Rubinstein, J. Plowman, M.R. Boyd, *J. Natl. Cancer*, 1989, 81, 1088-1092
- [29] R.L. Huang, A. Wallqvist, D.G. Covell, *Biochem. Pharmacol.*, 2005, 69, 1009-1039
- [30] V. Milacic, D. Chen, L. Ronconi, K.R. Landis-Piwowar, D. Fregona, Q.P. Dou, *Cancer Res.*, 200, 66, 10478-10486.
- [31] A.R. Timerbaev, K. Pawlak, C. Gabbiani, L. Messori, *Trends Anal. Chem.*, 2011, 30, 1120-1138.
- [32] A. Casini, A. Guerri, C. Gabbiani, Luigi Messori, *J. Inorg. Biochem.*, 2008, 102, 995-1006.
- [33] E.S. Arnér, A. Holmgren, *Semin. Cancer. Biol.*, 2006, 6, 420-426.

## Chapter 2

- [34] P. Nguyen, R.T. Awwad, D.D. Smart , D.R. Spitz, D. Gius., *Cancer Lett.*, 2006, 236, 164–174.
- [35] E. Vergara , A. Casini, F. Sorrentino, O. Zava, E. Cerrada, M.P. Rigobello , A. Bindoli, Laguna,P.J. Dyson, *Chem.Med.Chem.*,2010, 5(1), 96-102

## SECTION B: Gold(I) Compounds

## 1. Introduction

Following the introduction of auranofin in the clinics for the oral treatment of rheumatoid arthritis (1985) and the discovery of its remarkable antiproliferative properties in vitro, gold compounds were increasingly considered as a possible source of new and more effective metal-based anticancer agents.[1] This interest was also fuelled by the observation that gold compounds usually manifest a very different pharmacological profile compared to established anticancer platinum drugs implying the occurrence of original and innovative modes of action. Hence, over the last two decades, several promising families of Au-based drug candidates, with the gold centre in the oxidation states +3 or +1, featuring diverse structural motifs, were prepared and characterised and their biological and pharmacological profiles were initially assessed.[1] Relevant examples are offered by a few classical mononuclear gold(III) complexes,[2] such as gold(III) dithiocarbamates[3] and gold(III) porphyrins;[4] by some organogold(III) compounds;[5] a few binuclear gold(III) complexes;[6] various neutral, two-coordinate gold(I) complexes, inspired to auranofin;[7] lipophilic cationic gold(I) complexes such as  $[\text{Au}(\text{dppe})_2]^+$ , and others.[8]

N-Heterocyclic carbenes (NHC's) are very interesting gold(I) ligands as they manifest donor properties similar to phosphines thus affording very stable gold(I) complexes; in addition, their imidazolium salt precursors are often more easily synthesized than similarly-functionalized phosphines.[9] The azoles and azolium salts used in the synthesis of N-heterocyclic carbenes are generally air stable species and their synthesis and purification is, in most cases, relatively straightforward. Hydrophilic/lipophilic properties can be readily fine-tuned by the incorporation of appropriate functional groups.[9c] Within this frame, a number of gold carbene complexes were prepared and characterised during the last few years that turned out to be particularly effective and promising from the biological and pharmacological points of view. Accordingly, a number of reports concerning cytotoxic gold(I/III) NHC complexes have been published with many derivatives showing highly promising antiproliferative activity with IC<sub>50</sub> values in the micromolar or even nanomolar range.[9,10]

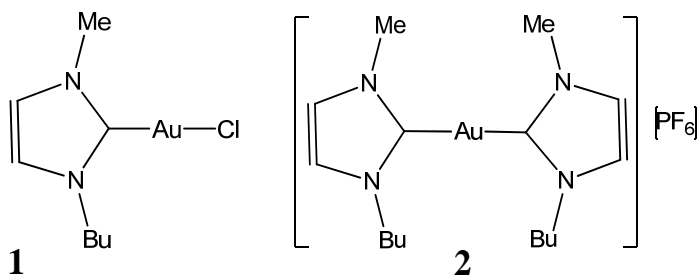
In 2004 Barnard et al. documented the induction of "mitochondrial permeability transition" by various dinuclear gold(I) NHC complexes.[11] The interference of gold(I) NHC complexes with mitochondrial biochemistry is a feature of particular interest that was further proved in subsequent studies. Baker et al. successfully synthesized a series of NHC gold(I) analogues of auranofin and reported on their biological activity.[12] More recently, Rubbiani et al. described a series of three

structurally related Au(I) complexes with benzimidazole derived NHC ligands that exerted selective inhibition of TrxR and significant antiproliferative effects.[13] Based on the reported findings, gold carbene complexes are now mainly considered as a class of antimetastatic agents.[1b,9c,10a,14]

Even though several studies have been carried out so far on the cellular effects of gold carbene compounds and valuable mechanistic information gathered, their precise mode of action, at the molecular level, is still unclear.

This led us to prepare and characterise two novel gold carbene complexes and to investigate in depth their main chemical and biological features through a variety of physicochemical and biochemical tests. The gold carbene complexes that were designed and prepared for the present investigation are schematically represented in figure 1.

They feature, respectively, a monocarbene gold(I) complex **1** and a dicarbene gold(I) complex **2** having the same carbene ligand. In both cases 1-butyl-3-methyl-imidazole-2-ylidene was chosen as the NHC ligand in order to obtain gold complexes showing high lipophilicity, in line with previous studies[9c]. Indeed, it is well documented that selectivity for cancer cells over normal cells can be ‘tuned’ by adjusting the hydrophilic/lipophilic balance in a series of related Au(I).[15]. In complex 1 the second gold ligand is a chloride ion that, in principle, is believed to act as a more labile ligand. The antiproliferative properties in vitro of these gold compounds were assessed toward the human ovarian carcinoma cell line A2780 either sensitive or resistant to cisplatin. Then, their reactivity with a few model proteins was explored as it is commonly believed that gold(I) compounds exert their biological actions mainly through interactions with protein targets.



Structures of the NHC Au(I) complexes synthesized in this study: **1** chloro(1-butyl-3-methylimidazol-2-ylidene)gold(I), **2** bis(1-butyl-3-methylimidazole-2-ylidene)gold(I) hexafluorophosphate. (figure 1)

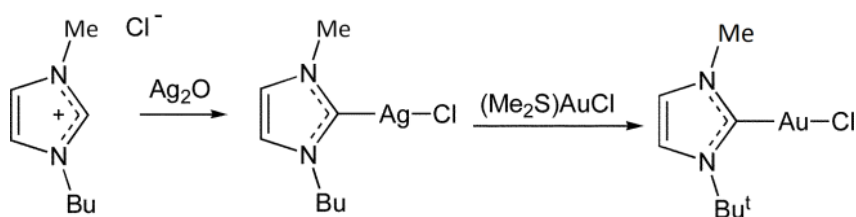


## 2. Results

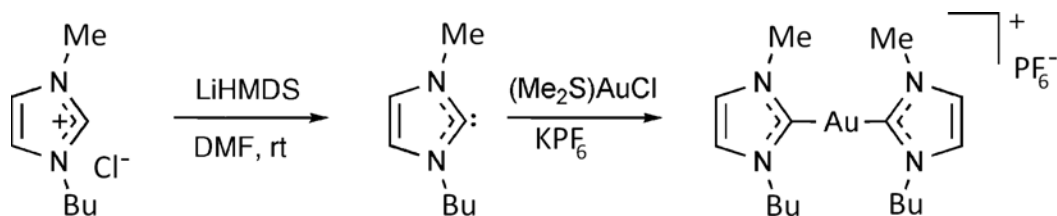
### 2.1 Synthesis and structural characterisation.

The gold(I) carbene complexes **1** and **2**, were prepared adapting the procedure developed by Baker and Berners-Price.[9c,16] The synthesis of complex **1** was achieved via the known route of transmetalation of the corresponding Ag(I) NHC complexes with [(Me<sub>2</sub>S)AuCl] (Scheme 1a). Complex **2** was synthesized by the reaction of [(Me<sub>2</sub>S)AuCl] with two equivalents of 1-butyl-3-methyl-imidazole-2-ylidene, prepared in situ by deprotonation of the imidazolium salt with lithium bis(trimethylsilyl)amide (lithium hexamethyldisilazide, LiHMDS) in DMF at room temperature (Scheme 1b).

(a)



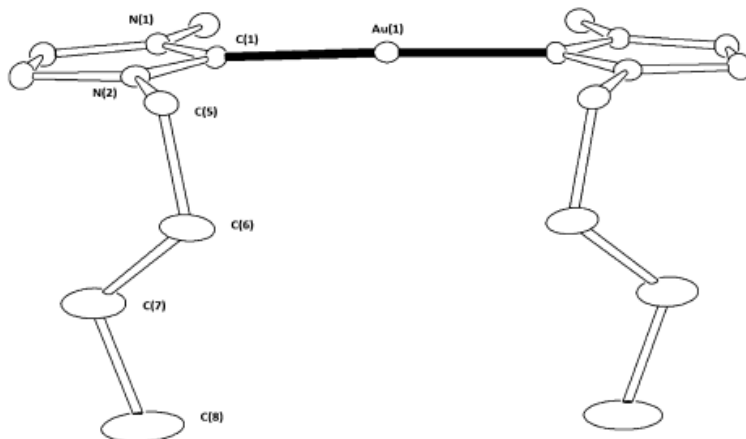
(b)



(a) synthesis of compound **1**; (b) synthesis of compound **2**. (scheme 1)

Complexes **1** and **2** were obtained in good yields as colourless solids, which are soluble in halogenated solvents, acetone, and dimethyl sulfoxide (DMSO). Complex **1** is soluble even in non-polar solvents as benzene, ether, hexane, etc. The new compounds were characterized in the solid state by elemental analysis and IR spectroscopy and then in solution by <sup>1</sup>H and <sup>13</sup>C NMR spectroscopy.

The solid-state structure for compound **2** was determined by single-crystal X-ray diffraction. The ORTEP view of compound **2** is shown in figure 1, and crystallographic data are reported in Table 1. Compound **2** gave pale yellow crystals, which hold half of the complex and half of the  $\text{PF}_6^-$  counterion in the asymmetric unit.



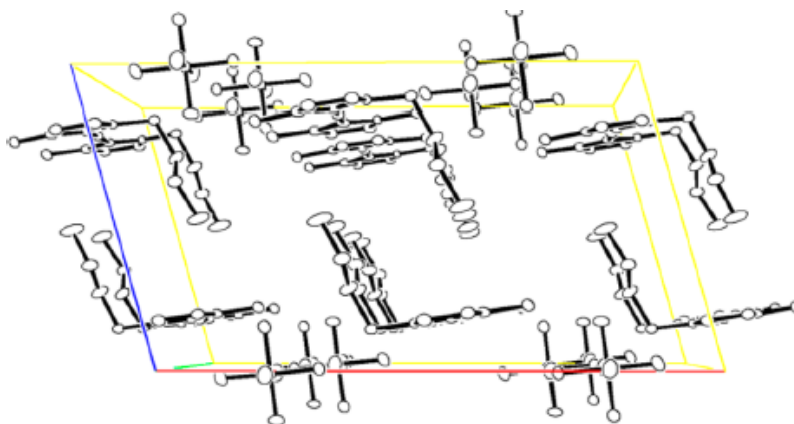
Molecular structures of **2** (figure1).

In both compounds, the NHC moiety is bound to the gold(I) center through the C atom. This gold(I) center displays the usual linear coordination with very modest distortions: in **2** the  $\text{C}(1)\text{-Au}(1)\text{-C}(1')$  angle is  $178.0(4)^\circ$  ( $'$  is reported by the symmetry operation  $x, -y, z$ ). The bond length  $\text{C}(1)\text{-Au}(1)$  is  $2.02(1) \text{ \AA}$ , and it is in the range found for similar compounds in a search performed in the Cambridge Structural Database (CSD)(v. 5.33 November 2011) [17]. Differences in  $\text{Au-C}$  bond lengths might imply some differences in the bond strength in the two cases (for **1** the bond length is  $1.94(2) \text{ \AA}$ ) as previously observed by Ott et al. when working on a similar series of gold(I) complexes [14a]. Also, the  $\text{Au}(1)\text{-Cl}(1)$  bond length is typical for these compounds ( $2.281(4) \text{ \AA}$ ) as previously reported [18] The aliphatic chain in the complex has the same dihedral conformation (see Table 2): the sequence of the dihedral angles being synclinal (sc) and antiperiplanar (ap).

complex	<b>2</b>
empirical formula	$C_8H_{14}Au_{0.50}F_3N_2O_{0.75}P_{0.50}$
formula weight	321.18
temperature (K)	120(2)
wavelength (Å)	wavelength (Å)
crystal system, space group	monoclinic, $C2/m$
unit cell dimensions (Å,deg)	$a = 18.3243(11)$ $b = 13.0863(8)$ $\beta = 105.088(5)$ $c = 10.6892(5)$
volume (Å <sup>3</sup> )	2474.9(2)
$Z$ , $D_c$ (mg/cm <sup>3</sup> )	8, 1.724
$\mu$ (mm <sup>-1</sup> )	6.069
$F(000)$	1248
crystal size (mm)	$0.2 \times 0.1 \times 0.05$
$\theta$ range (deg)	1.936 to 25.0
reflections collected	6738
data/restraints/parameters	3035/0/150
goodness-of-fit on $F^2$	1.047
final $R$ indices [ $I > 2\sigma(I)$ ]	$R1 = 0.0562$ , $wR2 = 0.1198$
$R$ indices (all data)	$R1 = 0.0800$ , $wR2 = 0.1480$

Crystallographic data for complex **2**. (table1)

Remarkably, in the crystal packing of **2** (figure 2), it is possible to detect a relatively strong aurophilic interaction  $Au \cdots Au$  3.5560(5) Å giving rise to dimers of the complex in the lattice. Moreover the crystal packing reveals a channel between the discrete molecule in which water molecules are located. The occupancy factors of these molecules are all set to 0.5, and this ribbon of water runs along the  $a$  axis.



Views of the packing in crystal of **2** (figure 2).

## 2.2 Solution chemistry

The solution chemistry of **1** and **2** was investigated through UV-Vis spectrophotometry and  $^1\text{H}$  NMR, under physiologically relevant conditions.

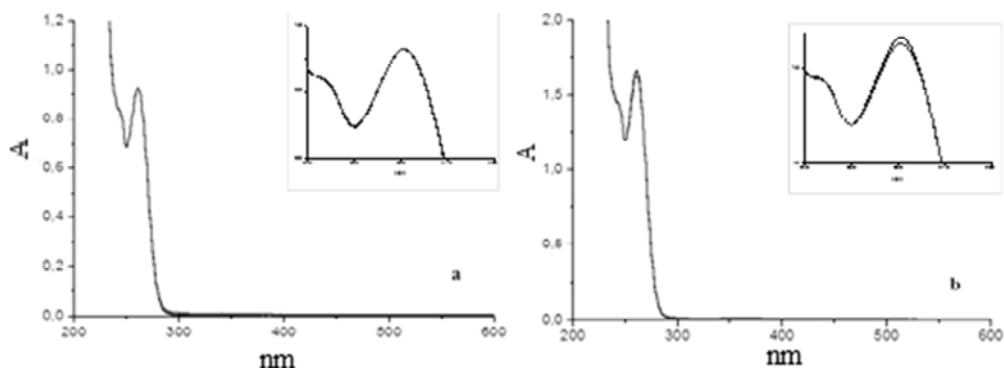
The UV-Visible spectra of the above complexes and, for comparison, of 1-butyl-3-methylimidazolium chloride, were recorded in 50 mM phosphate buffer, pH 7.4. All compounds are soluble in DMSO but poorly soluble in water. Thus, in line with previous studies, the compounds were first dissolved in DMSO and the resulting solutions were diluted with a reference aqueous buffer (50 mM phosphate buffer, pH 7.4). The percentage of DMSO in the final aqueous solution is 1%. No precipitation was apparent at dilution, using the described experimental procedure. Solutions were examined spectrophotometrically over 24 h; the resulting spectral profiles are shown in figure 3. Notably, the two compounds are soluble and stable within this medium, with full retention of their original structure. The spectra of the complexes showed absorbance maxima at ca. 250–260 nm, characteristic of the gold(I) chromophore, that may straightforwardly be assigned as metalto- ligand charge-transfer (MLCT) bands.

As gold(I) has a  $d^{10}$  configuration, ligand-to-metal charge-transfer (LMCT) transitions and ligand-field (LF) transitions are absent.[19] Since the imidazolium salt ( $\lambda_{\text{max}} = 210$  nm) does not show the transitions at ca. 250 and 260 nm, the bands were assigned to MLCT transitions.

Furthermore, the stability of the two compounds toward biologically occurring reductants was evaluated. Ascorbic acid (AsA) and Glutathione (GSH) were chosen as reference reducing agents. Interestingly, we observed that addition of even large molar excesses of the two reductants (up to 100 : 1 molar ratios) did not elicit any major spectral change thus ruling out occurrence of gold(I) reduction; also, no evidence was obtained for GSH coordination to the gold(I) center.

$^1\text{H}$  and  $^{13}\text{C}$  NMR spectra for **1** and **2** showed the signals commonly expected for this kind of complexes. For complex **2** all signals are sharp (until  $-50^\circ\text{C}$ ) as it is usual for a structure where free rotation about the  $\text{Au}-\text{C}_{(\text{carbene})}$  bond occurs. As the formation of the gold(I) complexes proceeded through deprotonation of the (NCHN) proton of the imidazolium chloride salt, the  $^1\text{H}$  NMR spectra lack the characteristic NCHN resonance in the downfield region of the spectrum. The  $^{13}\text{C}$  NMR spectrum, however, showed the appearance of the metal bound carbene signal significantly downfield shifted in comparison to that of the corresponding imidazolium NCN carbon.

Both complexes turned out to be very stable in solution over 24 h observation; no appreciable release of the chloride group is noticed in the case of complex **1**. In addition, both compounds are highly resistant toward GSH and ascorbic acid treatment.



Hydrolysis profiles of complexes **1** (a) and **2** (b) dissolved in phosphate buffer 50 mM pH 7.4. Spectra were recorded over 24 h at room temperature. Black line,  $t = 0$ ; red line,  $t = 24$  h. Inset: zoom of the main peak (figure 3)

### 2.3 Cellular studies/antiproliferative properties

Afterward, the antiproliferative properties of **1** and **2** were measured *in vitro* against the A2780 ovarian carcinoma human cell line sensitive to cisplatin (A2780/S) and its resistant subline (A2780/R) as reported in the Experimental Section. The  $IC_{50}$  values observed after 72 h exposure are reported in Table 3. These compounds show relevant antiproliferative effects with  $IC_{50}$  values falling in the low micromolar range for both A2780/S (from 1.68 to 1.98  $\mu\text{M}$ ) and A2780/R cells (from 0.68 to 0.75  $\mu\text{M}$ ).

This finding differs from the cytotoxicity results of Schuh *et al.*, [18] who suggest that the chloro-substituted NHC Au(I) complexes are expected to be less active since the chloride group may make the chloride derivatives more reactive and thus more prone to be deactivated by different cellular components.

Compound **2** was more active than cisplatin even in the A2780/S cell line. Interestingly, these two gold carbene complexes were more active toward cisplatin resistant cell line compared to the sensitive one (resistance index (RI) value ranging from 0.4 to 0.5) implying that the molecular mechanism of resistance to cisplatin are ineffective toward them. Additional experiments were carried out to assess at least qualitatively the time dependence of gold-induced cytotoxic effects. This led us to measure the cell growth inhibition values of the two gold compounds at 24 hours, on both A2780/S and A2780/R cell lines. Far higher  $IC_{50}$  values were determined. Indeed,  $IC_{50}$  values at 24 h for **1** were 31.10  $\mu\text{M}$  and 53.68  $\mu\text{M}$  in A2780/S and A2780/R respectively; those of **2** were 18.83  $\mu\text{M}$  and 42.55  $\mu\text{M}$  in A2780/S and A2780/R respectively, to be compared to  $\sim 1$   $\mu\text{M}$  values measured at 72 h.

Compounds	A2780/S IC50 ( $\mu\text{M}$ )	A2780/R IC50 ( $\mu\text{M}$ ) R	R <sup>a</sup>
1	1.98 $\pm$ 0.17	0.68 $\pm$ 0.07	0.3
n <sup>b</sup>	4	4	
2	1.68 $\pm$ 0.24	0.75 $\pm$ 0.05	0.4
n	4	4	
CDDP	1.84 $\pm$ 0.12	23.24 $\pm$ 0.75	12.6
n	6	6	

R<sup>a</sup>, resistance ratio. n<sup>b</sup>, number of determination

*In vitro* growth inhibition of the A2780 cisplatin sensitive or resistant cell lines by **1** and **2** after a 72 h drug exposure. (table 3)

These results imply that the antiproliferative effects induced by these gold carbenes require relatively long times to show up, being mediated-most likely-through a specific and relatively slow cellular response. A similar situation holds for cisplatin: indeed IC50 values of cisplatin at 24 h were 32.24  $\mu\text{M}$  and  $>100 \mu\text{M}$  in in A2780/S and A2780/R, respectively. The available literature shows that NHC gold carbines usually display a relevant cytotoxic activity. However, only the results of the study performed by Schuh *et al.*[18] are directly comparable with ours (same cell lines and same drug exposures). Results of Schuh show that their compounds have a slightly lower activity after a 72 h exposure (from 2.6 to 3.9  $\mu\text{M}$  in A2780/S; from 1.6 to 6.8  $\mu\text{M}$  in A2780/R) compared to our compounds, but higher activity after 24 h of drug exposure (from 3.2 to 11.5  $\mu\text{M}$  in A2780/S; from 4.9 to 12.7  $\mu\text{M}$  in A2780/R). Several other studies investigated the cytotoxic activity of NHC gold(I) carbenes but in tumor cell lines other than A2780[13,14,20] Although most compounds included in these studies reached activities in the low micromolar range, only some of those reported by Rubbiani *et al.*[14] showed IC50  $< 1 \mu\text{M}$ . Overall, our findings render both compounds well suitable for *in vivo* studies aimed at assessing their safety and anticancer activity in cisplatin-resistant animal models.

#### 2.4 Reactions with Cytochrome c and Lysozyme

To gain a deeper insight into the specific reactivity of these NHC Au(I) complexes with their potential biomolecular targets, compounds **1** and **2** were first reacted with hen egg white lysozyme (HEWL) and horse heart cyt c (cyt c), that are often used as model proteins [21] Reactions were monitored through ESI mass spectrometry (ESI-MS) and UV-Visible spectrophotometry in accordance with protocols previously established in our laboratory[22]. Deconvoluted ESI-MS spectra of HEWL and cyt c samples reacted with compounds **1** and **2** were recorded, after 72 h incubation, at 37  $^{\circ}\text{C}$ . No evidence of protein metalation was gained in all cases. Even addition of an

excess of the reducing agent dithiothreitol (DTT) to the solution did not lead to formation of protein adducts. The same reaction mixture (protein plus metallodrug), observed by UV-Visible spectrophotometry, leads to the same result: the spectrum remains unchanged throughout the whole incubation time.

### 3. Discussion

There is currently a great interest in the development of new gold-based compounds as cytotoxic agents and prospective antitumor drug candidates. Indeed, gold compounds appear very promising for this purpose as they usually exhibit outstanding antiproliferative properties *in vitro* while manifesting chemical and biological properties highly distinct from those of clinically established platinum drugs. This implies that they do exert their remarkable cytotoxic effects through innovative mechanisms of action. Accordingly, they typically exhibit a different spectrum of anticancer activities compared to platinum drugs and also overcome acquired resistance to platinum agents.[1] Various classes of potent cytotoxic gold compounds were identified in recent times including gold(III) porphyrins, gold(III) dithiocarbamates, gold(III) bipyridine complexes, gold(I) phosphine and gold(I) carbenes. For some of them very encouraging results were also obtained in various animal models of cancer.[25]

Gold carbene complexes appear particularly attractive as carbenes are tightly bonded ligands for soft metals and are not easily removed from gold(I) coordination; also, for a few gold(I) carbene complexes, a substantial body of evidences has been gathered at the cellular level showing that they are potent antiproliferative agents causing cell death most probably through direct mitochondrial damage.[1b,9c,10a,14]

Based on these arguments, we have designed, synthesised and characterised two novel, structurally-related gold(I) carbene compounds and analysed their biological behaviour. Specifically, a mono-carbene and a di-carbene gold(I) complex were prepared and structurally characterised using 1-butyl-3-methyl-imidazole-2-ylidene as the invariant NHC ligand. In the mono-carbene complex (1) a chloride ion acts as the second ligand. Afterwards, some key aspects of their solution chemistry, and their reactivity with biomolecules and of their cellular actions were comparatively explored and elucidated.

*Chemical aspects: structural and solution chemistry.*

The solid state chemistry of these two novel compounds was examined in depth as their respective crystal structures could be solved to high resolution. The two compounds show a nearly linear geometry around the di-coordinated gold(I) center. They just differ -modestly- in the length of the carbon-gold bonds being 1.94 Å for

compound **1** and 2.03 Å for compound **2** respectively. Reasonably, this might imply some differences in the strength of the carbon gold bond in the two cases as previously observed by Ott et al. when working on a similar series of gold(I) complexes [14a].

Notably, both gold carbenes investigated here manifest a rather modest but still acceptable solubility in water. Freshly prepared solutions of the two gold(I) carbenes were thus prepared and monitored over long observation periods to highlight the possible release of the chloride ligand. Contrary to expectations, both complexes resulted very stable and no spectral changes were noticed over 24 h observation at room temperature. In particular, no appreciable release of the chloride group was detected in the case of complex **1**. Both compounds turned out to be very resistant even toward reduction: indeed, neither GSH nor ascorbic acid were effective in causing gold(I) reduction.

#### *Antiproliferative properties in vitro.*

The antiproliferative effects of the two study compounds were specifically investigated toward human ovarian carcinoma A2780 cells either sensitive or resistant to cisplatin. Both compounds turned out to cause marked cancer cell growth inhibition at 72 hours with similar IC<sub>50</sub> values (around 1 μM in both cases) qualifying them as potent antiproliferative agents. Remarkably, no cross resistance with cisplatin was highlighted implying that the molecular mechanisms that counteract platinum related cell damage are ineffective toward cellular insults produced by these gold species. This interesting observation renders both compounds suitable for in vivo studies to investigate their safety and anticancer activity in cisplatin resistant animal models.

We also evaluated the antiproliferative effects of complexes **1** and **2** after a shorter exposition time (24 hours). Far greater IC<sub>50</sub> values were measured in the latter case implying that the antiproliferative effects of complexes **1** and **2** require relatively long time periods to manifest fully; it is straightforward to assign such a behaviour to the occurrence of relatively slow cellular responses to the chemical insult ultimately leading to apoptotic cancer cell death. Also, a weak cross-resistance was observed for both compounds after 24 hours incubation (R ranging from 1.8 and 2.5), although lower compared to that of cisplatin (R=4.2).

*Mechanistic aspects- reactions with proteins.* It is believed that the cytotoxic effects of gold compounds are mainly mediated by a few protein targets rather than by direct interactions with genomic DNA as it is the case for cisplatin.[1b] This is particularly true for gold(I) complexes due to the fact that the gold(I) center typically exhibits a poor affinity for DNA nucleobases. This led us to explore the reactions of the study gold compounds with some model proteins that might simulate real protein targets. In



particular, we have tested their interactions at first with the model proteins cytochrome c and lysozyme.

In conclusion, with the present study, we have designed, prepared and characterised two novel gold carbene complexes as anticancer drug candidates. The two novel gold complexes were exhaustively described from the structural point of view owing to obtainment of their respective crystal structures. Further, their behaviour in solution was elucidated. Both compounds show a high stability in physiological-like media with no evidence of NHC or chloride detachment even over long observation periods. Notably, both complexes manifested similar and very pronounced antiproliferative effects toward the reference cancer cell line A2780; interestingly, cisplatin resistance was fully overcome. As gold carbene compounds are believed to act on a few protein targets rather than on DNA, the reactivity of the present gold carbenes with two selected proteins was explored, mainly through ESI-MS analysis.

#### 4. Experimental sections

##### *Materials.*

Horse heart cytochrome c (C7752) and chicken hen egg white lysozyme (L7651) were purchased from Sigma and used as received. *Atox-1* – full length HAH1 (G09HA101) – was purchased from Giotto Biotech. RPMI 1640 cell culture medium, fetal calf serum (FCS) and phosphate-buffered saline (PBS) were obtained from Celbio (Milan, Italy); DMSO, sulforhodamine B (SRB) and cisplatin (purity >99.9%) were obtained from Sigma (Milan, Italy).

##### *Instruments*

Elemental analyses were performed by a Carlo Erba elemental analyzer model 1106. Infrared (IR) spectra were recorded with a Perkin-Elmer FT-IR spectrometer equipped with a universal attenuated total reflectance (UATR) sampling accessory. NMR spectra were recorded on a Varian Gemini 200 BB instrument ( $^1\text{H}$ , 200 MHz;  $^{13}\text{C}$ , 50.3 MHz) at room temperature; frequencies are referenced to the residual resonances of the deuterated solvent. UV–visible (UV-vis) spectra were recorded on a Varian Cary 50 spectrophotometer. Electrospray ionization mass spectrometry (ESI-MS) measurements were performed on a linear trap quadrupole (LTQ) linear ion trap

(Thermo, San Jose, CA) equipped with a conventional ESI source. Data collection for the sample was carried out on an Oxford Diffraction XCalibur Diffractometer with

charge-coupled device (CCD) area detector, equipped with Mo  $K\alpha$  radiation ( $\lambda = 0.7107 \text{ \AA}$ ) and a low-temperature device (data collection was performed at 120 K). The program suite used for the data collection was CrysAlis CCD,[23] while the data were reduced with the program CrysAlis RED, and the absorption correction was applied by the program ABSPACK [24].

### *Synthesis of [(NHC)AuCl](1).*

$\text{Ag}_2\text{O}$  (60 mg, 0.26 mmol) was added to a solution of 1-butyl-3-methylimidazolium chloride (80 mg, 0.46 mmol) in a mixture of  $\text{CH}_2\text{Cl}_2$  (4 mL) and MeOH (5 mL) under  $\text{N}_2$  atmosphere and stirred overnight under protection from light. Then  $\text{Me}_2\text{SAuCl}$  (135 mg, 0.46 mmol) was added and the suspension was stirred for an additional 3 h under  $\text{N}_2$ . The black precipitate was separated by filtration over celite and the filtrate was evaporated to dryness under reduced pressure to yield a colourless oil. This was further purified by column chromatography on silica gel ( $\text{CH}_2\text{Cl}_2$ /hexane, 1:4) to give **1** as a colourless powder (107 mg; 63% yield).  $^1\text{H}$  NMR (acetone- $d_6$ , 293K):  $\delta = 7.38$  (d,  $J = 1.6$  Hz, 1 H), 7.33 (d,  $J = 1.6$  Hz, 1 H), 4.20 (t,  $J = 6.8$  Hz, 2 H), 3.83 (s, 3 H), 1.85 (apparent quintet,  $J = 6.8$  Hz, 2 H), 1.34 (apparent sextet,  $J = 7.4$  Hz, 2 H), 0.94 ppm (t,  $J = 7.4$  Hz, 3 H);  $^{13}\text{C}\{^1\text{H}\}$  NMR ( $\text{C}_6\text{D}_6$ , 293K):  $\delta = 171.9$  (imidazolyl C2); 121.3, 120.9 (imidazolyl C4/C5), 50.7 (NCH<sub>2</sub>), 37.4 (NCH<sub>3</sub>), 33.0 (NCH<sub>2</sub>CH<sub>2</sub>), 19.7 (NCH<sub>2</sub>CH<sub>2</sub>CH<sub>2</sub>), 13.8 ppm (CH<sub>2</sub>CH<sub>3</sub>); IR (solid state):  $\nu = 3152, 3122, 2869, 1599, 1564, 1465, 1406, 1368, 1230, 1200, 752 \text{ cm}^{-1}$ ; elemental analysis calcd (%) for  $\text{C}_8\text{H}_{14}\text{AuClN}_2$ : C 25.9, H 3.81, N 7.56; found: C 25.7, H 3.65, N 7.39.

### *Synthesis of [Au(NHC)<sub>2</sub>PF<sub>6</sub>](2)*

LiHMDS (111 mg, 0.78 mmol) was added to a solution of 1-butyl-3-methylimidazolium chloride (130 mg, 0.74 mmol) in DMF (2 mL). After 30 min of stirring a solution of  $[(\text{Me}_2\text{S})\text{AuCl}]$  (103 mg, 0.35 mmol) in DMF (1 mL) was added dropwise. The resulting mixture was stirred for 4 h and the solvent was filtered and washed with ether. The hygroscopic solid was collected and then dissolved in water (2 mL). After the addition of saturated aqueous  $\text{KPF}_6$ , the resultant precipitate was collected and washed with water and dried in vacuo yielding a colourless solid (121 mg; 56% yield).  $^1\text{H}$  NMR (acetone- $d_6$ , 293K):  $\delta = 7.49$  (d,  $J = 1.6$  Hz, 1 H), 7.43 (d,  $J = 1.6$  Hz, 1 H), 4.33 (t,  $J = 7.0$  Hz, 2 H), 3.99 (s, 3 H), 1.93 (apparent quintet,  $J = 7.0$  Hz, 2 H), 1.37 (apparent sextet,  $J = 7.4$  Hz, 2 H), 0.95 ppm (t,  $J = 7.4$  Hz, 3 H);  $^{13}\text{C}\{^1\text{H}\}$  NMR (acetone- $d_6$ , 293K):  $\delta = 184.8$  (imidazolyl C2); 123.7, 122.6 (imidazolyl C4/C5), 51.4 (NCH<sub>2</sub>), 38.2 (NCH<sub>3</sub>), 34.3 (NCH<sub>2</sub>CH<sub>2</sub>), 20.3 (NCH<sub>2</sub>CH<sub>2</sub>CH<sub>2</sub>), 13.9 ppm (CH<sub>2</sub>CH<sub>3</sub>); IR (solid state):  $\nu = 3176, 3148, 2956, 2873, 1568, 1474, 1411, 1381, 1236,$

1205, 1118, 1084, 877, 831, 739, 692  $\text{cm}^{-1}$ ; elemental analysis calcd (%) for  $\text{C}_{16}\text{H}_{28}\text{AuF}_6\text{N}_4\text{P}$ : C 31.1, H 4.56, N 9.06; found: C 30.9, H 4.71, N 8.81.

### *X-ray Crystallography*

The structure of **2** was confirmed by Xray crystallography. Crystal of the compound was grown by the diffusion of  $\text{CHCl}_3$  vapors into an n-hexane solution of gold(I) complex. The structures of compound **2** was solved by direct methods executed by the program SIR97[25] and then refined by full-matrix leastsquares against  $F^2$  using all data (SHELXL 2012) [26]. In **2** the Au(1), P(1), F(1), F(2), F(3), F(4), and F(5) atoms lie on a special position, and the occupancy factors are all 0.5. For both complexes, all nonhydrogen atoms were refined anisotropically, while the hydrogen atoms were set in calculated positions as riding atoms and refined accordingly. Strong absorption has been detected for the crystal of **2**. This factor leads to strong peaks of residual electron density in the Fourier maps mainly, but not only, around the gold metal atom. Geometrical calculations were completed with PARST,[27] and molecular plots were produced with ORTEP3 program[28a] and Mercury [28b].

### *Cell lines and cell colture*

The human ovarian carcinoma cell line sensitive to cisplatin (A2780/S) and its cisplatin-resistant cell subline (A2780/R) were used for cytotoxicity studies. Cell lines were maintained in RPMI1640 medium supplemented with 10% of FCS and antibiotics at 37 °C in a 5%  $\text{CO}_2$  atmosphere and subcultured twice weekly.

### *Cell growth inhibition studies*

The cytotoxic effects of the study gold carbenes were evaluated on the growth of A2780/S and A2780/R cell lines according to the procedure described by Skehan *et al.*[29]. Both compounds were initially diluted in DMSO as stock solutions (20 mM), further dilutions have been performed in PBS (0.5% DMSO present at the higher tested concentration).

Exponentially growing cells were seeded in 96-well microplates at a density of  $5 \times 10^3$  cell/well. After cell inoculation, the microtiter plates were incubated under standard culture conditions (37°C, 5%  $\text{CO}_2$ , 95% air and 100% relative humidity) for 24 h prior to the addition of study compounds. After 24 h, the medium was removed and replaced with fresh medium containing drug concentrations ranging from 0.003 to 100  $\mu\text{M}$  for a continuous exposure of 24 and 72 h for both study compounds.

For comparison purposes the cytotoxicity effects of cisplatin measured in the same experimental conditions were also determined.

According to the procedure the assay was terminated by the addition of cold trichloroacetic acid (TCA). Cells were fixed in situ by 10% TCA and stained by sulforhodamine B (SRB) solution at 0.4% (w/v) in 1% acetic acid. After staining, unbound dye was removed by washing five times with 1% acetic acid and the plates were air dried. Bound stain was subsequently solubilized with 10 mM tris base, and the absorbance was read on an automated plate reader at a wavelength of 540 nm.

The  $IC_{50}$  drug concentration resulting in a 50% reduction in the net protein content (as measured by SRB staining) in drug treated cells as compared to untreated control cells was determined after 72 h of drug exposure. The  $IC_{50}$  data for the two carbenes and cisplatin represent the mean of at least three independent experiments.

To evaluate presence or lack of cross-resistance to study compounds of cisplatin-resistant cells, A2780/R as compared to the parental A2780/S cells, the resistance ratio (R) was calculated as the  $IC_{50}$  values in the resistant cell line and the  $IC_{50}$  values in the sensitive one.

### *Interaction with Lysozyme and Cytochrome c*

The gold complexes were added to the solution with cytc or HEWL (3:1 metal/protein ratio) in 20 mM ammonium acetate buffer, pH 7.4. Mono and dicarbene/protein adducts were prepared by mixing equivalent amounts of the two proteins ( $10^{-4}$  M). The solution was incubated at 37°C for 72h. After a 20-fold dilution with water, ESI-MS spectra were recorded by direct introduction at 5  $\mu$ l/min flow rate in an Orbitrap high-resolution mass spectrometer.

The working conditions were the following: spray voltage 3.1 kV, capillary voltage 45 V and capillary temperature 220°C. The sheath and the auxiliary gases were set, respectively, at 17 and 1 (arbitrary units). For acquisition, the Xcalibur 2.0. software (Thermo) was used and monoisotopic and average deconvoluted masses were obtained by using the integrated Xtract tool. For spectrum acquisition a nominal resolution (at m/z 400) of 100,000 was used.

## References

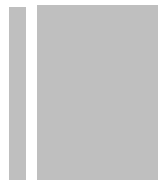
- [1] (a) F. Mohr, *Gold Chemistry. Applications and Future Directions in the Life Sciences*; Wiley: Weinheim, Germany, 2009. (b) S. Nobili, E. Mini, I. Landini, C. Gabbiani, A. Casini, L. Messori, *Med. Res. Rev.*, 2010, 30, 550–580. (c) S.J. Berners-Price, A. Filipovska, *Metallomics*, 2011, 3, 863–873.
- [2] L. Messori, F. Abbate, G. Marcon, P. Orioli, M. Fontani, E. Mini, T. Mazzei, S. Carotti, T. O’Connell, P. Zanello, *J. Med. Chem.*, 2000, 43, 3541–3548.
- [3] (a) L. Ronconi, L. Giovagnini, C. Marzano, F. Bettio, R. Graziani, G. Pilloni, D. Fregona, *Inorg. Chem.*, 2005, 44, 1867–1881. (b) V. Milacic, D. Chen, L. Ronconi, K.R.Landis-Piowar, D. Fregona, Q.P. Dou, *Cancer Res.*, 2006, 66, 10478–10486. (c) D. Saggiaro, M.P. Rigobello, L. Paloschi, A. Folda, S.A. Moggach, S. Parsons, L.Ronconi, D. Fregona, A. Bindoli, *Chem. Biol.*, 2007, 14, 1128–1139.
- [4] (a) R.W.-Y Sun, C.K.-L Li, D.-L Ma, J.J. Yan, C.-N Lok, C.-H Leung, N. Zhu, C.-M Che, *Chem. Eur. J.*, 2010, 16, 3097–3113. (b) R. W.-Y Sun, C.-M Che, *Coord. Chem. Rev.*, 2009, 253, 1682–1691. (c) C.T. Lum, Z.F. Yang, H.Y. Li, R.W.-Y Sun, S.T. Fan, R.T.P. Poon, R. T. P.; Lin, C.-M Che, H.F. Kung, *Int. Cancer Res.*, 2005, 65, 11553–11564.
- [5] (a) L. Messori, G. Marcon, M.A. Cinellu, M. Coronello, E. Mini, C. Gabbiani, P. Orioli, *Bioorg. Med. Chem.*, 2004, 12, 6039–6043. (b) M. Coronello, E. Mini, B. Caciagli, M.A. Cinellu, A. Bindoli, C. Gabbiani, L. Messori, *J. Med. Chem.*, 2005, 48, 6761–6765.
- [6] (a) C. K.-L. Li, R. W.-Y. Sun, S. C.-F. Kui, N. Zhu, C.-M Che, *Chem. Eur. J.*, 2006, 12, 5253–5266. (b) M.A. Cinellu, L. Maiore, M. Manassero, A. Casini, M. Arca, H.H. Fiebig, G. Kelter, E. Michelucci, G. Pieraccini, C. Gabbiani, L. Messori, *ACS Med. Chem. Lett.*, 2010, 1, 336–339. (c) C. Gabbiani, A. Casini, L. Messori, A. Guerri, M.A. Cinellu, G. Minghetti, M. Corsini, C. Rosani, P. Zanello, M. Arca, *Inorg. Chem.*, 2008, 47, 2368–2379. (d) A. Casini, M.A. Cinellu, G. Minghetti, C. Gabbiani, M. Coronello, E. Mini, L. Messori, *J. Med. Chem.*, 2006, 49, 5524–5531.
- [7] (a) L. Messori, G. Marcon, In *Metal Ions in Biological Systems*; Siegel, A.; Siegel, H. Eds.; Marcel Dekker, Inc.: New York, 2004, 41, 279–304. (b) C. F. Shaw III, *Inorg. Chem.*, 1989, 8, 233–267.
- [8] (a) G. D. N. Hoke, G. F. Rush, G. E. Bossard, J. V. McArdle, B. D. Jensen, C. K. Mirabelli, *J. Biol. Chem.*, 1988, 263, 11203–11210. (b) J. S. Modica-Napolitano, J. R. Aprille, *Adv. Drug Delivery Rev.*, 2001, 49, 63–70.

- [9] (a) W.A. Herrmann, L.J. Goossen, M. Spiegler, *Organometallics*, 1998, 17, 2162. (b) D.S. McGuinness, K.J. Cavell, B.W. Skelton, A.H. White, *Organometallics*, 1999, 18, 1596. (c) M.V. Baker, P.J. Barnard, S. J.; Berners-Price, S.K. Brayshaw, J.L. Hickey, B.W. Skelton, A.H. White, *Dalton Trans.*, 2006, 3708–3715. (d) L. Oehninger, R. Rubbiani, I. Ott, *Dalton Trans.* 2013, 42, 3269–3284. (e) W. Liua, R. Gust, *Chem. Soc. Rev.* 2013, 42, 755–773.
- [10] (a) J.L. Hickey, R.A. Ruhayel, P.J. Barnard, M.V. Baker, S.J. Berners-Price, A.J. Filipovska, *Am. Chem. Soc.*, 2008, 130, 12570–12571. (b) T. Zou, C.T. Lum, S.S.-Y Chui, S. C.-M Che, *Angew. Chem., Int. Ed.*, 2013, 52, 2930–2933.
- [11] P.J. Barnard, M.V. Baker, S.J. Berners-Price, D.A. Day, *J. Inorg. Biochem.*, 2004, 98, 1642–1647.
- [12] M.V. Baker, P.J. Barnard, S.J. Berners-Price, S.K. Brayshaw, J.L. Hickey, B.W. Skelton, A.H. White, *J. Organomet. Chem.*, 2005, 690, 5625–5635.
- [13] R. Rubbiani, I. Kitanovic, H. Alborzinia, S. Can, A. Kitanovic, L.A. Onambele, M. Stefanopoulou, Y. Geldmacher, W.S. Sheldrick, G. Wolber, A. Prokop, S. Wöfl, I. Ott, *J. Med. Chem.*, 2010, 53, 8608–8618.
- [14] (a) R. Rubbiani, S. Can, I. Kitanovic, H. Alborzinia, M. Stefanopoulou, M. Kokoschka, S. Mönchgesang, W.S. Sheldrick, S. Wöfl, I. Ott, *J. Med. Chem.* 2011, 54, 8646–8657. (b) P.J. Barnard, M.V. Baker, S.J. Berners-Price, D.A. Day, *J. Inorg. Biochem.*, 2004, 98, 1642–1647.
- [15] (a) J. Weaver, S. Gaillard, C. Toye, S. Macpherson, S.P. Nolan, A. Riches, *Chem. Eur. J.* 2011, 17, 6620–6624. (b) M.J. McKeage, S.J. Berners-Price, P. Galettis, R.J. Bowen, W. Brouwer, L. Ding, L. Zhuang, B.C. Baguley, *Cancer Chemother. Pharmacol.* 2000, 46343–350. (c) S.J. Berners-Price, R.J. Bowen, T.W. Hambley, P.C.J. Healy, *Chem. Soc., Dalton Trans.*, 1999, 1337–1346. (d) S.J. Berners-Price, R.J. Bowen, P. Galettis, P.C. Healy, M.J. McKeage, *Coord. Chem. Rev.* 1999, 185–186, 823–836.
- [16] M.V. Baker, P.J. Barnard, S.K. Brayshaw, J.L. Hickey, B.W. Skelton, A.H. White, *Dalton Trans.*, 2005, 37–43.
- [17] F.H. Allen, *Acta Cryst B* 2002, B58, 380–388.
- [18] E. Schuh, C. Pflüger, A. Citta, A. Folda, M.P.A.; Rigobello, A. Bindoli, A. Casini, F.J. Mohr, *Med. Chem.*, 2012, 55, 5518–5528.
- [19] (a) H. Kunkely, A.J. Vogler, *Organomet. Chem.* 2003, 684, 113. (b) H. Kunkely, A. Vogler, *Inorg. Chem. Commun.* 2000, 3, 143.

- [20] (a) J. Lemke, A. Pinto, P. Niehoff, V. Vasylyeva, N. Metzler- Nolte, *Dalton Trans.*, 2009, 21, 7063–7070. (b) L. Kaps, B. Biersack, H. Müller-Bunz, K. Mahal, J. Münzner, M. Tacke, T. Mueller, R.J. Schobert, *Inorg. Biochem.* 2012, 106, 52–58. (c) M. Pellei, V. Gandin, M. Marinelli, C. Marzano, M. Yousufuddin, H.V. Dias, C. Santini, *Inorg. Chem.*, 2012, 51, 9873–9882.
- [21] A. Casini, A. Guerri, C. Gabbiani, L. Messori, *J. Inorg. Biochem.*, 2008, 102, 995–1006.
- [22] A. Casini, C. Gabbiani, G. Mastrobuoni, L. Messori, G. Moneti, G. Pieraccini, *ChemMedChem*, 2006, 1, 413–417.
- [23] CrysAlisPro, Version 1.171.35.19; Agilent Technologies: San Jose, CA, (release 27–10–2011 CrysAlis171 .NET) (compiled Oct 27 2011,15:02:11).
- [24] CrysAlisPro, Version 1.171.35.19; Agilent Technologies: San Jose, CA, (release 27–10–2011 CrysAlis171 .NET) (compiled Oct 27 2011,15:02:11) Empirical absorption correction using spherical harmonics, implemented in SCALE3 ABSPACK scaling algorithm.
- [25] A. Altomare, M.C. Burla, M. Camalli, G.L. Cascarano, C. Giacovazzo, A. Guagliardi, A.G.G. Moliterni, G. Polidori, R.J. Spagna, *Appl. Crystallogr.*, 1999, 32, 115–119
- [26] G.M. Sheldrick, *Acta Crystallogr.* 2008, A64, 112–122.
- [27] M.J. Nardelli, *Appl. Crystallogr.* 1995, 28, 659–673
- [28] (a) L.J.J. Farrugia, *Appl. Crystallogr.*, 1997, 30, 565. (b) C. F. Macrae, I. J. Bruno, J. A. Chisholm, P. R. Edgington, P. McCabe, E. Pidcock, L. Rodriguez-Monge, R. Taylor, J. vande Streek, P. A. Wood. *J. Appl. Crystallogr.* 2008, 41, 466–470.
- [29] P. Skekan, R. Stroeng, D. Scudiero, A. Monks, J. McMahon, D. Vistica, J.T. Warren, H. Bokesch, S. Kenney, M.R. Boyd, *J. Natl. Cancer Inst.*, 1990, 82, 1107–1112







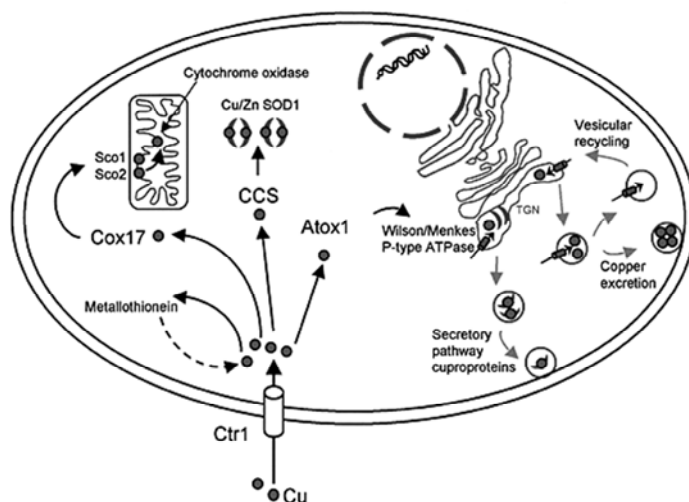
## **Chapter 3**

### **Medicinal Gold Compounds Tight form Adducts with the Copper Chaperone Atox-1: Biological and Pharmacological Implications\***

\* The results presented in this chapter have been published in “Medicinal Gold Compounds form Tight Adducts with the Copper Chaperone Atox-1: Biological and Pharmacological Implications” . C. Gabbiani, F. Scaletti, L. Massai, E. Michelucci, M. A. Cinellu, L. Messori; Chem. Commun. (2012) 48, 11623-11625 And in “Chemistry and Biology of Two Novel Gold(I) Carbene Complexes as Prospective Anticancer Agents”, L. Messori, L. Marchetti; L. Massai, F. Scaletti, A. Guerri, I. Landini, S. Nobili; G. Perrone, E. Mini, P. Leoni, M. Pasquali, C. Gabbiani, Inorg.Chem.( 2014) 53(5), 2396-2

## 1. Introduction

The so called “copper trafficking system” is primarily involved in the regulation of copper transport and homeostasis inside cells. Details of the copper trafficking system were recently disclosed [1]. This system consists of a few proteins that assist copper entrance inside cells and then promote its transfer and delivery to essential copper dependent cellular proteins [1]. (figure 1).

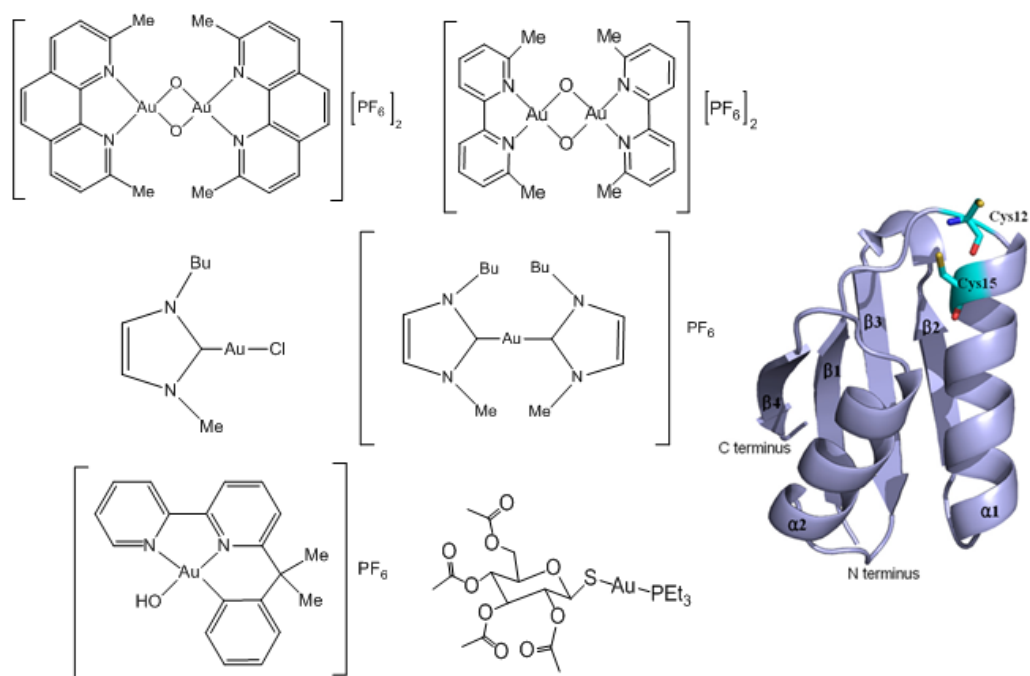


Pathways of copper trafficking within a mammalian cell. Reproduced from ref 5 (figure 1)

The sophisticated biochemical machinery of the *copper trafficking system* ensures a tight control of the intracellular concentrations of free copper ions that are potentially very deleterious to cells and are kept well below  $10^{-15}$  M. *Atox-1* is an intracellular metallochaperone crucially involved in copper trafficking; structural details of *Atox-1* were clarified through a few recent studies [2]. Most *Atox-1* homologues are  $\sim 70$  amino acid proteins containing a conserved CXXC motif for copper(I) binding in the vicinity of the N-terminus. Previous investigations revealed that platinum based drugs do interact strongly with proteins belonging to the copper trafficking system; the latter, in turn, seems to play a key role in modulating cisplatin uptake [3]. A strict linkage between the copper trafficking system and resistance to cisplatin was also pinpointed [4]. More recent studies proved that cisplatin reacts eagerly with *Atox-1* forming stable derivatives [5]. The structures of cisplatin derivatives of *Atox-1* have been solved through X-ray diffraction [2] or NMR measurements [5] proving the interaction of the platinum center with the CXXC motif. Interestingly, Arnesano *et al.* showed that cisplatin binding to *Atox-1* comprises at least two steps: initially a cisplatin-*Atox-1* adduct is formed; afterward, protein dimerization and concomitant loss of amines

## Medicinal Gold Compounds Tight form Adducts with the Copper Chaperone Atox-1: Biological and Pharmacological Implications

from cisplatin take place. In turn, a study by Pernilla Wittung *et al.* analysed the reaction of cisplatin with *Atox-1* through various biophysical methods and demonstrated that copper(I) and platinum(II) ions may bind simultaneously to this protein to nearby, yet independent and not mutually exclusive, anchoring sites [6]. During the last decade we were engaged in preparing and characterising a number of medicinal gold compounds as experimental cytotoxic and anticancer agents [7].



Structures of the tested compounds and *Atox1* (chart 1)

On the ground of basic concepts of coordination chemistry and of established HSAB principles, we hypothesised that medicinal gold compounds, especially those in the oxidation state +1, might interact strongly with proteins of the *copper trafficking system*. Indeed, a previous study had revealed that the copper trafficking system is substantially inhibited by “soft”  $d^{10}$  silver(I) ions, capable of binding *Atox-1* [8]. Gold(I) ions -with a  $d^{10}$  electronic configuration- are even “softer” Lewis acids than silver(I) ions and, as such, should react eagerly with the copper(I) binding site of *Atox-1*; remarkably, a very recent study reported that copper transport proteins are involved in the uptake of some gold(I) carbene compounds [9]. Interference with other

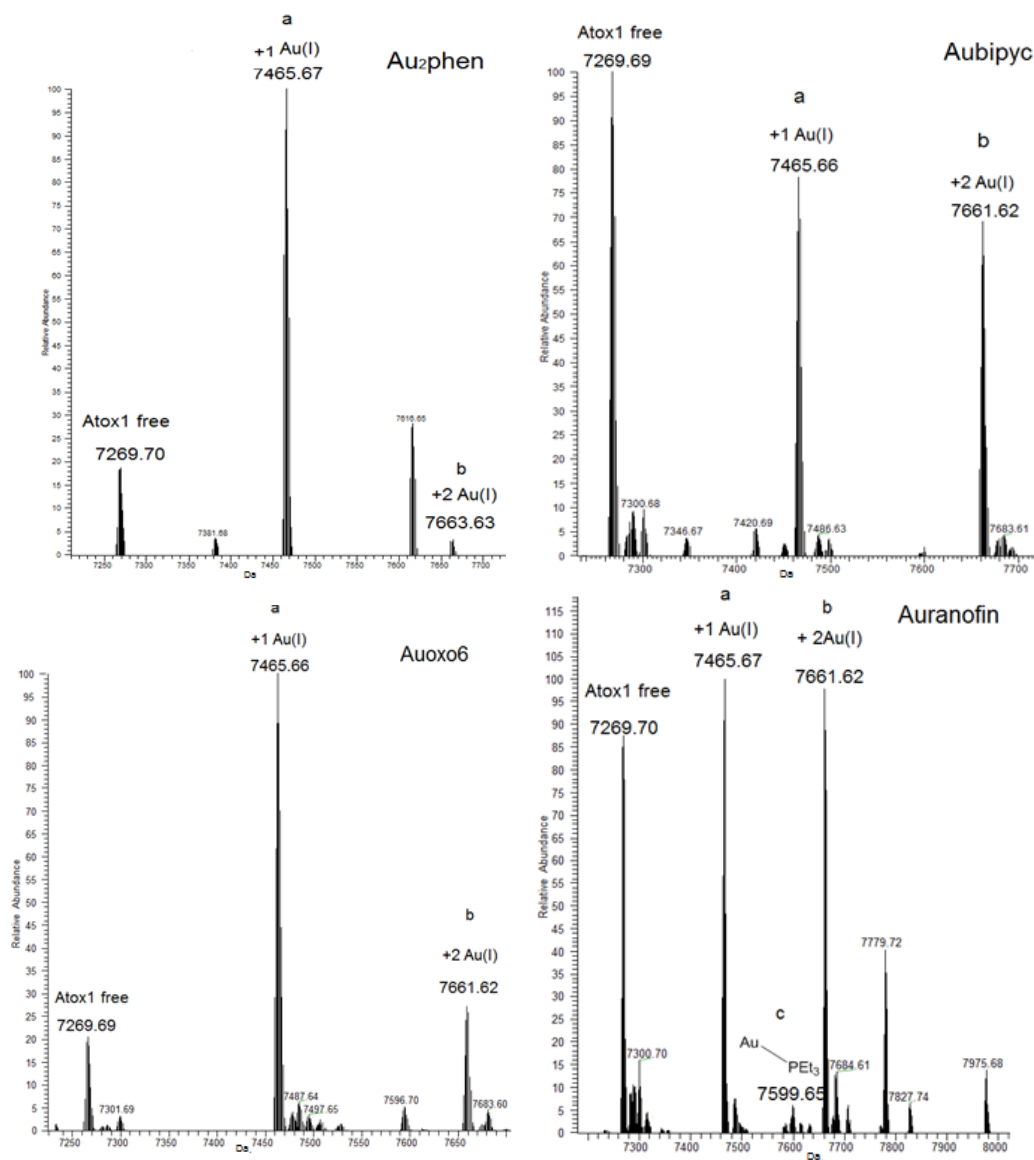
biochemical pathways of transport and storage that regulate the homeostasis of divalent/trivalent transition metal ions [10] cannot be ruled out at this stage.

## 2. Results

### 2.1 Interaction with gold compounds and Atox1

Based on the above arguments, we decided to investigate the interactions of three representative cytotoxic gold(III) compounds developed in our laboratory –namely Auoxo [11], Au<sub>2</sub>phen [12] and Aubipic [13]- and also of the clinically established gold(I) drug auranofin with human Atox-1. Schematic structures of the study compounds are shown in Chart 1. The investigational gold(III) compounds, in particular Auoxo6 and Au<sub>2</sub>phen, have been reported to undergo rather facile reduction to gold(I), even under mildly reducing conditions, thus being an effective source of “soft” gold(I) ions. Typically, gold(III) reduction causes complete breakdown of the starting metal complex and release of its bulky bidentate organic ligands. The interactions of the mentioned gold(III) compounds with Atox-1 were analysed through ESI-MS as the latter method appears very suitable and informative to monitor the Atox-1 protein in solution, as recently reported.<sup>5</sup> For the ESI MS measurements, Atox-1 was dissolved in 25 mM tetramethylammonium acetate buffer (TMeAmAc), containing DTT (with a 1:5 protein/DTT molar ratio) at physiological pH, and reacted with a stoichiometric amount of the above gold(III) compounds according to established experimental protocols (see ESI). Samples were collected after 24 hours incubation and comparatively analysed through ESI-MS. Parallel studies were carried out with auranofin under identical solution conditions. The resulting deconvoluted ESI-MS spectra are shown in figure 2. Formation of metal-protein adducts is clearly documented by the appearance of peaks of higher molecular mass than that of the native protein falling at ~7269 Da. The new peaks may be straightforwardly assigned to protein binding of gold containing molecular fragments. In the case of the three gold(III) compounds, a same major adduct was invariantly formed (with a peak falling at ~7465 Da) matching protein binding of a single gold(I) ion. Formation of this adduct implies disruption of the starting gold(III) complex, loss of ligands and reduction of gold(III) to gold(I). Auranofin gave the same adduct as its major reaction product; however, the weak peak observed at ~7599 Da well matches an adduct bearing the Au(PEt<sub>3</sub>)<sup>+</sup> fragment. In all cases the monometalated derivative resulted to be the predominant adduct; however, a second intense peak was invariantly observed at ~7661 Da that corresponds to protein binding of two gold(I) ions. In two cases i.e. Aubipyc and Auranofin this latter peak manifests an intensity absolutely comparable to that of the monometalated adduct, implying that adducts containing two metal centers may be formed in large amounts.

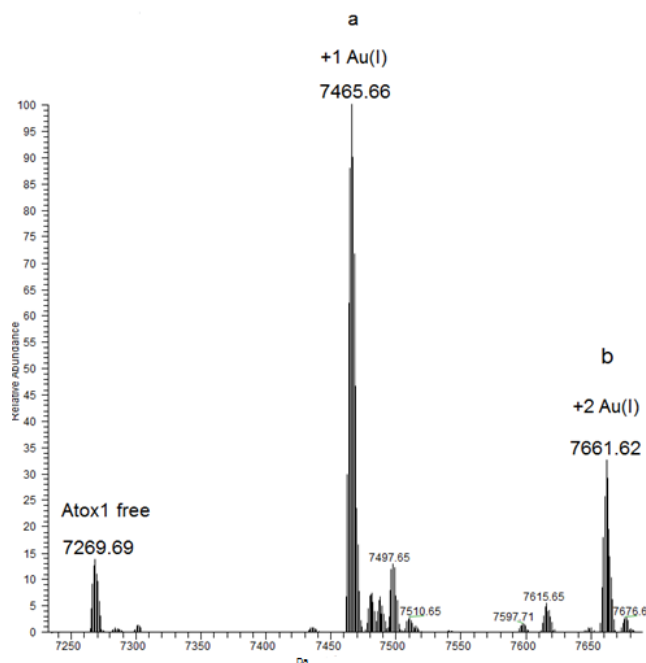
# Medicinal Gold Compounds Tight form Adducts with the Copper Chaperone Atox-1: Biological and Pharmacological Implications



LTQ-Orbitrap ESI-MS spectra of Atox-1 treated with gold compounds. Atox1 adducts are formed with: 1 Au<sup>+</sup> (a) or 2 Au<sup>+</sup> (b) bound to the protein; in the case of auranofin there is an additional adduct with a Au(PEt<sub>3</sub>)<sup>+</sup> (c) fragment. Incubation time 24 h. (figure 2)

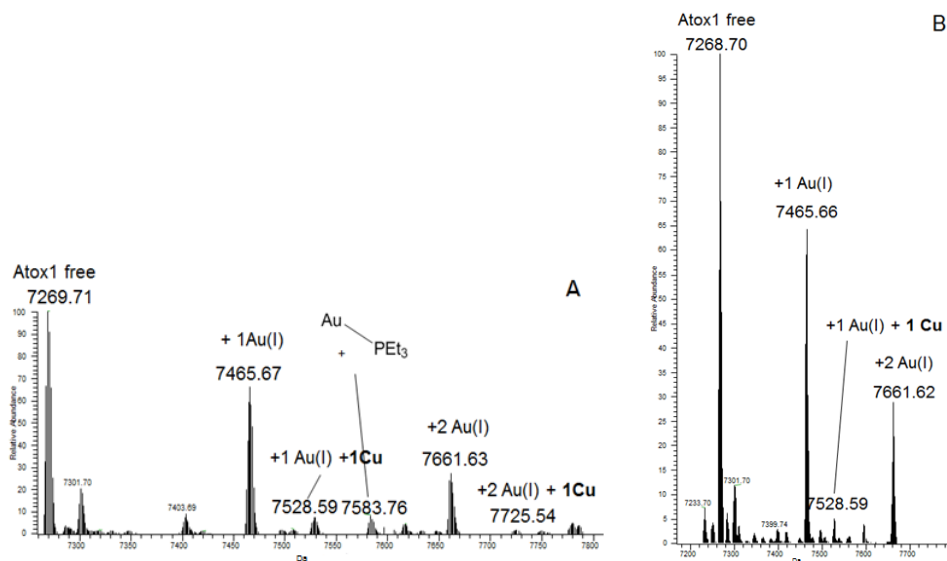
The stability of the obtained gold Atox-1 adducts in solution, at room temperature, was further assessed by recording ESI-MS spectra at regular time intervals over 72 hours. An appreciable stability of gold Atox-1 adducts could be documented in selected cases.

The behaviour of Aubipic is very representative (figure 3). Indeed, its gold-protein adducts turned out to be fairly stable with time over 72 hours; yet, the total amount of gold adducts increased significantly with time as it emerges from comparative analysis of peak intensities at 24 hours (figure 2) versus 72 hours (figure 3). In contrast, the adducts formed with Auoxo6 and Au<sub>2</sub>phen manifested a lower stability over incubation times longer than 24 h showing evident signs of adduct and protein degradation (data not shown).



LTQ-Orbitrap ESI-MS spectrum of Atox-treated with Aubipyc after 72 h incubation; other conditions as in figure 2. (figure 3).

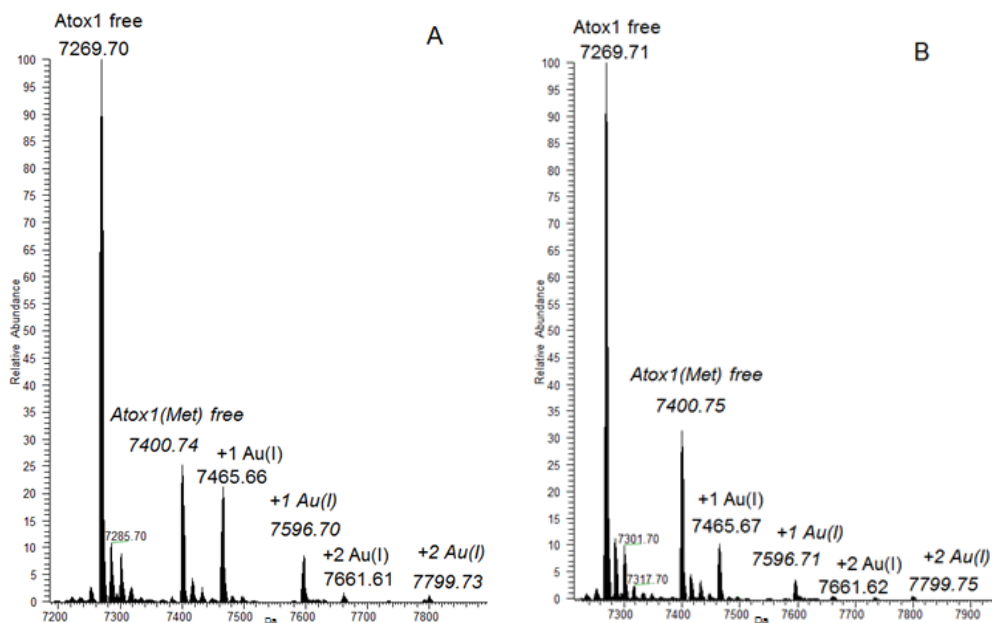
The above reported results well document that Atox-1 can form tight derivatives with gold(I) ions implying that the resulting metal-protein interactions are strong. To better elucidate this point competition studies were carried out with copper. More precisely, Atox-1 was preincubated with copper(II) ions in the presence of DTT, according to previous preparative procedures ; then, gold compounds were added. ESI-MS spectra were taken for the final samples after 12 hours incubation with gold compounds(Auoxo6 and Auranofin). Remarkably, large amounts of gold/Atox-1 derivatives were formed while copper/Atox-1 derivatives are hardly seen. Again, these results point out that gold ions apparently form far stronger Atox-1 complexes than copper ions(figure 4)



LTQ-Orbitrap ESI-MS spectrum of Atox-1 sequentially treated with  $\text{CuCl}_2$  and Auranofin (A) or Auoxo6 (B), (1:2:1 molar ratio) at room temperature. Incubation time 24 h (see: I. Anastassopoulou, L. Banci, I. Bertini, F. Cantini, E. Katsari, A. Rosato, *Biochemistry* 2004, 43, 13046-53 for details of sample preparation). (figure 4)

## 2.2 Interactions with NHC gold(I) complexes and Atox1

Similar reactivity studies were subsequently carried out in the presence of the copper chaperone Atox-1 and NHC gold(I) complexes. Protein adducts with the selected compounds were prepared by mixing equivalent amounts of Atox-1 ( $10^{-4}$  M) with  $[\text{Au}(\text{NHC})\text{Cl}]$  or  $\text{Au}(\text{NHC})_2\text{PF}_6$ , in the presence of ammonium acetate buffer (pH 7.4), and DTT ( $10^{-4}$  M). Notably, the resulting ESI-MS spectra show that incubation of Atox-1 with NHC gold(I) complexes leads, after 24 h, to the formation of metal-protein adducts (figure 5). This is clearly documented by the appearance of peaks of higher molecular mass than those assigned to the native protein falling at 7269 Da (protein without the first methionine, Met) and at 7400 Da (protein with the first methionine). The new peaks may be straightforwardly assigned to formal binding of  $\text{Au}^+$  to the protein. In the formation of the adduct the starting gold(I) complex loses the ligands. In the two cases the monometalated derivative resulted to be the predominant adduct; however, a second weak peak is observed at 7661 Da that corresponds to protein binding of two  $\text{Au}^+$  ions. All samples show additional peaks corresponding to adducts formed between gold(I) and the Atox1 protein still bearing the N-terminal methionine (Met-1).



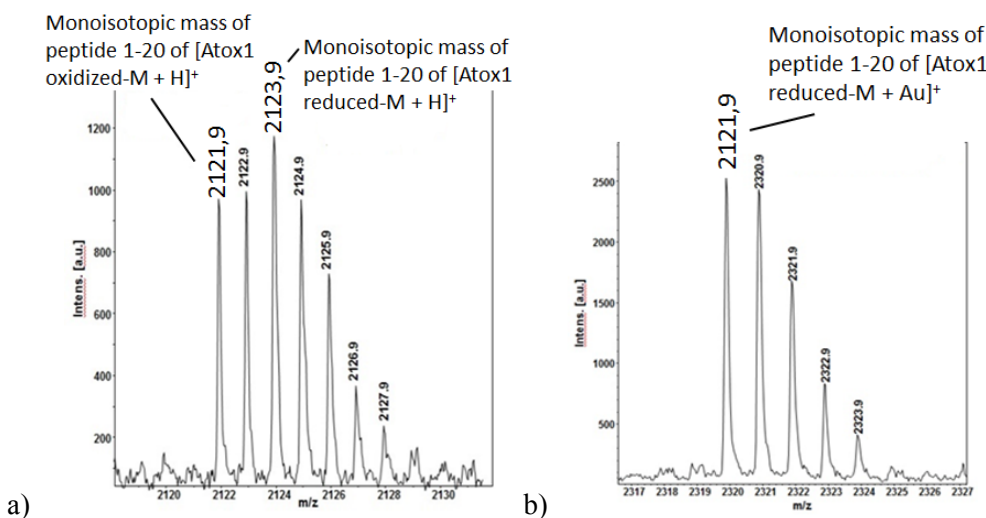
LTQ-Orbitrap ESI-MS spectra of Atox-1 (7269 Da) treated with Au(NHC)Cl (a) and Au(NHC)<sub>2</sub>PF<sub>6</sub> (b). Atox-1 adducts are formed with: Au<sup>+</sup> (7465 Da) or 2 Au<sup>+</sup> (7661 Da) bound to the protein. Incubation time was 24 h. The peak of Atox-1 with a methionine (7400 Da) is also visible, and the respective adducts with 1 Au<sup>+</sup> (7596 Da) and 2 Au<sup>+</sup> (7799 Da) (figure 5)

### 2.3 Characterisation of gold binding in Aubipic/Atox1

It was previously shown that Atox1 may form stable derivatives with a variety of gold compounds of medicinal interest. In particular, Aubipyc is an established organogold(III) complex with promising antiproliferative and anticancer properties, extensively studied in recent years [7]. Notably, under the solution conditions used to monitor metal binding to Atox1, i.e. within the strongly reducing environment created by DTT, the gold(III) center of Aubipyc is reduced to gold(I), the terdentate ligand is released and the resulting gold(I) species binds Atox1. The main -and virtually only- derivative that is formed corresponds to Atox1 bound to a single bare gold(I) ion. We decided to study in more depth this derivative and identify the exact location of the gold binding site. Adduct formation is well witnessed by deconvoluted ESI MS spectra showing a clear peak at ~7465 Da. Based on simple coordination chemistry considerations and HSAB concepts, it is straightforward to hypothesise that gold(I) binding may occur at the level of the copper(I) binding site. However, to better ascertain this point, tryptic digestion was carried out either on the Atox1/Atox1-M mixture alone or on the same mixture incubated with Aubipyc. Then, MALDI spectra



were recorded on both tryptic digests. Notably, the most abundant tryptic fragment obtained from the first mixture was the 1-20 peptide of Atox1-M (figure 6a). Upon comparing this spectrum with the one obtained from tryptic digestion of the second mixture (i.e. Atox1/Atox1-M incubated with Aubipyc) we noticed the appearance of a relatively intense peak at 2319.8 Da due to the binding of  $\text{Au}^+$  to 1-20 peptide of reduced Atox1-M (figure 6b). Further, the absence of peaks at 2317 Da implies that the oxidised form of peptide 1-20 is unable to coordinate the  $\text{Au}^+$  ion. This result is nicely consistent with the hypothesis that gold binding takes place at the CXXC motif, as reported for cisplatin by Rosenzweig et al [14].



(a) MALDI spectrum of 1-20 fragment obtained through tryptic digestion of Atox1-M. (b) MALDI spectrum of 1-20 fragment obtained through tryptic digestion of Atox1-M + Aubipyc (incubated for 24 h at RT, 1:1 complex to protein ratio in 20 mM ammonium acetate buffer solution,  $\text{N}_2$  inert atmosphere). (figure 6)

#### 2.4 Metal binding properties of Atox1 versus other soft metals

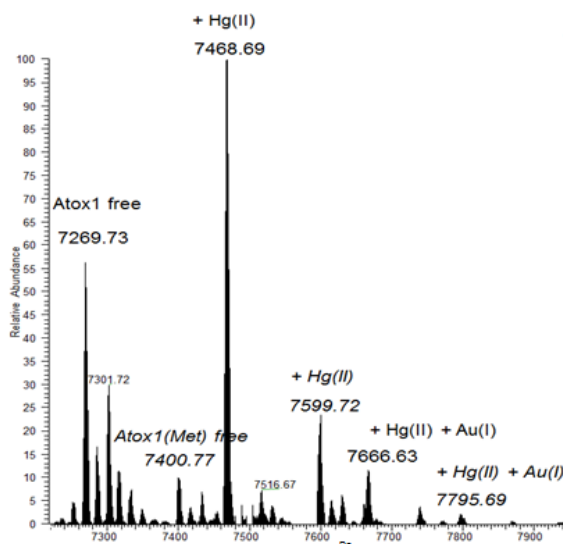
Next, an ESI MS approach (analogous to that reported for medicinal gold compounds in our previous work) [5] was exploited to assess Atox1 metal binding abilities toward a variety of metal species of medicinal or toxicological interest [15,16]. In particular we selected a number of metal (or metalloid) species, namely antimony, arsenic, bismuth and mercury, exhibiting a pronounced thiophilic character. At first, a screening was carried out for each metal under the same experimental conditions. As the result of this screening adduct formation was demonstrated for bismuth and mercury while the other species failed to form adducts, at least under the here adopted

experimental conditions. Deconvoluted ESI MS spectra documenting adduct formation in the case of mercury and bismuth are shown in figure 3. Notably, the peak of the adduct, in the case of mercury, is significantly higher than that of the native apoprotein implying a large binding affinity of Atox1 for mercury. For both mercury and bismuth the ESI-MS spectrum is dominated by a major peak corresponding to the monometalated derivative, suggesting the existence of a single metal binding site. In the case of bismuth we could ascertain that the abundance of this derivative increases with increasing the metal: protein ratio, with no evidence of bis-metalated species

The structure of a Hg-Atox1 derivative had been previously reported by Rosenzweig *et al.* [15] within a comparative crystallographic study; in contrast, formation of a tight adduct between Atox1 and the tripositive bismuth(III) ion is described for the first time.

### 2.5 Metal competition studies

Having documented the strong affinity of the above metal species - *i.e.* Aubipyc, and mercury- for Atox1, we moved to investigate possible competition among them in protein binding. In principle, observation of a direct competition may support the hypothesis that these metal species share the same metal binding site; in addition initial information may be inferred on the relative stabilities of the various metal-protein species. This goal could be accomplished straightforwardly through a single experiment where Atox1 was challenged simultaneously with mercury and gold, presented at 1:1 metal to protein ratio, under the same experimental conditions reported above. The resulting sample was analysed through ESI-MS and found to exhibit a single major peak at 7468 Da, corresponding to the Hg-Atox1 derivative, described above; minor peaks are also seen, assignable to others derivatives including a 2Hg-Atox1 derivative (figure 7). Remarkably, no evidence was obtained for any Au-Atox1 derivatives. These spectral features tell us quite unambiguously, that the two tested metal species do compete for the same metal binding site or region which realistically corresponds to the CXXC motif. Mercury turns out to be- by far- the strongest agonist for the Atox1 metal binding site, completely abolishing the binding Aubipyc to the same site. Strong evidence of a direct competition between the three considered metal species is thus offered.



Deconvoluted ESI-MS spectrum of competition experiment between Au, Hg, incubated with Atox1/Atox1-M mixture for 24 h at RT, 1:1 metals to protein ratio in 20 mM ammonium acetate buffer solution, N<sub>2</sub> inert atmosphere. (figure 7)

### 3. Discussion

In conclusion, we have explored here whether a few representative cytotoxic gold compounds might manifest high affinity and form stable adducts with the copper chaperone Atox-1. Notably, large metal-protein affinities and relevant adduct formation were unambiguously proved through ESI MS analysis; the nature of the adducts and their metal-protein stoichiometries were elucidated at the molecular level. Based on the above ESI MS results, some general trends may be proposed for the investigated reactions. Under the applied experimental conditions- i.e the reducing environment provided by DTT-the gold(III) centers are invariably reduced to gold(I) with simultaneous loss of the starting ligands. In turn, the resulting gold(I) species bind Atox-1 strongly. Two major gold binding sites were disclosed on the protein that may well correspond to previously described metal binding sites.

Notably, our gold carbene complexes were NOT able to form adducts with the two model proteins – i.e. cytochrome c and lysozyme- in contrast both reacted eagerly with the Atox-1 protein bearing a characteristic CXXC motif. Monometalated derivatives turned out to be predominant. In both cases covalent (coordinative) adducts were formed where the NHC moiety is released and gold(I) ions are found associated to the protein. This implies that the CXXC motif possesses such a high affinity for the gold(I)

center as to bind it coordinatively in the place of chloride or of the first NHC ligand and then to displace even the other NHC ligand, oppositely located. These results suggest that gold(I) NHC complexes are highly selective in protein metalation, having the chance to interact only with those few proteins possessing specific metal binding motifs.

Competition studies with copper were also carried out showing that gold-Atox1 adducts are far more stable than copper adducts. In view of these findings, it may be suggested that gold compounds will interfere importantly with the intracellular copper trafficking system. This observation contains important pharmacological implications: i) It is likely that gold based medicinal compounds may exploit the copper trafficking system to enter cells and to be delivered to a number of cellular sites; this kind of processing, however, causes disruption of the original gold(III) species and gold(III) reduction to gold(I); ii) it can be hypothesised that gold compounds may drastically inhibit the copper trafficking system and be effective in modulating its efficiency; iii) such effects might be relevant even for a modulation of cisplatin activity and for the control of its uptake. Thus, the present results strongly warrant that gold compounds are tested *in vitro* on appropriate cellular systems to ascertain whether the predicted effects truly occur. Moreover, our study further stresses the importance of ESI MS methods to elucidate adduct formation between metallodrugs and proteins and delineate the respective mechanisms of interaction.

Here, we have deepened the characterisation of the Atox1 binding properties toward the antiproliferative organogold(III) complex Aubipyc. We have shown that Aubipyc, in its reaction with Atox1, produces a monometalated gold(I)/Atox1 derivative; that gold(I) binding primarily occurs at the tryptic peptide 1-20 in its reduced form; that gold binding is completely inhibited by mercury. Direct competition with mercury offers clear evidence that gold(I) binding occurs at the primary metal binding site of Atox1 i.e. the copper binding site

#### 4. Experimental section

##### *Materials*

The various gold(III) complexes were synthesized as previously described (see the respective refs). Auranofin was purchased at Vinci-Biochem. Copper transport protein Atox1 was purchased from Giotto Biotech.

### *ESI Mass Spectrometry*

For the analysis Atox-1 was dissolved ( $10^{-4}$  M) in 25 mM tetramethylammonium acetate buffer (TMeAmAc), pH 7.4 containing DTT (1:5 protein:DTT molar ratio). Then the three gold (III) complexes and Auranofin were added (1:1 metal/protein ratio) to the solution and incubated at room temperature for 24 or 72h. After a 10-fold dilution with 1% HCOOH, ESI-MS spectrum was recorded by direct introduction at 5  $\mu$ l/min flow rate in an LTQ-Orbitrap high-resolution mass spectrometer (Thermo, San Jose, CA, USA), equipped with a conventional ESI source. The working conditions were the following: spray voltage 3.1 kV, capillary voltage 45 V and capillary temperature 220 °C. The sheath and the auxiliary gases were set, respectively, at 17 (arbitrary units) and 1 (arbitrary units). For acquisition, Xcalibur 2.0. software (Thermo) was used and monoisotopic and average deconvoluted masses were obtained by using the integrated Xtract tool. For spectrum acquisition a nominal resolution (at m/z 400) of 100,000 was used.

### *Digestion and MALDI-TOF analyses*

Two 100  $\mu$ M solutions of Atox1/Atox1-M in ammonium acetate buffer solution at pH 6.8 containing DTT (500  $\mu$ M) were prepared with or without adding Aubipyc (protein to metal ratio 1:1, at RT for 24 h, N<sub>2</sub> inert atmosphere). At 5  $\mu$ L of both solutions were added 30  $\mu$ L of Ambic 40mM. Both solutions were digested on immobilized trypsin tips (DigesTip, ProteoGen Bio, Siena, Italy) and 0.4  $\mu$ L of tryptic digests were spotted on an AnchorChip 400 MALDI target (Bruker Daltonics, Bremen, Germany) together with 0.4  $\mu$ L of matrix solution (10 mg/ml  $\alpha$ -cyano-4-hydroxycinnamic acid in 70/30 acetonitrile/0.1% TFA). The solvent was allowed to evaporate and the two dried spots were analyzed with a MALDI-TOF spectrometer (Ultraflex III MALDI-TOF/TOF, Bruker Daltonics, Bremen, Germany). The working conditions were the following: reflectron positive mode, mass range 850-5000 m/z. The spectra were processed using Flex Analysis software 3.0 from Bruker Daltonics.

References

- [1] a) A. K. Boal, A. C. Rosenzweig, *Chem. Rev.*, 2009, 109, 4760-4779; b) L. Banci, F. Cantini, S. Ciofi-Baffoni, *Cell. Mol. Life Sci.*, 2010, 67, 2563-2589.
- [2] A. K. Boal, A. C. Rosenzweig, *J. Am. Chem. Soc.*, 2009, 131, 14196-14197.
- [3] a) R. Safaei, S.B. Howell, *Crit Rev Oncol Hematol.*, 2005, 53, 13-23; b) S.B. Howell, R. Safaei, C.A. Larson, M.J. Sailor, *Mol Pharmacol.* 2010, 77, 887-894.
- [4] K. Katano, A. Kondo, R. Safaei, A. Holzer, G. Samimi, M. Mishima, Y.M. Kuo, M. Rochdi, S. B. Howell, *Cancer Research*, 2002, 62, 6559-6565.
- [5] F. Arnesano, L. Banci, I. Bertini, I. C. Felli, M. Losacco, G. Natile, *J. Am. Chem. Soc.* 2011, 133, 18361-18369.
- [6] a) M. E. Palm, C. F. Weise, C. Lundin, G. Wingsle, Y. Nygren, E. Björn, P. Naredi, M. Wolf-Watz, P. Wittung-Stafshede, *PNAS*, 2011, 108, 6951-6956; b) M. E. Palm-Espling, P. Wittung-Stafshede, *Biochem Pharm.*, 2012, 83, 874-881.
- [7] S. Nobili, E. Mini, I. Landini, C. Gabbiani, A. Casini, L. Messori, *Medicinal Research Reviews*, 2010, 30, 550-580
- [8] J. Lee, M. M. O. Peña, Y. Nose, D. J. Thiele, *J. Biol. Chem.*, 2002, 277, 4380-4387.
- [9] L. Kaps, B. Biersack, H. Müller-Bunz, K. Mahal, J. Münzner, M. Tacke, T. Mueller, R. Schobert, *J Inorg Biochem.* 2012, 106, 52-58.
- [10] a) V.C. Culotta, M. Yang, M.D. Hall, *Eukaryot Cell.* 2005, 4, 1159-1165; b) M. Stola, F. Musiani, S. Mangani, P. Turano, N. Safarov, B. Zambelli, S. Ciurli, *Biochemistry*, 2006, 45, 6495-6509; c) B. Zambelli, N. Cremades, P. Neyroz, P. Turano, V.N. Uversky, S. Ciurli, *Molecular BioSystems* 2012, 8, 220-228; d) I. Bertini, D. Lalli, S. Mangani, C. Pozzi, C. Rosa, E.C. Theil, P. Turano *J. American Chemical Society*, 134, 6169-6176.
- [11] A. Casini, M.A. Cinellu, G. Minghetti, C. Gabbiani, M. Coronello, E. Mini, L. Messori, *J. Med. Chem.*, 2006, 49, 5524-5531.
- [12] C. Gabbiani, A. Casini, G. Kelter, F. Cocco, M.A. Cinellu, H.H. Fiebig, L. Messori, *Metallomics*, 2011, 3, 1318-1323.
- [13] G. Marcon, S. Carotti, M. Coronello, L. Messori, E. Mini, P. Orioli, T. Mazzei, M.A. Cinellu, G. Minghetti, *J. Med. Chem.*, 2002, 45, 1672-1677.
- [14] A.C. Rosenzweig, D.L. Huffman, M.Y. Hou, A.K. Wernimont, R.A. Pufahl, T.V. O' Halloran, *Structure*, 1999, 7, 605-617

Medicinal Gold Compounds Tight form Adducts with the Copper Chaperone Atox-1:  
Biological and Pharmacological Implications

[15] Dabrowiak, J. C. *Metals in Medicine*, first ed.; Jhon Wiley and Sons, Ltd, UK, 2009.

[16] J.A.R. Salvador, A.C. Figueiredo, R.M.A. Pinto, S.M. Silvestre, *Future Med. Chem.*, 2012, 4,1495-1523





## Chapter 4

### **Interactions of Gold-Based Drugs with proteins: a structural perspective\***

\* The results presented in this chapter have been published in “The mode of action of anticancer gold-based drugs: a structural perspective” L. Messori, F. Scaletti, L. Massai, M.A. Cinellu, C. Gabbiani, A. Vergara, A. Merlino. And in “Interactions of gold-based drugs with proteins: crystal structure of the adduct formed between ribonuclease A and a cytotoxic gold(III)Compound” , L. Messori, F. Scaletti, L. Massai, M. A. Cinellu, I. Russo Krauss, G. di Martino, A. Vergara, L. Paduano, A Merlino

### 1. Introduction

Gold based compounds form a new family of cytotoxic agents of current, great interest as anticancer drug candidates. Indeed, many structurally diverse gold complexes – either gold(III) or gold(I) – were designed, synthesised and characterised in recent years, showing potent antiproliferative properties *in vitro* against several cancer cell lines.[1] So far, the most important classes of cytotoxic gold compounds under study have been gold porphyrins,[2] gold dithiocarbamates,[3] cyclometalated gold(III) complexes,[4,5] dinuclear gold complexes,[6] and gold carbenes;[7] for some of them encouraging – though preliminary – *in vivo* results have been gathered.[2b,c;3a,b;5a,d] Recent investigations well documented that cytotoxic gold compounds behave, in most cases, as prodrugs; in other words they exert their pharmacological actions only after chemical activation and conversion into more reactive species. The latter react with various biomolecular targets, thus producing their pharmacological actions. They behave as “functional metal compounds” according to Enzo Alessio’s categorization[8]. Previous studies highlighted that DNA is not a good target for most gold-based cytotoxic agents – at variance with the case of platinum drugs[9]. Conversely, there is some solid evidence that gold based drugs mainly act through modification of selected proteins with consequent loss of function. This implies that selective “protein metalation” is the key feature in the mechanism of action of anticancer gold drugs. An excellent example is offered by the case of the selenoenzyme thioredoxin reductase [10], a putative and now partially validated target for many cytotoxic gold compounds [11]. Irreversible inhibition of human glutathione reductase by phosphine–metal complexes, which results in a unique S–Au(I)–S coordination, has also been found [12a]. The apparent importance of the reactions of medicinal gold compounds with proteins prompted us to analyse these processes in more depth from the structural point of view. Indeed, only very few crystallographic studies are available to date concerning structures of proteins modified with gold drugs[12] determining a substantial information gap. This led us to perform a careful crystallographic analysis of the products formed in the reaction between some representative gold compounds and hen egg white lysozyme (HEWL), a model protein extensively used to characterise metallodrug–protein interactions [13] and RNase A. Hen egg white lysozyme is well known among crystallographers as a protein very prone to crystallization, thus turning out very appropriate for X-ray diffraction studies of our metallodrugs adducts.

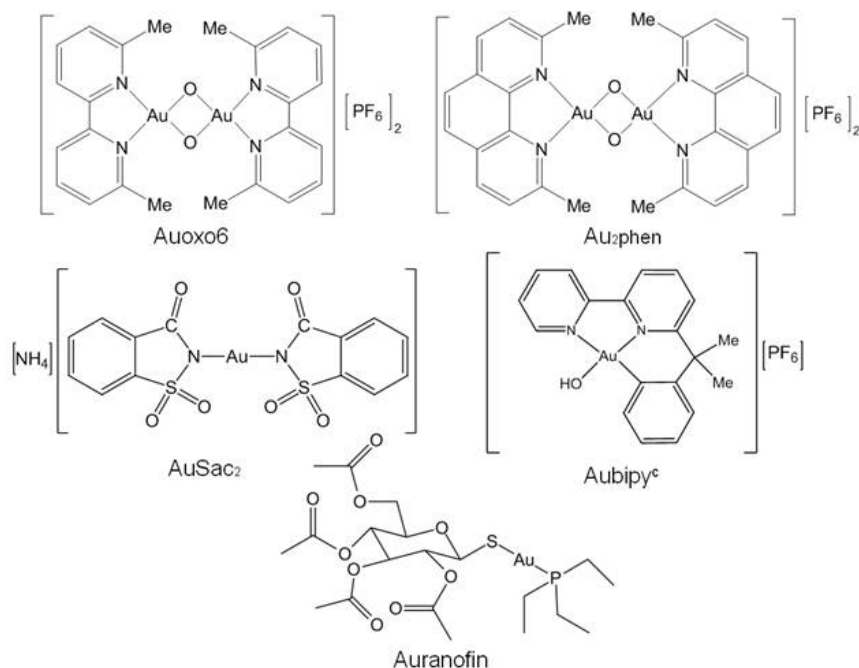
Bovine pancreatic ribonuclease (RNase A) is a small (124 residues)protein that cleaves and hydrolyzes single-stranded RNA [14–17]. RNase A has been used as a model system for pioneering studies in protein chemistry: it was the first protein to have its sequence fully synthesized[18]; its crystal structure was solved already in 1967 [19]; it

## Interactions of Gold-Based Drugs with proteins: a structural perspective

is a stable protein[20] and is able to crystallize under many different crystallization conditions [20]. Owing to its favourable properties, RNase A has been used as a suitable model system for protein metalation studies [21,22]. The above arguments prompted us to use this protein to perform structural characterization of complexes with medicinal gold species to model the gold drug–protein interactions. Notably, reactions of RNase A with gold compounds have been described in two previous studies [23,24] Pioneering experiments in this field were performed by Isab and Sadler in 1977, showing the reaction of Au(III) with methionine residues [23]. Later on, Maruyama et al. demonstrated that gold(III) ions exhibit inhibitory effects on RNase A [24] and suggested that Au(III) ions could be linked to the catalytic His or methionine residues.

### 2. Results

A small panel of structurally diverse gold compounds featuring the oxidation states +3 and +1 was chosen for the present study. Namely, the investigational panel included Auoxo6, Au<sub>2</sub>phen, AuSac<sub>2</sub>, Aubipyc and Auranofin (figure 1).

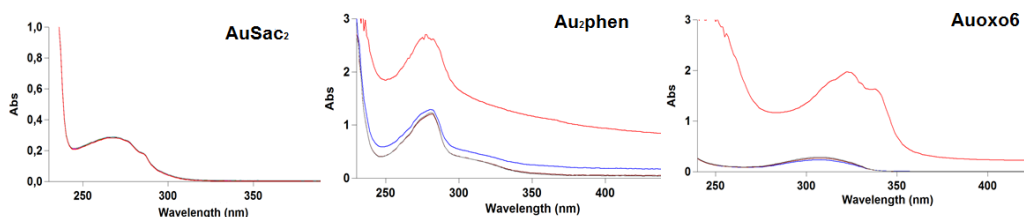


Structures of Auoxo6, Au<sub>2</sub>phen, AuSac<sub>2</sub>, Aubipyc, and Auranofin (figure 1)

$[\text{NH}_4][\text{Au}(\text{Sac})_2]$  or  $\text{AuSac}_2$  is a homoleptic gold(I) complex with the saccharinate ligand.[25]. All these compounds formerly revealed promising and potent antiproliferative properties when tested in vitro against a few cancer cell lines [26].

## 2.1 Gold-Based drugs and Lysozyme

Crystals of the adducts between HEWL and gold compounds have been prepared according to two different protein crystallization strategies, namely crystal soaking and co-crystallisation. The HEWL crystals have been already used to study the interactions of protein with metallodrugs [13a], including cisplatin [27]. Crystals were grown for all five panel compounds; however, only in three cases – i.e.  $\text{AuSac}_2$ ,  $\text{Au}_2\text{phen}$  and  $\text{Auoxo6}$  – gold adducts formed in significant amounts. Spectrophotometric studies have already been carried out on these systems [25,27], but new experiments have now been done under the same solution conditions of the crystallisation experiments.

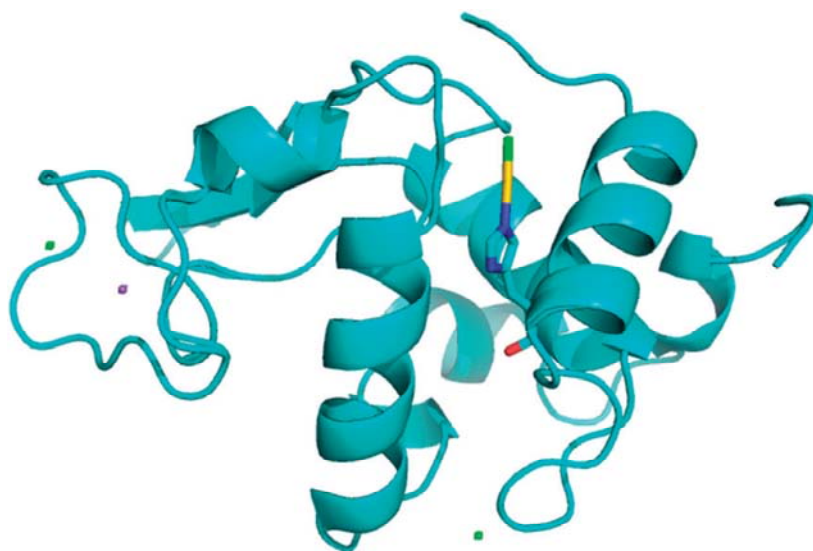


Time course UV-vis spectra of each gold compound in the presence of HEWL (green line) dissolved in 50 mM acetate buffer/ 1M NaCl pH 4.5 over 24 h incubation. Concentration of the complex is  $10^{-5}$  M (with a metallodrug-protein molar ratio of 10:1). The figure shows spectra recorded after 0 h (red line), 1 h (blue line), 12h (brown line) and 24 h (grey line). (figure 2)

$\text{Auoxo6}$  and  $\text{Au}_2\text{phen}$  manifest large spectral changes when incubated in the reference buffer, implying that they are undergoing relevant chemical transformations and/or degradation (most likely gold(III) reduction and consequent ligand detachment). Reduction attenuates the interaction of gold center to its ligands and facilitates gold transfer to other ligands and ultimately to the protein. This means that probably, in the case of  $\text{Auoxo6}$  and  $\text{Au}_2\text{phen}$ , gold is first reduced and released from its original ligands; then it binds the protein, though the two latter processes -ligand release and protein binding- may be somewhat overlapped. The case of the gold(I) complex  $\text{Ausac}_2$  features a different situation where ligand exchange is the main molecular mechanism

accounting for adduct formation. In our case, it is evident that upon interactions with the protein both saccharinate ligands are displaced. Moreover, the presence of high concentrations of chloride in the medium may play a role in the overall reaction process.

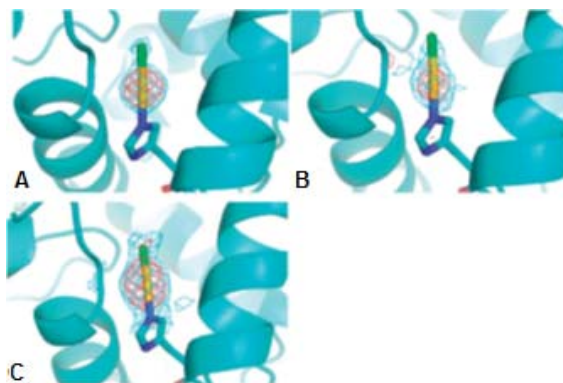
High resolution crystal structures (1.72–2.10 Å resolution) were solved for the three mentioned metal–protein adducts – i.e. HEWL-AuSac<sub>2</sub>, HEWL-Au<sub>2</sub>phen and HEWL-Auoxo6 . The structures have been deposited in the Protein Data Bank with codes 4LFP, 4LGK and 4LFX for HEWL-AuSac<sub>2</sub>, HEWL-Au<sub>2</sub>phen and HEWL-Auoxo6, respectively. Most notably and rather surprisingly, these three adducts turned out to be almost indistinguishable as described below. In all cases, the overall protein conformation was not significantly affected by gold binding implying that HEWL structure in the complexes is nearly identical to that of native protein (PDB code 193L), with rootmean square deviation in positions of the CA atoms within the range 0.20–0.29 Å. The structure of the adduct HEWL-AuSac<sub>2</sub> is depicted in figure 3.



Overall structure of HEWL-AuSac<sub>2</sub>, which is very similar to those of HEWL Auoxo6 and HEWL-Au<sub>2</sub>phen. In all cases, Au(I) is covalently attached to the His15 NE2 atom and to a Cl<sup>-</sup> ion. (figure 3)

Very interestingly, for all three crystal structures, difference Fourier electron-density maps ( $F_o - F_c$ ) invariantly revealed one  $>10\sigma$  peak near His15 (figure 4A–C), which has been attributed to the presence of a gold ion. These peaks reside close to a lower peak, which – in consideration of the dependence of HEWL crystal growth in the presence of NaCl and in previous findings[12] – was modelled as a Cl<sup>-</sup> ion. In all cases,

the coordination geometry around the gold center is approximately linear, which strongly suggests that the oxidation state of Au is +1. The Au–NE2 (His15) distances [average: 2.2 (0.1) Å] and the NE2–Au–Cl angle [average: 174 (5)°] are in good agreement with the expected value. Structural refinements suggested an occupancy value for the Au atom to be around 0.4–0.6, thus representing a quite relevant degree of protein metalation. The electron density maps were carefully inspected to reveal additional Au binding sites, but no other features of this kind were detected.



Details of the binding site of Au(I) in HEWL-AuSac2 (A), HEWL-Auoxo6 (B) and HEWL-Au<sub>2</sub>phen (C) showing the Au ion bound to His15 and Cl<sup>-</sup> ion. 2Fo – Fc electron density maps are contoured at 5s (red) and 3s (cyan) levels in the case of HEWL-AuSac2 and 3s (red) and 1.5s (cyan) levels in the other two cases. (figure 4)

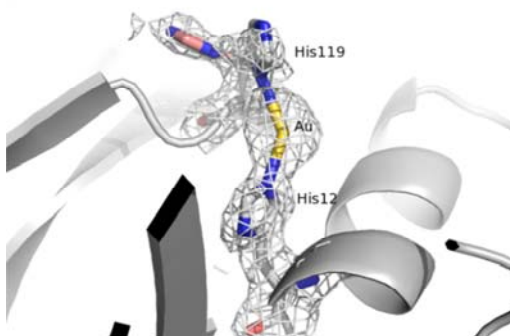
## 2.2 Gold-Based drugs and RNase A

Specifically, we reacted RNase A with a few representative medicinal gold compounds and tried to characterise structurally the gold drug–protein adducts that might have been formed in these reactions. Since RNase A crystals are particularly well suitable for soaking experiments, gold drug–protein adducts were obtained by soaking pre-grown monoclinic RNase A crystals in solutions containing three different gold compounds Auoxo6, Au<sub>2</sub>phen and Auranofin (figure 1). X-ray diffraction data have been collected for these crystals; structures have been solved and refined. Inspection of electron density maps revealed that a clear derivative has been obtained only in the case of Auoxo6.

The structure of the RNase A–Auoxo6 derivative was solved at 2.25 Å resolution. The overall structure of the two molecules in the asymmetric unit is not significantly affected by the soaking procedure (CA root mean square deviation, RMSD, from the starting model is as low as 0.4–1.3 Å), although a subtle but significant modification of the protein structure is induced by the gold binding. A gold atom (occupancy 0.5) is

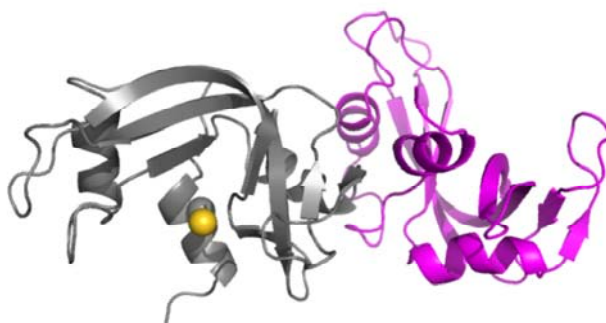
## Interactions of Gold-Based Drugs with proteins: a structural perspective

clearly detected in the active site of molecule A. The occupancy of 0.5 is an indication of a good degree of protein metalation. The Au atom is simultaneously coordinated to imidazoles of His12 and His119. The coordination geometry is nearly linear, strongly indicating that gold is in the +1 oxidation state (figure 5). These observations point out that, upon reaction with RNase A, Auoxo6 undergoes breakdown, ligand detachment and gold(III) reduction, producing gold(I) species.



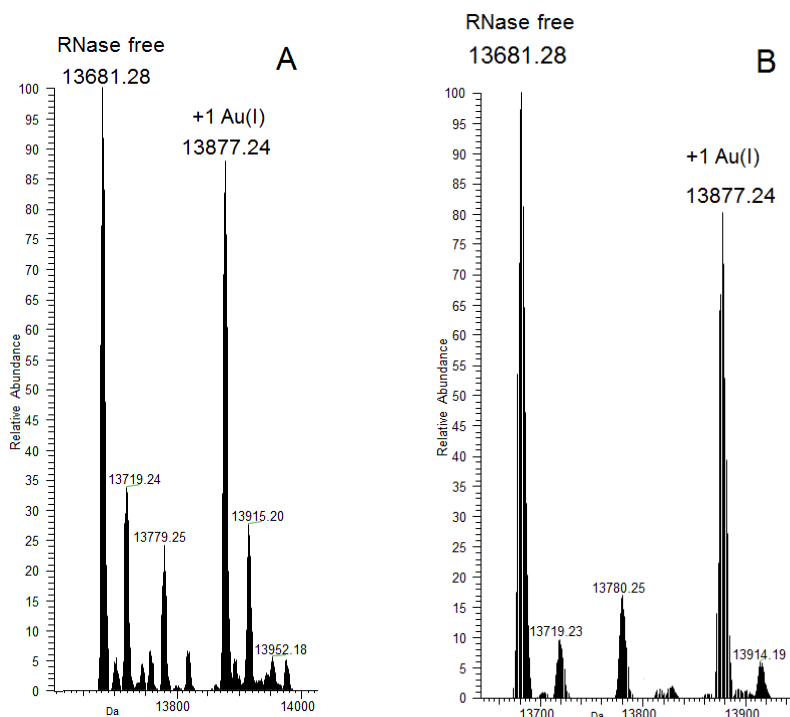
Structural details of the gold center in the RNase A–gold adduct. The 2Fo Fc electron density map is contoured at 1s. His119 adopts two distinct conformations. (figure 5 )

In the present case, gold(I) ions coordinate to the two His residues located in the molecule A active site affording the described derivative. Molecule A of RNase A–Auoxo6 has been superimposed onto molecule B. The superimposed Ca traces are shown in figure 6 The structural superimposition clearly reveals that the binding of the gold is associated with an opposite shift of the b-sheets. The movement of b-sheets is a dynamic feature of the RNase A structure that has been already associated with substrate binding and catalytic action [28,29,30].



Ribbon representation of the asymmetric unit of RNase A-Auoxo6 crystals. The two RNase A molecules are coloured grey and magenta, respectively. The gold ion is shown as a yellow sphere.(figure 6)

The above intriguing structural data prompted us to perform further studies in solution. Mass spectrometry experiments of the protein samples reacted with Auoxo6 were carried out both at physiological pH and at pH 5.5, according to previously reported protocols. Under the applied solution conditions, ESI MS spectra revealed that RNase A reacts extensively with Auoxo6 and forms a monometalated derivative containing a bare gold(I) ion bound to the protein (figure 7). Thus, solution studies carried out in a buffer appropriate for ESI MS experiments offer further evidence of gold(III) reduction to gold(I).



LTQ-orbitrap ESI mass spectra of Auoxo6 dissolved in 20 mM ammonium acetate buffer at pH 5.5 (A) and at pH 7.4 (B) in the presence of RNase A after 24 h incubation. The protein concentration is  $10^{-4}$  M with a metal complex to protein molar ratio of 3 : 1. Adducts are formed by 1  $\text{Au}^+$  bound to RNase A.(figure 7).

Overall, with the present investigation, we have succeeded in determining the crystal structure of the adduct formed between a medicinal gold(III) compound and RNase A; the structural results are in agreement with those obtained in solution through ESI MS. These results contribute to extending the structural and mechanistic information on gold–protein interactions that is still quite limited.



### 3. Discussion

Comparative analysis of the above described high resolution crystal structures permits highlighting some relevant features in the reactions of medicinal gold compounds with HEWL, thus providing a rather accurate description of the underlying protein metalation processes. The main aspects that emerge from our crystallographic results are summarised below:

(i) Three structurally different medicinal gold compounds i.e. AuSac<sub>2</sub>, Au<sub>2</sub>phen and Auoxo6 afforded – upon reaction with HEWL – the same metal–protein adduct bearing a gold(I) ion tightly anchored to His15 with Cl<sup>-</sup> as the second ligand. Such an adduct, which is the common end-product of three independent reactions, appears to be highly stable. In the case of the reaction with RNase Auoxo6, breaks down and undergoes reduction, loses its bipyridyl ligands and produces reactive gold(I) species; in turn, the latter species tightly bind RNase A at the level of the two catalytic histidines affording a stable monometalated derivative.

(ii) The binding of [AuCl] fragments to His15 did not significantly affect the overall structure of the protein: only minor local changes were observed. The same case for RNase, where the overall structure of protein is not affected by interaction with this gold(I) species;

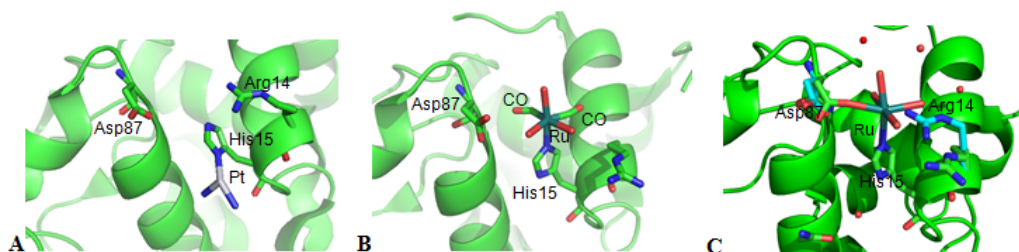
(iii) HEWL-gold adducts were formed in different amounts that depend on the nature of the starting gold compound: this implies that some gold compounds are very efficient in metalating HEWL while others are nearly ineffective. These results are in agreement with those of a previous ESI-MS study [25,26]; the poor reactivity of Aubipyc and Auranofin with HEWL prevented us from obtaining structural information on the respective adducts.

(iv) The three gold compounds forming HEWL adducts undergo extensive degradation and react with this protein confirming their prodrug nature; no evidence of the presence of the original metal ligands is indeed gained from the crystal structures of the respective adducts. The same result, i.e. extensive ligand loss, has been obtained in previous ESI-MS studies [25,26]. Of particular interest is the case of the two dinuclear gold(III) compounds where not only the whole structural organisation of the starting metal complexes is completely lost but also the metal is reduced owing to the appreciable oxidising character of these gold(III) centers. It follows that protein bound gold is invariantly found in the oxidation state +1 independently of the nature of the starting compounds, as documented by its linear coordination. Our data suggest that in the buffer used for the crystallization experiments, Auoxo6 and Au<sub>2</sub>phen undergo large chemical transformations. Probably, gold(III) is first reduced and released from its

original ligands, and then it binds the protein, though the two latter processes – ligand release and protein binding – may be somewhat overlapped.

(v) Gold binding is observed only at the level of His15 pointing out that the interaction of gold with HEWL is highly selective. In spite of the reported broad reactivity of gold species toward a variety of nucleophiles and the presence of various methionine residues, no other binding site of HEWL was affected by these gold compounds, even in the presence of a large stoichiometric excess of the metallodrug.

Notably, His15 was previously implicated in the interaction of HEWL with various other metals or metallodrugs [13] including cisplatin [27]. A comparison between our findings and those obtained by studying the interactions between HEWL and Ru or Pt containing drugs is reported in figure 4. Interestingly, in spite of the pronounced differences in the chemistry of these three metal centers (gold, platinum and ruthenium) in all cases metal binding preferentially occurs at His 15



Interactions between HEWL and metal (Pt and Ru) containing drugs. In all cases, metal binding preferentially occurs at His 15. A) complex with cisplatin, pdb code 2I6Z [31]; Pt(II) has occupancy equal to 0.3. It is bound to the the ND1 of His 15 and to the nitrogens of two ammonia molecules in cisplatin. The fourth ligand is not detected. B) complex with [fac-Ru(CO)(3)Cl( $\kappa$ (2)-H(2)NCH(2)CO(2))], a Ru(III) containing CO releasing molecule, pdb code 2XJW; C) complex with AziRu, a Ru(III) containing complex analogous to NAMI-A, pdb code 4J1A [32]. In the last two cases, Ru(III) is coordinated to NE2 atom of His15. (figure 4)

The high quality of the reported structural data underlines the pivotal role of protein metalation in the mode of action of metal based drugs and contributes to the elucidation of the protein metalation mechanism at the molecular level. Clear evidence is offered that metal containing fragments (the [AuCl] moiety in our case) – derived from a few gold-based drugs – bind tightly and selectively the model protein HEWL affording the same type of monometalated adduct of Au(I). Interestingly, in the course

of the reaction, the various gold complexes lose all their original ligands so that only the [AuCl] fragment is eventually bound to HEWL.

Specifically, in the case of Auoxo6-RNase, it can be inferred that the anti-tumor activity of Auoxo6 probably arises from tight inhibition of target enzymes by Au(I) ions originated from gold(III) reduction. In particular, the anti-tumor activity can be the result of the formation of stable gold(I)-thiolate-selenolate complexes leading to inhibition of relevant target enzymes such as thioredoxin reductase or peroxiredoxin.

The concept that selected gold drugs behave as extreme prodrugs capable of delivering the naked metal ion to their protein targets is thus experimentally supported. The here-described metal-protein interactions are crucial for understanding the molecular mechanisms of “functional” metal-based drugs.

#### 4. Experimental

##### *Materials*

Hen egg white lysozyme (HEWL- L7651), Ribonuclease A from bovine pancreas type XII-A (RNase 055K7695), sodium citrate, PEG4K, sodium chloride, sodium acetate, acetic acid were purchased from Sigma. Au<sub>2</sub>phen, Auoxo6, Aubipyc and AuSac<sub>2</sub> were synthesized and characterized as described previously. Auranofin (EI-206-0100) was purchased from Vinci-Biochem.

##### *Methods*

##### *UV-vis spectrophotometric studies*

To assess the compound interactions with HEWL, spectrophotometric studies were performed by a Varian Cary 50 Bio UV-vis spectrophotometer. 10 μl of freshly prepared concentrated solutions (10<sup>-2</sup>M) of the individual complex in a proper solvent (DMSO) for Auoxo6 and Au<sub>2</sub>phen; ethanol for Auranofin, and acetone for AuSac<sub>2</sub>) were added to a solution of HEWL (10<sup>-5</sup>M) in 50 mM acetate buffer and 1M NaCl at pH 4.5. The concentration of each gold compound in the final sample was 10<sup>-4</sup> M. Electronic spectra of HEWL were recorded before and after the addition of each gold compound at a stoichiometric ratio of 10:1 (metal to protein). Each sample was monitored by collection of the electronic spectra for 24 hours at room temperature.

### *Crystallization and X-ray diffraction data collection*

Crystals of HEWL-gold compound adducts were obtained by both co-crystallization and soaking procedures. Ligand-free HEWL crystals were grown at 293 K using the hanging drop vapour diffusion method, 1.0-1.4 M NaCl as a precipitating agent in 0.050 M acetate buffer at pH 4.5 and protein concentration 15 mg/mL. Crystals of 0.3-0.4 mm size appeared within 24 hours. After two days, crystals were soaked in a solution formed by gold based drugs dissolved in a proper solvent (DMSO for Aubipyc, Auoxo6 and Au<sub>2</sub>phen; ethanol for Auranofin, and acetone for AuSac<sub>2</sub>) and 1.2 M NaCl in the same buffer. At the final, concentrations of metallodrugs and protein were in at least in 1:1 ratio. Crystals of HEWL in the presence of the gold-based drugs have been also obtained by co-crystallization using complex in a 1:1 ratio.

Crystals of RNase A-gold compound complexes were obtained by soaking procedures. Ligand-free RNase A crystals were grown at 298 K using the hanging drop vapour diffusion method, protein concentration 15 mg/mL and a precipitant solution containing 20% PEG4000 and 20 mM sodium citrate buffer pH 5.0. Crystals appeared within 7 days. After two weeks, crystals were soaked for two weeks in a solution of gold-based drugs dissolved in a proper solvent (DMSO for Auoxo6 and Au<sub>2</sub>phen; ethanol for Auranofin) and in 50 mM sodium citrate buffer pH 5.0. At the final, concentrations of metallodrugs and protein were in at least 1:1 ratio. All the crystals were fished with nylon loops and flash-frozen at 100 K using nitrogen gas produced by an Oxford Cryosystem (and maintained at 100 K during the data collection) without cryoprotectant, using a procedure recently developed [33]. This procedure partly dehydrates the crystals, enhancing in some cases the resolution of X-ray diffraction data [34] Complete data sets were collected at the CNR Institute of Biostructure and Bioimages, Naples, Italy using a Saturn944 CCD detector equipped with CuK $\alpha$  X-ray radiation from a Rigaku Micromax 007 HF generator. Data were processed and scaled using HKL2000 [35]. The structures were solved with Fourier difference method, using the PDB file 4L55 [36], without water molecules and ligands, as the starting model. The refinement was carried out with CNS [37] or REFMAC [38], model building and map inspections were performed using O [39] and COOT [40] Structure validation has been carried out using Procheck [41]. Coordinates and structure factors for the RNase A-Auoxo6 adduct have been deposited in the Protein Data Bank (PDB code 4MXF).

### *Electrospray Mass Spectrometry*

Metal complex/protein adducts were prepared by mixing equivalent amounts of the RNase A ( $10^{-4}$  M) in 20 mM ammonium acetate buffer (AmAc), pH 7.4 or pH 5.5.

## Interactions of Gold-Based Drugs with proteins: a structural perspective

Then gold(III) complexes were added (3:1 metal/protein ratio) to the solution and incubated for 24 hours at room temperature. After a 10-fold dilution with water, ESI-MS spectra were recorded by direct introduction at 30  $\mu\text{l}/\text{min}$  flow rate in an Orbitrap high-resolution mass spectrometer (Thermo, San Jose, CA, USA), equipped with a conventional ESI source. The working conditions were the following: spray voltage 3.1 kV, capillary voltage 45 V and capillary temperature 220° C. The sheath and the auxiliary gases were set, respectively, at 17 (arbitrary units) and 1 (arbitrary units). For acquisition, Xcalibur 2.0. software (Thermo) was used and monoisotopic and average deconvoluted masses were obtained by using the integrated Xtract tool. For spectrum acquisition a nominal resolution (at  $m/z$  400) of 100,000 was used.

## References

- [1] S. Nobili, E. Mini, I. Landini, C. Gabbiani, A. Casini, L. Messori, *Med. Res. Rev.*, 2010, 30, 550-580.
- [2] (a) R. W.-Y. Sun, C. K.-L. Li, D.-L. Ma, J. J. Yan, C.-N. Lock, C.-H. Leung, N. Zhu, C.-M. Che, *Chem.–Eur. J.*, 2010, 16, 3097-3113; (b) K. H.-M. Chow, R. W.-Y. Sun, J. B. B. Lam, C. K.-L. Li, A. Xu, D.-L. Ma, R. Abagyan, Y. Wang, C.-M. Che, *Cancer Res.*, 2010, 70, 329-337; (c) C. T. Lum, Z. F. Yang, H. J. Li, R. W.-Y. Sun, S. T. Fan, R. T. Poon, M. C. M. Lin, C.-M. Che, H. F. Kung, *Int. J. Cancer*, 2006, 118, 1527-1538; (d) Y. Wang, Q. Y. He, R. W.-Y. Sun, C.-M. Che, J. F. Chiu, *Cancer Res.*, 2005, 65, 11553-11564; (e) C.-M. Che, R. W.-Y. Sun, W.-Y. Yu, C.-B. Ko, N. Zhu, H. Sun, *Chem. Commun.*, 2003, 1718-1719.
- [3] (a) L. Cattaruzza, D. Fregona, M. Mongiat, L. Ronconi, A. Fassina, A. Colombatti, D. Aldinucci, *Int. J. Cancer*, 2011, 128, 206-215; (b) V. Milacic, D. Chen, L. Ronconi, K. R. Landis-Piwowar, D. Fregona, Q. P. Dou, *Cancer Res.*, 2006, 66, 10478-1486; (c) L. Ronconi, L. Giovagnini, C. Marzano, F. Bettio, R. Graziani, G. Pilloni, D. Fregona, *Inorg. Chem.*, 2005, 44, 1867-1871; (d) L. Giovagnini, L. Ronconi, D. Aldinucci, D. Lorenzon, S. Sitran, D. Fregona, *J. Med. Chem.*, 2005, 48, 1588-1595; (e) D. de Vos, S. Y. Ho, E. R. Tiekink, *Bioinorg. Chem. Appl.*, 2004, 2, 141-154.
- [4] (a) M. Coronello, E. Mini, B. Caciagli, M. A. Cinellu, A. Bindoli, C. Gabbiani, L. Messori, *J. Med. Chem.*, 2005, 48, 6761-6765; (b) L. Messori, G. Marcon, M. A. Cinellu, M. Coronello, E. Mini, C. Gabbiani, P. Orioli, *Bioinorg. Med. Chem.*, 2004, 12, 6039-6043 (c) G. Marcon, S. Carotti, M. Coronello, L. Messori, E. Mini, P. Orioli, T. Mazzei, M. A. Cinellu, G. Minghetti, *J. Med. Chem.*, 2002, 45, 1672-1677.
- [5] (a) R. W.-Y. Sun, C.-N. Lok, T. T.-H. Fong, C. K.-L. Li, Z. F. Yang, T. Zou, A. F.-M. Siu, C.-M. Che, *Chem. Sci.*, 2013, 4, 1979-1988; (b) J.-J. Zhang, R. W.-Y. Sun, C.-M. Che, *Chem. Commun.*, 2012, 48, 3388-3390; (c) J.-J. Zhang, W. Lu, R. W.-Y. Sun, C.-M. Che, *Angew. Chem., Int. Ed.*, 2012, 51, 4882-4886; (d) J. J. Yan, A. L.-F. Chow, C. H. Leung, R. W.-Y. Sun, D. L. Ma, C.-M. Che, *Chem. Commun.*, 2010, 46, 3893-3895; (e) C. K.-L. Li, R. W.-Y. Sun, S. C.-F. Kui, N. Zhu, C.-M. Che, *Chem. Eur. J.*, 2006, 12, 253.
- [6] (a) M. A. Cinellu, L. Maiore, M. Manassero, A. Casini, M. Arca, H.-H. Fiebig, G. Kelter, E. Michelucci, G. Pieraccini, C. Gabbiani, L. Messori, *ACS Med. Chem. Lett.*, 2010, 1, 336-339; (b) C. Gabbiani, A. Casini, L. Messori, A. Guerri, M. A. Cinellu, G. Minghetti, M. Corsini, C. Rosani, P. Zanello, M. Arca, *Inorg. Chem.*, 2008, 47, 2368-

2379; (c) A. Casini, M. A. Cinellu, G. Minghetti, C. Gabbiani, M. Coronello, E. Mini, L. Messori, *J. Med. Chem.*, 2006, 49, 5524-5531.

[7] (a) T. Zou, C. T. Lum, S. S.-Y. Chui, C.-M. Che, *Angew. Chem., Int. Ed.*, 2013, 52, 2930-2933; (b) R. Rubbiani, S. Can, I. Kitanovic, H. Alborzinia, M. Stefanopoulou, M. Kokoschka, S. Mo¨nchgesang, W. S. Sheldrick, S. Wo¨lfl, I. Ott, *J. Med. Chem.*, 2011, 54, 8646-8657; (c) M. W. Baker, P. J. Barnard, S. J. Berners-Price, S. K. Brayshaw, J. L. Hickey, B. W. Skelton, A. H. White, *Dalton Trans.*, 2006, 14(30), 3708-3715.

[8] T. Gianferrara, I. Bratsos, E. Alessio, *Dalton Trans.*, 2009, 7588-7598.

[9] C. K. Mirabelli, C. M. Sung, J. P. Zimmerman, D. T. Hill, S. Mong, S. T. Crooke, *Biochem. Pharmacol.*, 1986, 35, 1427-1433.

[10] (a) C. Marzano, V. Gandin, A. Folda, G. Scutari, A. Bindoli, M. P. Rigobello, *Free Radicals Biol. Med.*, 2007, 42, 872-881; (b) E. Schuh, C. Pflüger, A. Citta, A. Folda, M. P. Rigobello, A. Bindoli, A. Casini, F. Mohr, *J. Med. Chem.*, 2012, 55, 5518-5528.

[11] A. Pratesi, C. Gabbiani, M. Ginanneschi, L. Messori, *Chem. Commun.*, 2010, 46, 7001-7003.

[12] (a) S. Urig, K. Fritz-Wolf, R. Re´au, C. Herold-Mende, K. To´th, E. Davioud-Charvet, K. Becker, *Angew. Chem., Int. Ed.*, 2006, 45, 1881-1886; (b) H. Wei, Z. Wang, J. Zhang, S. House, Y.-G. Gao, L. Yang, H. Robinson, L. H. Tan, H. Xing, C. Hou, I. M. Robertson, J.-M. Zuo, Y. Lu, *Nat. Nanotechnol.*, 2011, 6, 93-97; (c) A. Ilari, P. Baiocco, L. Messori, A. Fiorillo, A. Boffi, M. Gramiccia, T. Di Muccio, G. Colotti, *Amino Acids*, 2012, 42, 803-811.

[13] (a) A. Vergara, G. D'Errico, D. Montesarchio, G. Mangiapia, L. Paduano, A. Merlino, *Inorg. Chem.*, 2013, 52, 4157-4159; (b) M. J. Panzner, S. M. Bilinovich, W. J. Youngs, T. C. Leeper, *Chem. Commun.*, 2011, 47, 12479-12481; (c) S. Abe, M. Tsujimoto, K. Yoneda, M. Ohba, T. Hikage, M. Takano, S. Kitagawa, T. Ueno, *Small*, 2012, 8, 1314-1319; (d) J. R. Helliwell, S. W. Tanley, *Acta Crystallogr., Sect. D*, 2013, 69, 121-125.

[14] F. M. Richards and H. W. Wyckoff, in *The Enzymes*, ed. P. D. Boyer, Academic Press, San Diego, 1971, vol. IV, pp. 647-806.

[15] R. T. Raines, *Chem. Rev.*, 1998, 98, 1045-1066.

[16] G. R. Marshal, J. A. Fengand, D. J. Kuster, *Biopolymers*, 2008, 90, 259-277.


[17] G. D'Alessio and J. F. Riordan, *Ribonucleases. Structures and functions*, Academic Press, New York, 1997

- [18] B. Gutte, R. B. Merryfield, *J. Biol. Chem.*, 1971, 246, 1922-1941.
- [19] G. Kartha, J. Bello, D. Harker, *Nature*, 1967, 213, 862-865.
- [20] A. Merlino, F. Sica, L. Mazzarella, *J. Phys. Chem.*, 2007, 111, 5483-5486.
- [21] R. Balakrishnan, N. Ramasubbu, K. I. Varughese, R. Parthasarathy, *Proc. Natl. Acad. Sci. U. S. A.*, 1997, 94, 9620-9625.
- [22] A. Vergara, D. Montesarchio, I. Russo Krauss, L. Paduano, A. Merlino, *Inorg. Chem.*, 2013, 52, 10714-10716.
- [23] A. A. Isab, P. J. Sadler, *Biochim. Biophys. Acta*, 1977, 492, 322-330.
- [24] T. Maruyama, S. Sonokawa, H. Matsushita, M. Goto, *J. Inorg. Biochem*, 2007, 101, 180-186.
- [25] L. Maiore, M. A. Cinellu, E. Michelucci, G. Moneti, S. Nobili, I. Landini, E. Mini, A. Guerri, C. Gabbiani, L. Messori, *J. Inorg. Biochem.*, 2011, 105, 230-237.
- [26] A. Casini, G. Kelter, C. Gabbiani, M. A. Cinellu, G. Minghetti, D. D. Fregona, H. H. Fiebig, L. Messori, *JBIC, J. Biol. Inorg. Chem.*, 2009, 14, 1139-1149.
- [27] (a) A. Casini, G. Mastrobuoni, C. Temperini, C. Gabbiani, S. Francese, G. Moneti, C. T. Supuran, A. Scozzafava, L. Messori, *Chem. Commun.*, 2007, 156-158; (b) S.W. M. Tanley, A.M. Schreurs, L.M. J. Kroon-Batenburg, J. Meredith, R. Prendergast, D. Walsh, P. Bryant, C. Levy, J. R. Helliwel, *Acta Crystallogr., Sect. D*, 2012, 68, 601-612.
- [28] L. Vitagliano, A. Merlino, A. Zagari, L. Mazzarella, *Proteins*, 2002, 46, 97-104.
- [29] A. Merlino, L. Vitagliano, M. A. Ceruso, A. Di Nola, L. Mazzarella, *Biopolymers*, 2002, 65, 274-283.
- [30] A. Merlino, L. Vitagliano, M. A. Ceruso, L. Mazzarella, *Proteins*, 2003, 53, 101-110.
- [31] A. Casini, G. Mastrobuoni, C. Temperini, C. Gabbiani, S. Francese, G. Moneti, C.T. Supuran, A. Scozzafava, L. Messori, *Chem. Commun*, 2007, 156-158
- [32] A. Vergara, G. D'Errico, D. Montesarchio, G. Mangiapia, L. Paduano, A. Merlino, *Inorg Chem* 2013, 52, 4157-4159
- [33] E. Pellegrini, D. Piano, M. W. Bowler *Acta Cryst.D* 2011, 67, 902-906.
- [34] I. Russo Krauss, F. Sica, C.A. Mattia, A. Merlino. *Int. J. Mol. Sci.* 2012, 13, 3782-3800.
- [35] Z. Otwinowski, W. Minor. *Methods Enzymol.* 1997, 276, 307-326.



- [36] A. Vergara, D. Montesarchio, I. Russo Krauss, L. Paduano, A. Merlino. *Inorg Chem* 2013, 52, 10714-10716.
- [37] A.T. Brunger, P.D. Adams, G.M. Clore, P. Gros, R.W. Grosse-Kunstleve, J.S. Jiang, J. Kuszewski, N. Nilges, N.S. Pannu, R.J. Read, L.M. Rice, T. Simonson, G.L. Warren, *Acta Cryst. D*. 1998, 54, 905-921.
- [38] G.N. Murshudov, P. Skubak, A.A. Lebedev, N.S. Pannu, R.A. Steiner, R.A. Nicholls, M.D. Winn, F. Long, A.A. Vagin. *Acta Cryst. D*, 2011, 67, 355-367.
- [39] T.A. Jones, J.Y. Zou, S.W. Cowan, M. Kjeldgaard, *Acta Cryst. D*. 1991, 56, 714-721.
- [40] P. Emsley, K. Cowtan, *Acta Cryst. D*. 2004, 60, 2126-2132.
- [41] R.A. Laskowski, M.W. Macarthur, D.S. Moss, J.M. Thornton, *J. Appl. Cryst.* 1993, 26, 283-291.





## **Chapter 5**

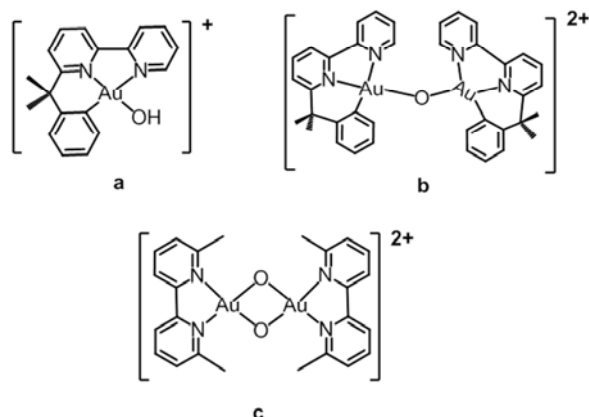
### **Interactions of Selected Gold(III) Complexes with DNA G Quadruplexes\***

\* The results presented in this chapter have been published in “Interactions of Selected Gold(III) Complexes with DNA G Quadruplexes” P. Gratteri, L. Massai, E. Michelucci, R. Rigo, L. Messori, M. A. Cinellu, C. Musetti, C. Sissi, C. Bazzicalupi.

### 1. Introduction

DNA G-quadruplexes are promising targets for the development of novel anticancer agents[1,2]. Indeed, solid evidences have now been gathered on their formation in living cells and their relevant role in cancer [3]. Consistently, well documented data relate efficient binding of small molecules to human telomeric G-quadruplex with efficient impairment of tumor growth and progression [4,5]. So far, several ligands, based on different scaffolds, have been tested for their affinity toward telomeric G-quadruplex. Recently, a great interest has been focused on the development of innovative metal based agents directed towards this target. Actually, this strategy provided several metal complexes highly effective in inducing G-quadruplex structures in G-rich regions and in stabilizing them; several examples for this kind of experimental approach are reported in the recent studies [6-9]. Most of the active metal complexes studied so far recognize the G-quadruplex motif by stacking over the terminal tetrads (the structural elements deriving from the pairing of four guanines). Such interaction is generally supported by a planar aromatic organic portion whereas the metal centre cooperates by neutralizing the central electron-dense channel generated by the carbonyl oxygens of the paired guanines[10]. Despite the strong interest toward targeting DNA G-quadruplexes with metal complexes, well testified by the growing number of reported active metal complexes, very few examples concern gold complexes [9,11].

During the last 15 years we have been working on the development of new gold based complexes as cytotoxic and prospective anticancer agents [12]. Their mechanisms of action appear to be variegate and not fully elucidated, still being a matter of intense debate in the scientific community. Interestingly, upon selection of proper organic ligands, the peculiar coordination properties of the gold(III) center allow the obtainment of metal complexes showing an almost co-planar localization of extended aromatic surfaces [13]. These complexes seem highly suitable for nucleic acid targeting, despite the preliminary studies on their interactions with double helix DNA revealed overall weak binding. [14].



Chemical structures of Aubipyc (a), Au<sub>2</sub>bipyc (b) and Auoxo6 (c). (chart 1)

Starting from these observations, we decided to explore whether a few representative gold(III) complexes selected from our internal library might bind tightly well-known G-quadruplex forming DNA sequences.

To this end, we chose three previously characterised gold(III) complexes, namely, [(bipy<sup>2Me</sup>)<sub>2</sub>Au<sub>2</sub>(μ-O)<sub>2</sub>][PF<sub>6</sub>]<sub>2</sub> (bipy<sup>2Me</sup> = 6,6'-dimethyl-2,2'-bipyridine) – Auoxo6, [15,16], Au[(bipy<sup>dmb</sup>-H)(OH)][PF<sub>6</sub>] (bipy<sup>dmb</sup>-H = deprotonated 6-(1,1-dimethylbenzyl)-2,2'-bipyridine) – Aubipyc [17] and Au<sub>2</sub>[(bipy<sup>dmb</sup>-H)<sub>2</sub>(μ-O)][PF<sub>6</sub>]<sub>2</sub> – Au<sub>2</sub>bipyc, [18] and these structures are schematically represented in Chart 1. Notably, the hydroxo complex Aubipyc is a gold(III) cyclometalated derivative and Au<sub>2</sub>bipyc its dinuclear oxo-bridged version. (Chart 1); on the other hand, Auoxo6 is a dinuclear gold(III) complex featuring a Au<sub>2</sub>O<sub>2</sub> “diamond core” linked to two bipyridine ligands. As a result, the three selected complexes explore different chemical spaces. These gold complexes manifest an acceptable solubility and stability profile in aqueous solutions for a few days at room temperature and physiological pH that render them suitable models for pharmaceutical applications. [19,21]

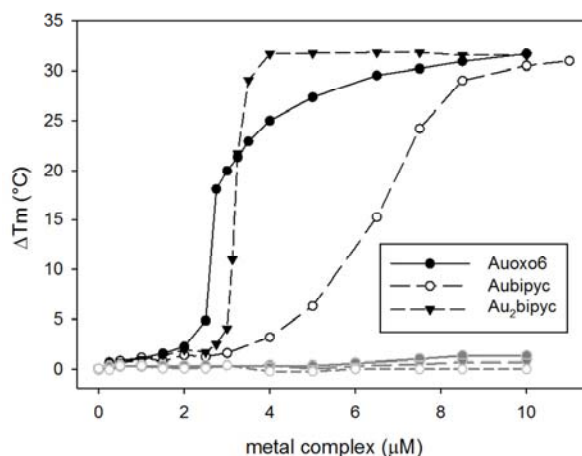
Interestingly, all of them exist in solution as cations, either monomeric (Aubipyc) or dimeric (Au<sub>2</sub>bipyc and Auoxo6); as such, they are expected to interact with polyanionic DNA sequences to different extents, according to their net charge. The cytotoxic properties of the three compounds were previously tested at Oncotest according to specific in home screening strategies, revealing that Auoxo6 exhibits the greatest cytotoxicity and a high selectivity [19,20]. Overall, the above mentioned properties make these metal complexes good starting models to define the potential of Au(III) complexes for G-quadruplex recognition. To perform our investigation, we used the human telomeric sequence as target G-quadruplex: its interactions with metal complexes were studied through different biophysical methods including DNA

melting, circular dichroism, SPR and ESI MS. For comparison purposes the interactions of the same metal compounds with a canonical DNA duplex were evaluated as well.

## 2. Results

### 2.1 The DNA thermal stabilization promoted by gold(III) complexes is a function of their structure and of nucleic acid folding.

The interactions of the selected gold(III) complexes with nucleic acids were first screened through a simple DNA melting assay in which the variations of the melting temperature of the polynucleotides were analysed as a function of the concentration of tested metal complexes. To preliminarily assess the target selectivity, the telomeric sequence HTS (d[AG3(T2AG3)3T]) and a double stranded DNA of the same length and composition, dsDNA, were comparatively assayed. As shown in figure 1, the tested gold(III) complexes produced a marked increase in DNA melting temperature only in the case of the G-quadruplex folded sequence; the extent of such stabilization is related to ligand concentration according to a sigmoidal relationship. At variance, no significant increment of the thermal stability was observed when the same ligands were added to the canonical double stranded DNA sequence. These observations suggest the occurrence of a unique interaction between the three gold(III) species and G-quadruplex DNA.



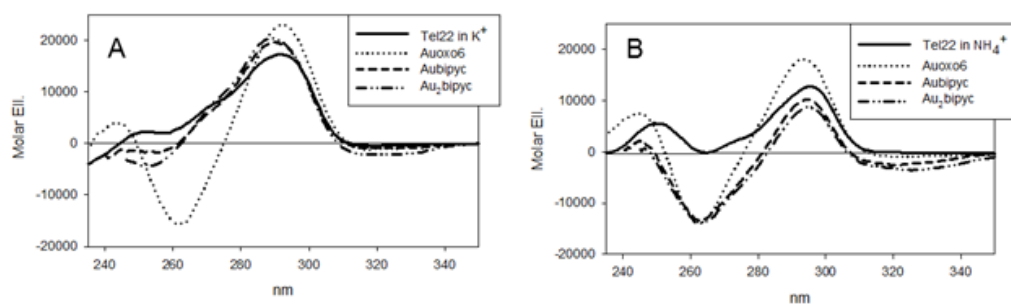
Changes of DNA melting temperature ( $\Delta T_m$ ) induced by increasing concentrations of tested metal complexes. Black and grey symbols refer to HTS and dsDNA, respectively. Errors were  $\pm 0.4$  °C. (figure 1)

Interestingly, the dinuclear complexes Auoxo6 and Au<sub>2</sub>bipyc appeared to be more efficient than mononuclear Aubipyc in stabilising G-quadruplex DNA. However, these results may be affected by temperature increments that can actually impair the stability of the tested metal complexes, *e.g.*, Au<sub>2</sub>bipyc, which can undergo partial hydrolysis, releasing two monomeric units of Aubipyc [19]. Consistently, when we compared the efficiency of Aubipyc and Au<sub>2</sub>bipyc in terms of monomeric species concentration, perfectly superimposed EC<sub>50</sub> values of 6.5 μM were found (figure 1). Thus, to better establish the reason for the apparent increased efficiency of the two bimetallic complexes, we used other analytical methods capable of preserving the chemical structure of the metal complexes. The hydrolysis of Au<sub>2</sub>bipyc is complete after 1 h at 50 °C, whereas it is quite less at room temperature even after 24 h [19].

## 2.2 Auoxo6 forms conserved complexes with telomeric G-quadruplex irrespectively of solution conditions.

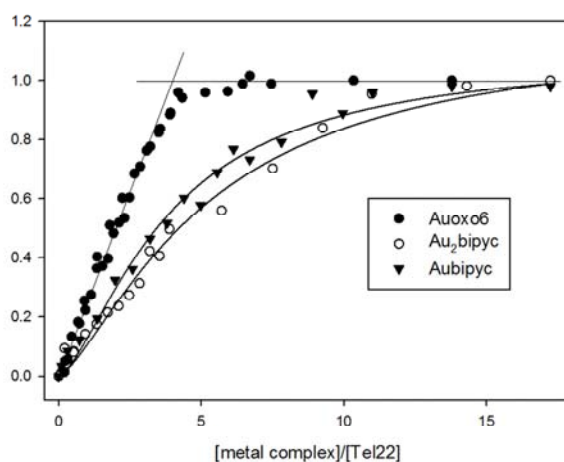
Accordingly, the interactions of the three gold(III) complexes with human telomeric DNA were subsequently analysed by mean of circular dichroism. Indeed, human telomeric sequences are well characterized in terms of their dichroic features; the CD technique allows monitoring perturbations in their folding topology caused by the presence of different ligands [22-24]. CD results obtained on Tel22 (d[AG<sub>3</sub>(T<sub>2</sub>AG<sub>3</sub>)<sub>3</sub>]), previously folded into an intramolecular G-quadruplex, upon addition of the tested Au(III) complexes, are synoptically shown in figure 2.

From these data it is evident that, in potassium containing solutions, addition of saturating concentrations of the three gold(III) complexes to Tel22 influenced the CD spectrum of the nucleic acid to different extents. In particular, Aubipyc and its corresponding dimeric species Au<sub>2</sub>bipyc scarcely affect the chiroptical features of telomeric G-quadruplex. Nevertheless, an increment of the positive contribution at 290 nm was always observed. This supports the view that some metallodrug-nucleic acid interaction is actually taking place though it does not produce relevant structural rearrangements of the G-quadruplex conformation.



CD spectra of 4  $\mu\text{M}$  Tel22 folded into intramolecular G-quadruplex in the absence (solid lines) or in the presence of 10 fold excess of the tested Au(III) metal complexes. Spectra were acquired in 10 mM Tris, 50 mM KCl (PANEL A) or 50 mM  $\text{NH}_4\text{Cl}$  (PANEL B), pH 7.5, 25  $^\circ\text{C}$ . (figure 2)

Distinctly, upon addition of Auoxo6, a more intense variation at 290 nm was induced; this feature is paired with the appearance of a strong negative band centred at about 260 nm. An almost superimposable spectrum was obtained when potassium ions were replaced by ammonium ions suggesting the formation of the same bound form irrespective of the ionic composition of the buffer. It is worth noting that a similar overall arrangement was promoted when Tel22 was treated with Aubipyc and  $\text{Au}_2\text{bipyc}$  in the presence of ammonium salts.

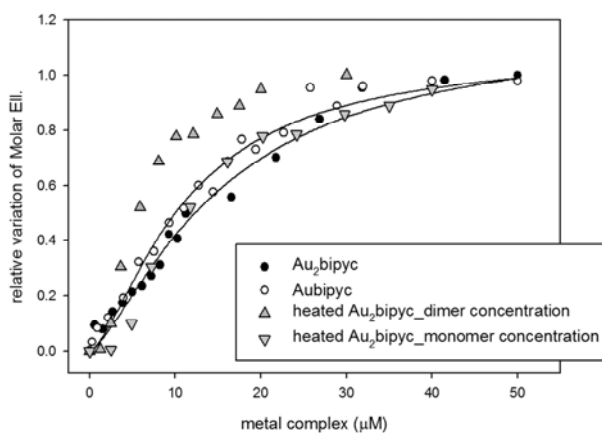


Relative variation the 260 nm CD signal recorded for Tel22 upon addition of the tested Au(III) metal complexes in 10 mM Tris, 50 mM KCl, pH 7.5, 25  $^\circ\text{C}$ . (figure 3)

The relative variations of the CD signals were then plotted as a function of tested metal



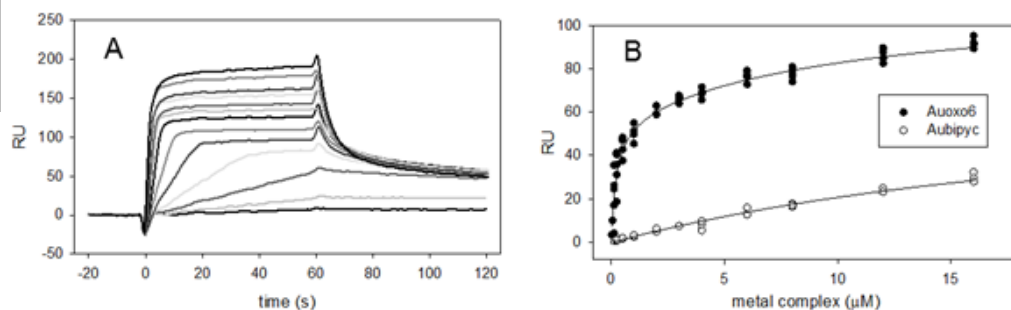
complexes concentrations (figure 3). Results are in good agreement with the above melting data since they confirm Auoxo6 as being the most efficient binder. An unexpected result arises from comparison of data relative to Aubipyc and Au<sub>2</sub>bipyc. Indeed, similar amount of the two metal complexes was required to fully convert Tel22 to the bound form. Conversely, when we hydrolysed Au<sub>2</sub>bipyc before use (by heating the metal complex solutions for 1 h at 50 °C), a good superposition to Aubipyc was achieved only taking into account the concentration of the monomers released. (figure 4)



Comparison of the relative variation the 260 nm CD signal recorded in 10 mM Tris, 50 mM KCl, pH 7.5, 25 °C, for Tel22 upon addition of fresh solution of Aubipyc or Au<sub>2</sub>bipyc or of a solution of Au<sub>2</sub>bipyc that was previously heated at 50 °C for 1 h. For this data set, results are reported as a function of added Au<sub>2</sub>(bipyc) or as concentration of released Aubipyc monomeric units. (figure 4)

### 2.3 Quantitative analysis of binding affinity of gold(III) complexes for telomeric G-quadruplex

The changes of the DNA CD signal promoted by Auoxo6 turned out to be almost linearly related to metal complex concentration until a plateau level is reached. This points out a high efficiency for the Auoxo6-Tel22 interaction while preventing a safe evaluation of the corresponding binding affinity from analysis of CD data. Thus, in order to properly quantify this parameter, SPR titrations were carried out. Tel22 was immobilized on the chip to guarantee proper DNA folding along the titrations.

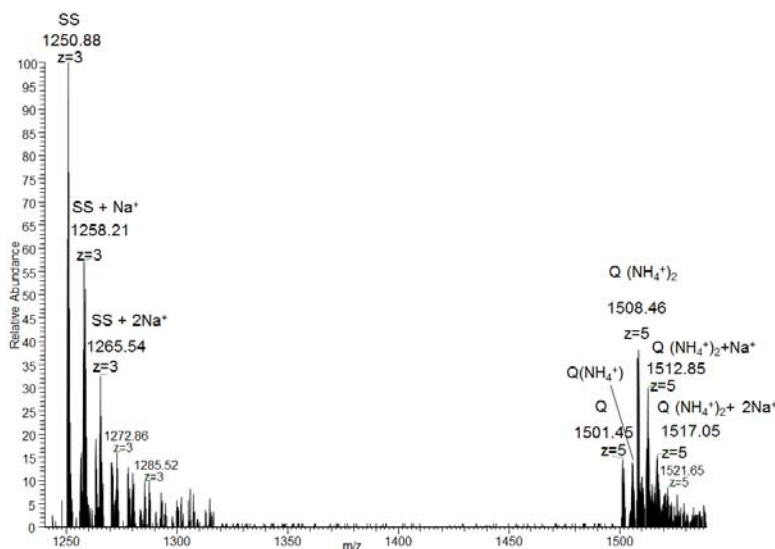


SPR sensograms obtained by flowing increasing concentrations of Auoxo6 (0-30  $\mu\text{M}$ ) on immobilized Tel22 (Panel A). The response units (RU) recorded at the steady state were plotted as a function of metal complexes concentrations in flow solutions (Panel B). Lines represent the best fit using the appropriate binding model described in the text. (figure 5)

Data summarized in figure 5 clearly support the occurrence of different binding profiles when Auoxo6 and Aubipyc are compared. The steady-state data were quantitatively analysed according to different binding modes. As far as Auoxo6 is concerned, the best fitting results were obtained when a two-sites model was applied. The analysis reveals the occurrence of a strong binding process ( $K_a 4.62 \pm 0.43 \cdot 10^6 \text{ M}^{-1}$ ) that is followed by a second one of far lower affinity. Analysis of the sensograms suggests that this second event may actually reflect aspecific binding to the target and not to the chip surface. Conversely, for Aubipyc, a binding affinity of  $K_a 4.1 \pm 0.5 \cdot 10^4 \text{ M}^{-1}$  was determined. This value reflects a very poor interaction with the telomeric sequence being well consistent with a comparable analysis performed using data acquired from CD titrations ( $5.0 \pm 0.4 \cdot 10^4 \text{ M}^{-1}$ ).

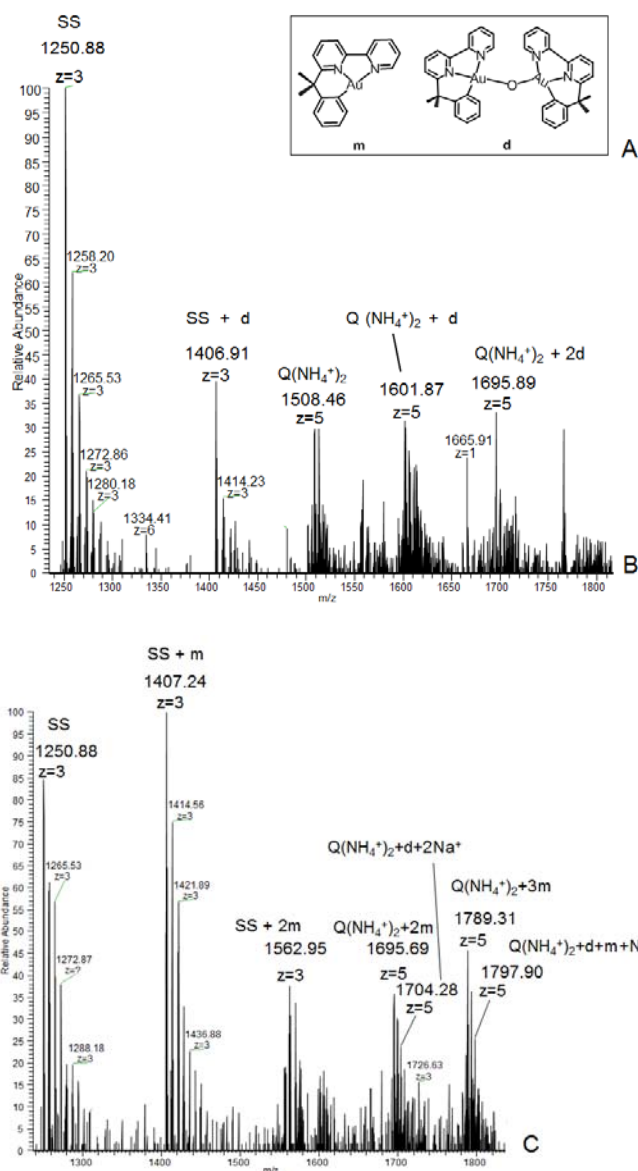
#### 2.4 Binding stoichiometry of gold(III) complexes toward telomeric G-quadruplex.

To fully characterize the interaction mode of our metal complexes with G-quadruplex DNA, ESI-mass spectrometry was also applied. To identify the metal complexes selectively bound only to G-quadruplex folded DNA we used as target the human telomeric sequence Tel12 (d[ $\text{TAG}_3\text{T}_2\text{AG}_3\text{T}$ ]). The latter sequence contains only two  $\text{T}_2\text{AG}_3$  repeats, so that it must dimerize in order to fold into a G-quadruplex. Accordingly, this makes possible to discriminate signals referring to the unfolded monomeric oligonucleotide from those related to dimeric G-quadruplex. For this analysis, samples were prepared in 60% EtOH. Indeed, this solvent promotes the formation of dimeric G-quadruplex, prevalently into a parallel conformation and allows improving signal detection [25] The ESI-mass spectrum obtained under these conditions is shown in figure 6. Two main peaks are easily detected which correspond to unfolded Tel12 and to dimeric G-quadruplex.



ESI-mass spectra of 20  $\mu\text{M}$  Tel12 annealed in 150 mM ammonium acetate in the presence of 60% EtOH (figure 6)

As confirmed by CD measurements, also in the conditions required for the MS experiments, the amounts of Aubipyc and Au<sub>2</sub>bipyc bound to the dimeric G-quadruplex were quite modest (data not shown). Nevertheless, when Tel12-complex solutions were analysed, new peaks corresponding to adducts with both the unfolded Tel12 as well as the G-quadruplex structure were detected (figure. 7). In particular, depending on the studied system, we found adducts containing the complex as such or fragments (m and d in figure 7A) related with the starting complex structure. Actually, when Tel12-Aubipyc solutions were analysed (figure 7B), new peaks corresponding to the fragment m bound both to unfolded Tel12 as well as to the G-quadruplex structure were detected. In particular, only one monomeric fragment was found associated to unfolded DNA and peaks corresponding to both the 1 : 1 and 1 : 2 G-quadruplex/Aubipyc adducts were identified.

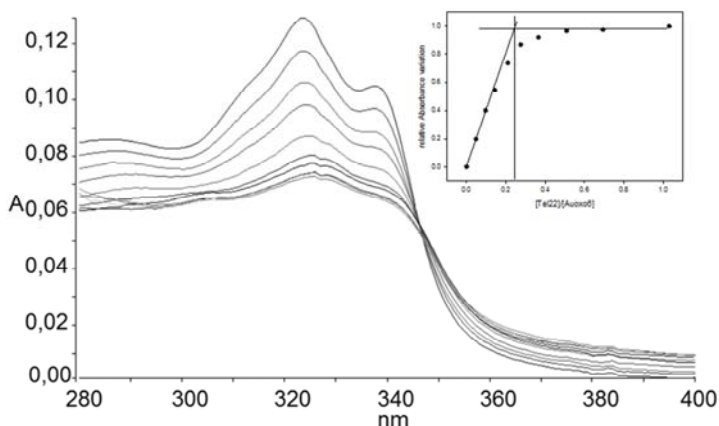


(A) Bound metallic species:  $m = [(bipy^{dmb}-H)Au]$  moiety;  $d = Au_2bipyC$ . (B) ESI-mass spectra of the adduct formed by Tel12 (SS = unfolded; Q = G-quadruplex) with AubipyC and (C)  $Au_2bipyC$ . Experimental conditions: 20  $\mu M$  in 150 mM ammonium acetate in the presence of 60% EtOH, 3 : 1 metal complex : G4 molar ratio. (figure 7)

The residual binding to the unfolded DNA fraction probably arises from the poor binding affinity of this metal complex to Tel12 and from its charged nature which allows unspecific interactions with the negatively charged unfolded nucleic acid. For

the Au<sub>2</sub>bipyc system (figure 7C) different peaks were observed. The expected peak corresponding to the 1:1 Au<sub>2</sub>bipyc/G-quadruplex (or d fragment/G-quadruplex) was detected; however, peaks corresponding to the monomeric fragment m bound to both G-quadruplex and unfolded Tel12, with different stoichiometry, were also observed. This finding suggests that the dimer may break down during the ionization process releasing two monomeric species.

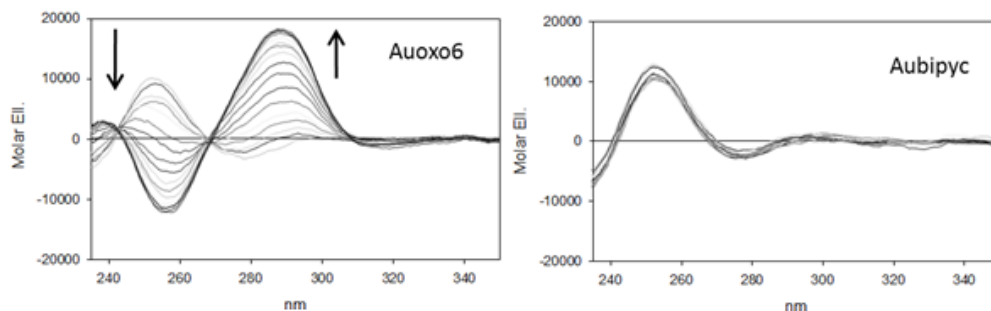
As far Auoxo6 is concerned, MS data indicated an even more extensive cleavage of the metal complex under the applied ionization conditions. In this case, an indication of the complex stoichiometry can be actually derived from the above presented CD titrations. Indeed, the intersection of the two lines describing the experimental data should occur at the 4:1 molar ratio of Auoxo6/Tel22, so defining the overall stoichiometry of the complex. The same result was derived by monitoring the UV absorption changes of the metal complex by increasing the concentration of the telomeric G-quadruplex (figure 8). Having characterized the absorption properties for the free and DNA-bound form of Auoxo6, we also evaluated the binding stoichiometry by ultrafiltration measurements on Tel22. Indeed, the large binding affinity of Auoxo6 for Tel22 should prevent significant loss of bound complex during the separation step. A full agreement with the three experimental results was found thus allowing us to infer that four molecules of Auoxo6 can be accommodated on the G-quadruplex conformation assumed by Tel22. Conversely, when the ultrafiltration measurements were repeated in the presence of Aubipyc, a stoichiometry of two metal complexes for each G-quadruplex was found. Although in this case the result can be underestimated due to the lower binding affinity of the metal complex for the target G-quadruplex, this finding is basically in line with the MS data.(data not shown).



Variation of the UV absorption spectrum of Auoxo6 upon addition of Tel22 in 10 mM Tris, 50 mM KCl, pH 7.5, 25 °C. Arrow indicates the direction of spectral variation upon increase of DNA concentration. In the insert, the relative variation of the absorbance readings at 323 nm is plotted vs the molar ratio of Tel22:Auoxo6.(figure 8)

### 2.5 Auoxo6 is efficient in inducing G-quadruplex formation

A relevant issue about G-quadruplex ligands concerns their ability to promote this nucleic acid conformation starting from a substantially unfolded sequence. To elucidate this point, additional CD titrations were carried out using the above mentioned telomeric sequence, Tel12, as target for the tested metal complexes. Suitably to our purposes, in the absence of cosolvents and at low molar concentration (4  $\mu\text{M}$ ), this sequence is poorly folded even in the presence of  $\text{K}^+$  or  $\text{NH}_4^+$ . Nevertheless, Auoxo6 was readily able to promote G-quadruplex assembly of Tel12; again, the final arrangement superimposed the one observed in the presence of Tel22 in  $\text{K}^+$  or  $\text{NH}_4^+$  containing solutions (figure 9). Conversely, Aubipyc as well as dimeric  $\text{Au}_2\text{bipyc}$  were not able to promote any relevant G-quadruplex formation from Tel12.



CD spectra of Tel12 in the presence of increasing metal complexes concentrations (0 – 50  $\mu\text{M}$ ) recorded in 10 mM Tris, 50 mM KCl, pH 7.5, 25 °C. Arrows indicated the main changes induced by Auoxo6. (figure 9)

### 3. Discussion

The interactions of three representative gold(III) complexes, namely, Aubipyc,  $\text{Au}_2\text{bipyc}$  and Auoxo6, with human telomeric DNA G-quadruplexes were analysed in depth through a variety of complementary physico-chemical methods. Remarkably, all three investigated metal complexes are able to bind the G-quadruplex form of telomeric DNA, whereas a canonical DNA double helix is not affected at all. This finding is in agreement with previous results obtained for similar gold(III) complexes that highlighted a poor interaction with calf-thymus DNA [14].

Interestingly, significant differences were highlighted among tested gold(III) complexes in their respective DNA binding modes. For Aubipyc and  $\text{Au}_2\text{bipyc}$ , we

found that both behave comparably at room temperature; in fact, they bind telomeric G-quadruplex with similar efficiency and force it to a common three-dimensional arrangement. Notably, upon increasing the temperature, the dimer may break down, releasing two monomeric species that interact independently with the nucleic acid. However, the most intriguing results were provided by Auoxo6. The latter compound showed the greatest binding affinity for human telomeric G-quadruplex under all applied conditions. Its binding affinity ( $K_a = 4.62 \pm 0.43 \times 10^6 \text{ M}^{-1}$ ) is in the usual range found for the metal complexes reported to be good G-quadruplex binders [11]. Our data point out an overall conserved structural arrangement of the G-quadruplex when it is bound by this metal complex. This indicates that Auoxo6 may show an interesting degree of selectivity among different G-quadruplex structures. Interestingly, it turned out that the Auoxo6 recognition process does not require DNA to be previously organized in the target secondary structure. This underscores the potential relevance of telomere targeting in the description of the overall cytotoxic profile of Auoxo6. In conclusion, the herein tested gold(III) complexes demonstrated peculiar DNA binding properties that might be mechanistically important and might also provide novel applications for this class of metal complexes.

#### 4. Experimental section

##### *Fluorescence melting studies*

Melting experiments were performed using a Roche LightCycler, using an excitation source at 488 nm and recording the fluorescence emission at 520 nm. Target DNA were the human telomeric sequence HTS d[AG<sub>3</sub>(T<sub>2</sub>AG<sub>3</sub>)<sub>3</sub>T], labeled with Dabcyl at the 5'-end and FAM at the 3'-end and a double stranded DNA d[G<sub>2</sub>ATGTGAGTGTGAGTGTGAG<sub>2</sub>]. DNA solutions (0.25 μM) were prepared in 50 mM potassium buffer (10 mM LiOH; 50 mM KCl pH 7.5 with H<sub>3</sub>PO<sub>4</sub>), slowly annealed and then added of increasing concentrations of tested derivatives. The resulting samples were slowly heated to 95 °C (1 °C/min). T<sub>m</sub> values were determined from the first derivatives of the melting profiles using the Roche LightCycler software. Each curve was repeated at least three times and errors were ± 0.4 °C. ΔT<sub>m</sub> were calculated by subtracting the T<sub>m</sub> value recorded in the presence of the ligand from the corresponding value in the absence of ligand.

*Circular dichroism measurements*

Circular dichroism spectra were recorded on a Jasco J-810 spectropolarimeter equipped with a Peltier temperature controller set at 25 °C. DNA substrates were the four-repeat human telomeric sequences Tel22 d[AG<sub>3</sub>(T<sub>2</sub>AG<sub>3</sub>)<sub>3</sub>] and the Tel12 d[TAG<sub>3</sub>T<sub>2</sub>AG<sub>3</sub>T]. DNA solutions (4 μM strand concentration) were prepared in 10 mM Tris, at pH 7.5 added of 50 mM KCl or NH<sub>4</sub>Cl. Before data acquisition, they were heated at 95 °C for 5 min and left to cool down at room temperature overnight. The spectra of nucleic acid alone and in the presence of increasing ligand concentrations (0-20 μM) were acquired using a 10 mm path-length cell. Each reported spectrum represents the average of 3 scans recorded with 1 nm step resolution. Observed CD signals were converted to mean residue ellipticity [Θ] = deg x cm<sup>2</sup> x d mol<sup>-1</sup> (Mol. Ellip.).

*SPR*

Surface plasmon resonance measurements were performed using a Biocore X100 set up with streptavidin-coated sensorchips prepared for use by conditioning with 1 min injections of 1 M NaCl, 50 mM NaOH in 50% isopropanol and finally extensively washed with a 0.22 μm filtered buffer (10 mM Tris, 50 mM KCl, 0.025% P20). Previously annealed 5'-biotinylated Tel22 was then immobilized on one cell of the chip surface by adding a 50 nM DNA solution at a 1 μl min<sup>-1</sup> flow rate until a 400 RU response was obtained. The second cell was left blank as control. Sensograms were acquired using serial dilutions of metal complexes in the same buffer. To avoid interference by DMSO, its concentration was kept constant and added to the running buffer as well (1.7%). Compounds solutions were injected at a 25 μl min<sup>-1</sup> flow rate until a constant steady-state was reached (60–200 seconds). After each run, a 30 seconds regeneration step was performed with 10 mM glycine (pH 2.5) followed by a 60 seconds stabilization period in running buffer. The experimental RU values were recorded at the steady state. Data were fitted according to a two binding sites model

$$RU = RU_{\max} \times (K_1 \times C_{\text{free}} + 2 \times K_1 \times K_2 \times C_{\text{free}}^2) / (1 + K_1 \times C_{\text{free}} + 2 \times K_1 \times K_2 \times C_{\text{free}}^2)$$

where  $K_1$  and  $K_2$  are the macroscopic thermodynamic binding constant and  $C_{\text{free}}$  is the complex concentration in the added solution



### *Electrospray Mass Spectroscopy*

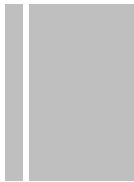
Metal complex/tel12 adducts were prepared by mixing equivalent amounts of the TEL12 (20  $\mu\text{M}$ ) in 150 mM ammonium acetate buffer (AmAc), 60% EtOH, pH 7.4. Then Au(III) complexes were added (3:1 metal/tel12 ratio). After a 10-fold dilution with water, ESI-MS spectra were recorded by direct injection at 30  $\mu\text{l}/\text{min}$  flow rate in an Orbitrap high-resolution mass spectrometer (Thermo, San Jose, CA, USA), equipped with a conventional ESI source. The working conditions were the following: spray voltage 3.1 kV, capillary voltage 45 V and capillary temperature 220° C. The sheath and the auxiliary gases were set, respectively, at 17 (arbitrary units) and 1 (arbitrary units). For acquisition, Xcalibur 2.0. software (Thermo) was used and monoisotopic and average deconvoluted masses were obtained by using the integrated Xtract tool. For spectrum acquisition a nominal resolution (at  $m/z$  400) of 100,000 was used.

## References

- [1] B. Maji, S. Bhattacharya, *Chem. Commun.*, 2014, 50, 6422-6438.
- [2] T. Shalaby, G. Fiaschetti, K. Nagasawa, K. Shin-ya, M. Baumgartner, M. Grotzer, *Molecules*, 2013, 18(10), 12500-12537.
- [3] G. Biffi, D. Tannahill, J. McCafferty, S. Balasubramanian, *Nature Chemistry*, 2013, 5, 182-186.
- [4] S. Lagah, I-L. Tan, P. Radhakrishnan, R.A. Hirst, J.H. Ward, C. O'Callaghan, S.J. Smith, M.F.G. Stevens, R.G. Grundy, R. Rahman, *PLOS ONE*, 2014, 9, e86187.
- [5] M. Ruden, N. Puri, *Canc. Treat. Rev.*, 2013, 39(5), 444-456.
- [6] S. Ghosh, O. Mendoza, L. Cubo, F. Rosu, V. Gabelica, A.J.P. White, R. Vilar, *Chem. Eur. J.*, 2014, 20(16), 4772-4779.
- [7] K. Abd, H. Nurul, O. Mendoza, A. Shivalingam, A.J. Thompson, S. Ghosh, M.K. Kuimova, R. Vilar, *RSC Advances* 2014, 4(7), 3355-3363.
- [8] H. Yaku, T. Murashima, D. Miyoshi, N. Sugimoto, *Molecules*, 2012, 17, 10586-10613.
- [9] J. Zhang, F. Zhang, H. Li, C. Liu, J. Xia, L. Ma, W. Chu, Z. Zhang, C. Chen, S. Li, S. Wang, *Curr. Med. Chem.*, 2012, 19(18), 2957-2975.
- [10] S.N. Georgiades, N.H. Abd Karim, K. Suntharalingam, R. Vilar, *Angew. Chem. Int. Ed.*, 2010, 49, 4020-4034 .
- [11] S.F. Ralph, *Curr. Top. Med. Chem*, 2011, 11, 572-590.
- [12] E.R.T. Tiekink *Crit. Rev. Onco. Hematol*, 2002, 42, 225-248.
- [13] A. Casini, G. Kelter, C. Gabbiani, M.A. Cinellu, G. Minghetti, D. Fregona H.H Fiebi, L. Messori, *J. Biol. Inorg. Chem.*, 2009, 14, 1139-1149.
- [14] L. Messori, P. Orioli, C. Tempi, G. Marcon, *Biochem. Biophys. Res. Comm*, 2001, 281, 352-360.
- [15] M. A. Cinellu, G. Minghetti, M. V. Pinna, S. Stoccoro, A. Zucca, M. Manassero and M. Sansoni, *J. Chem. Soc., Dalton Trans.*, 1998, 1735.
- [16] A. Casini, M. A. Cinellu, G. Minghetti, C. Gabbiani, M. Coronello, E. Mini and L. Messori, *J. Med. Chem.*, 2006, 49, 5524-5531.
- [17] G. Marcon, S. Carotti, M. Coronello, L. Messori, E. Mini, P. Orioli, T. Mazzei, M. A. Cinellu and G. Minghetti, *J. Med. Chem.*, 2002, 45, 1672-1677.
- [18] M.A. Cinellu, G. Minghetti, M.V. Pinna, S. Stoccoro, A.Zucca, M. Manassero, *Chem.Comm*, 1998, 2397-2398.
- [19] C. Gabbiani, A. Casini, G. Kelter, F. Cocco, M.A. Cinellu, H-H. Fiebig, L.Messori, *Metallomics*, 2011, 3, 1318-1323.
- [20] A. Casini, G Kelter, C. Gabbiani, M A Cinellu, G. Minghetti, D. Fregona, H-H Fiebig, L. Messori, *J Biol Inorg Chem*, 2009, 14, 1139-1149.

- [21] C. Gabbiani, L. Massai, F. Scaletti, E. Michelucci, L. Maiore, M.A. Cinellu, L. Messori, *J. Biol. Inorg. Chem.*, 2012, 17, 1293-1302.
- [22] A. Randazzo, G.P. Spada, M. Webba da Silva, *Top. Curr. Chem.*, 2013, 330, 67-86.
- [23] M. Vorlickova, I. Kejnovska, J. Sagi, D. Renciuk, K. Bednarova, J. Motlova, J. Kypr, *Methods*, 2012, 57(1), 64-75.
- [24] J. Kypr, I. Kejnovska, D. Renciuk, M. Vorlickova, *Nucl. Acids Res.*, 2009, 37(6), 1713-1725.
- [25] R. Ferreira, A. Marchand, V. Gabelica, *Methods*, 2012, 57, 56-63.





## **Chapter 6**

### **The future: Heterometallic Compounds?**

## 1. Heterometallic compounds.

As described in the previous chapters, metals, look very attractive in the field of cancer therapy. Recently, a new approach to obtain different and better anticancer compounds has been developed; on the ground of these previous studies and considering that multinuclearity may lead to innovative chemical and biological properties, heterometallic systems have been synthesized and characterized at chemico-physical and biological level [1,2].

The hypothesis is that the incorporation of two different cytotoxic metals, in the same molecule, may improve their activity as antitumor agents because of the interaction of the different metals with multiple biological targets or by the improved chemico-physical properties of the resulting hetero-polymetallic compound.

The strategy consists in using multimetallic systems, in this way the neighboring metals can cooperate and the interaction between metals in close proximity might lead to novel modes of action.

Contel *et al.* [3] synthesized a panel of coordination iminophosphorane complexes of gold(III) and palladium(II) derived from ferrocenyl phosphanes. The most stable of these compounds exhibit important cytotoxic effects in the low micromolar range against cancer cells, especially the resistant to cisplatin, A2780R and MCF7. This can indicate a possible synergistic antiproliferative effect of the two different metals and a different mechanisms of action than cisplatin.

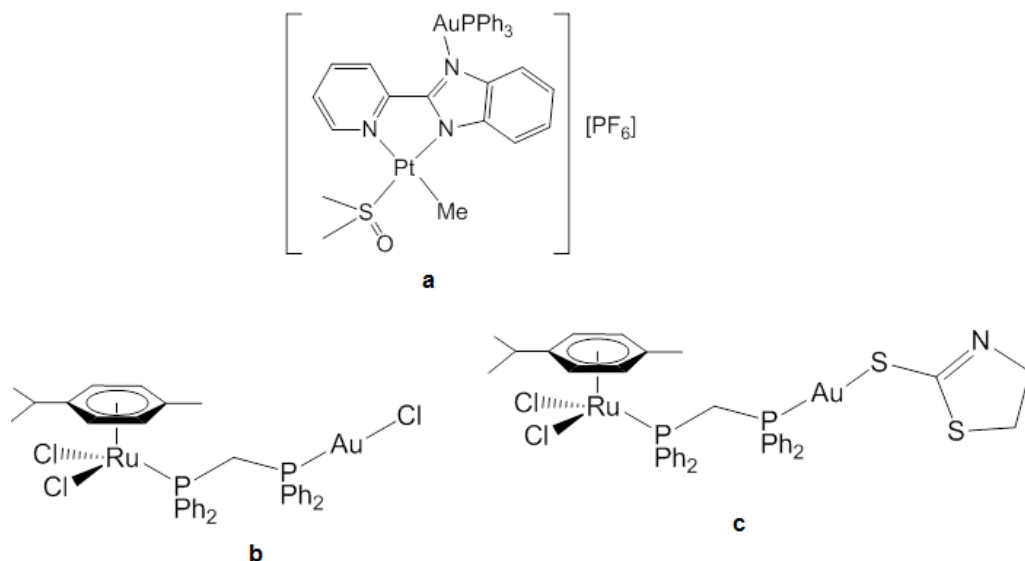
Casini *et al.*[4] synthesized hetero-bimetallic complexes of Au(I) and Pt(II) which showed marked antiproliferative properties and in some cases were able to overcome possible resistance phenomena to cisplatin against human lung cancer cell line (A549), and human ovarian cancer cells (A2780 and A2780R).

Very recently, some studies on the synthesis and biological properties of titanocene-Au(I), titanocene-Ru(II) and titanocene-Pt(II) [5–7] have been published. In general, a significant improvement of the cytotoxic properties for bimetallic complexes in comparison with a mixture of the two monometallic precursors was noticed.

Within this frame, some of polynuclear platinum, ruthenium, and gold compounds have been developed and biologically characterized (figure 1).

Compound **a** [(PPh<sub>3</sub>)Au(μ-pbi)Pt(dmsO)(CH<sub>3</sub>)](PF<sub>6</sub>), has been synthesized by M.A. Cinellu group of the Department of Chemistry and Pharmacy, University of Sassari.

Compound **b** RuCl<sub>2</sub>(p-cymene)(Ph<sub>2</sub>PCH<sub>2</sub>PPh<sub>2</sub>)AuCl] and compound **c** [RuCl<sub>2</sub>(p-cymene)(Ph<sub>2</sub>PCH<sub>2</sub>PPh<sub>2</sub>)Au(S-thiazoline)] have been synthesized in collaboration with the M. Contel group of the Department of Chemistry, Brooklyn College, CUNY, New York.



a)  $[(PPh_3)Au(\mu\text{-pbi})Pt(dmsO)(CH_3)](PF_6)_6$ ; b)  $[RuCl_2(p\text{-cymene})(Ph_2PCH_2PPh_2)AuCl]$ ; c)  $[RuCl_2(p\text{-cymene})(Ph_2PCH_2PPh_2)Au(S\text{-thiazoline})]$  (figure 1)

Compound (a) contains platinum(II) and gold(I) center, gold bound a triphenylphosphine ligand and is linked to platinum through a 2-(2-pyridyl)benzimidazole ligand. The other two compounds (b,c) contain ruthenium(II) center and gold(I) center that are linked through a bifunctional diphosphine ligand. The two compounds only differ in the nature of the gold(I) coordination environment; in one case a chloride ion is present as terminal ligand while in the other case chloride is replaced by a stronger thiol ligand.

## 2. UV-Vis studies

The solution behaviour of these heterodimetallc complexes was investigated to assess their suitability for biological studies. The electronic spectra were recorded diluting small amounts of freshly prepared concentrated solutions of the individual complexes in DMSO in the reference buffer (20 mM ammonium acetate buffer, pH 6.8). The concentration of each compound in the final sample was 10  $\mu$ M. These compounds are very soluble in organic solvents but only moderately soluble in water. Nevertheless, aqueous solutions may be straightforwardly prepared by diluting concentrated solutions of the complexes in organic solvents with a suitable aqueous buffer. From

spectra inspection it emerges that the various compounds manifest a substantial stability with no evidence of major changes even over a period of days (72h) sufficiently long for them to reach their biological target. Some minor alterations were noticed in the long-wave band of the aqueous buffer that may be ascribed to partial detachment of the weak ligands (chloride or DMSO) in the metal coordination sphere.

Electronic spectra of the model proteins (lysozyme, cytochrome c and RNase) at 10  $\mu\text{M}$  were recorded after the addition of each complex at a stoichiometric ratio of 3:1 (metal-to-protein) over 24 h at room temperature, in 20 mM ammonium acetate buffer, pH 6.8. From spectral inspection, it is apparent that protein addition does not affect importantly the behavior of the various metal chromophores. For example the spectra of the various metallodrug-cyt c systems reveal that the protein chromophore is substantially stable over 24 hours, with cyt c remaining in its oxidised ferric form.

### 3. ESI-MS studies : proteins/complexes interactions

To better elucidate the mode of interaction of heterometallic complexes with likely protein targets at the molecular level, ESI MS studies were performed. Metal complex/protein adducts were prepared by mixing equivalent amounts of the three proteins (100  $\mu\text{M}$ ) in 20 mM ammonium acetate buffer pH 6.8. Then the complexes were added (3:1 metal/protein ratio) to the solution and incubated at room temperature for 24h.

All these compounds typically behave as classical prodrugs; upon “chemical activation”, they react with proteins in two different way: partial disruption of the starting complex or in some cases, total disruption, with bare metal as reacting species. ESI MS spectra, recorded on metallodrug-protein samples at the end of the incubation period, turned out particularly informative in revealing adduct formation and in determining the final metal to protein stoichiometry and the nature of protein bound metallic fragments. The number and the nature of protein bound metallic species were determined unambiguously. A rough estimate of the amount of protein metalation was achieved by comparing the experimental peak intensities- i.e. the peak of the free protein versus those of its metal adducts.

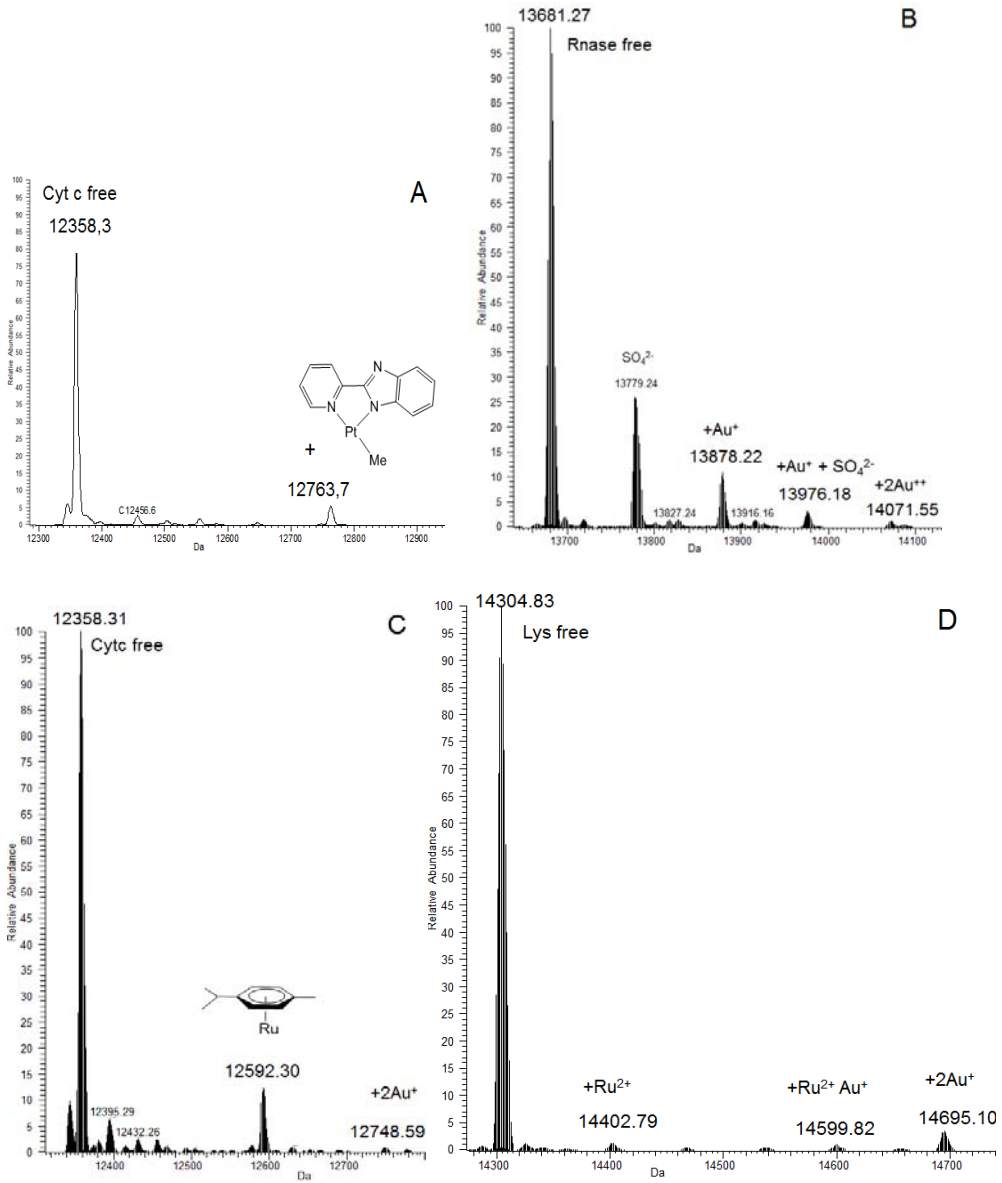
Three main types of metallodrug-protein adducts were identified in our studies:

- a) complex disruption and binding of the resulting gold(I) ions with different stoichiometry
- b) complex disruption and binding of the resulting ruthenium(II) ions
- c) binding of Ru (p-cymene) fragment or Pt ( $\mu$ -pbi) fragment to the protein.

Some differences were highlighted in the relative efficiency of the various metalation processes and in the quantities of formed adducts.



In the figure below are shown some example of our results



A) Interaction between compound **a** and cytochrome c; B) Interaction between compound **a** and RNase; C) Interaction between compound **c** and cytochrome c; D) Interaction between compound **b** and lysozyme.

## 4. Cellular studies

Afterward, the antiproliferative properties of **a** were measured in vitro against the A2780 ovarian carcinoma human cell line sensitive to cisplatin (A2780/S) and its resistant subline (A2780/R). The IC<sub>50</sub> values observed after 72 h exposure are reported in Table 1. This compound shows relevant antiproliferative effects with IC<sub>50</sub> values falling in the low micromolar range for both A2780/S and A2780/R cells

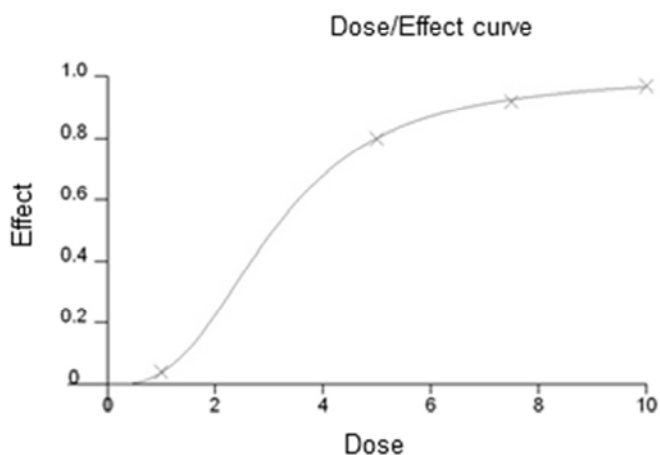
	IC <sub>50</sub> (μM) ± SD	
	A2780/S	A2780/R
Pt(pbi)(DMSO)(CH <sub>3</sub> )	1.07±0.13	1.61±0.48
[(PPh <sub>3</sub> )Au(μ-pbi)Pt(DMSO)Me][PF <sub>6</sub> ]	0.19±0.03	0.37±0.05
Auranofin	0.5±0.39	0.3±0.60
CDDP	1.81±0.68	27.54±5.02

In vitro growth inhibition of the A2780 cisplatin sensitive or resistant cell lines by **a** after a 72 h drug exposure. (table 1)

Compound **a** was more active than cisplatin even in the A2780/S cell line. Interestingly, this gold-platinum complex was more active toward cisplatin resistant cell line compared to the monomeric platinum compound, implying that the molecular mechanism of resistance to cisplatin is lower toward this heterometallic compound.

On the other hand, compounds **b** and **c** were screened against two different cancer cell line: HCT 116 (colon) and Mia Paca 1 (pancreas).

A dose-dependent inhibition of cell growth was observed in all cell lines with LD<sub>50</sub> values ranging in micromolar scale as depicted in the table 2 and 3.



Dose/Effect curve for compound **b** against Mia Paca 1 cells.

Comparing the dinuclear complex with the mononuclear Ru(II) complex, an enhancement of cytotoxicity is observed.

	LD50
$[\text{RuCl}_2(\text{p-cymene})]_2$	73.71 $\mu\text{M}$
$[\text{RuCl}_2(\text{p-cymene})(\text{Ph}_2\text{PCH}_2\text{PPh}_2)\text{AuCl}]$ ;	4.64 $\mu\text{M}$
$[\text{RuCl}_2(\text{p-cymene})(\text{Ph}_2\text{PCH}_2\text{PPh}_2)\text{Au}(\text{S-thiazoline})]$	6.49 $\mu\text{M}$

In vitro cytotoxicity effect against HCT 116 cell line (table 2)

	LD50
$[\text{RuCl}_2(\text{p-cymene})]_2$	27.80 $\mu\text{M}$
$[\text{RuCl}_2(\text{p-cymene})(\text{Ph}_2\text{PCH}_2\text{PPh}_2)\text{AuCl}]$ ;	3,06 $\mu\text{M}$
$[\text{RuCl}_2(\text{p-cymene})(\text{Ph}_2\text{PCH}_2\text{PPh}_2)\text{Au}(\text{S-thiazoline})]$	2.50 $\mu\text{M}$

In vitro cytotoxicity effect against Mia Paca 1 cell line (table 3)

## 5. Conclusion

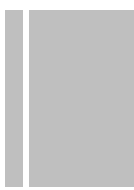
All compounds were screened for their cytotoxicity, against selected cancer cell lines, and according to these preliminary studies, they were found to be considerably more active than their parent mononuclear ruthenium compound.

The latter results together with the cytotoxicity profiles support the idea that the Au center in the bimetallic scaffold plays a fundamental role in determining the biological activity of the reported compounds, possibly due to its known high affinity for binding to amino acid residues in proteins/enzymes. These observations support the hypothesis that this family of heteronuclear potential metallodrugs operates through a pharmacological mechanism in which nucleic acids are not the only or primary target.

## References

- [1] J. Schulz, A.K. Renfrew, I. Císárová, P.J. Dyson, P. Štěpnička, *Appl. Organometal. Chem.*, 2010, 24(5), 392-397.
- [2] R. A. Khan, A. Asim, R. Kakkar, D. Gupta, V. Bagchi, F. Arjmand, S. Tabassum, *Organometal.*, 2013, 32, 2546–2551.
- [3] N. Lease, V. Vasilevski, M. Carreira, A. de Almeida, M. Sanaú, P. Hirva, A. Casini, María Contel *J. Med. Chem.*, 2013, 56 (14), 5806–5818.
- [4] M. Wenzel, E. Bigaeva, P. Richard, P. Le Gendre, M. Picquet, A. Casini, E. Bodio *J. Inorg. Biochem.* 2014, 141, 10–16.
- [5] M. Wenzel, B. Bertrand, M.J. Eymin, V. Comte, J.A. Harvey, P. Richard, M. Groessel, O. Zava, H. Amrouche, P.D. Le Gendre, M. Piquet, A. Casini, *Inorg. Chem.*, 2011, 50, 9472-9480.
- [6] F. Pelletier, V. Comte, A. Massard, M. Wenzel, S. Toulot, P. Richard, M. Piquet, P.D. Le Gendre, O. Zava, F. Edafe, A. Casini, P.J. Dyson, *J. Med. Chem.*, 2010, 53, 6923-6933.
- [7] J.F. Gonzales-Pantoja, M. Stern, A.A. Jarzecki, E. Royo, E. Robles-Escajeda, A. Varela-Ramirez, R.J. Aguilera, M. Contel, *Inorg. Chem.*, 2011, 50, 11099-11110.





**Chapter 7**  
**Conclusion**

### 1. Conclusion

This work was focused on the molecular characterization of adducts formed between cytotoxic gold compound and a few proteins, either models or targets. ESI-MS and X-ray diffraction have tounred out a powerful methods to describe the formation of protein adduct and identify the nature of bound metal fragments.

Metallodrugs behave frequently as a *prodrugs*. They must undergo an activation step before they can react with protein targets. The resulting “activated metallodrugs” usually contain a weakly coordinated ligand that is easily removed and replace by a stronger ligand provided by protein itself. Only a few protein residues perform this function with the “soft” metal ion, mainly histidine, methionines, cysteines through nitrogen or sulphur donors. This ligand substitution reaction leads to the formation of protein-metallodrug adduct.

However these studies have been conductes on simple two compenent systems containing a single metallodrugs and a single protein, real cellular systems are, of course, more complicated as they contain thousands of different proteins at highly variable concentration. In addition, these various components are highly organized and compartmentalized wiyjin the various intracellular structures thus offering a peculiar spatial distribution inside cells. It is obvious that studying the interaction of metallodrugs with protein at cellular level, represent today an important task for researchers to understand the mode of action of metallodrugs, endowed with potent cytotoxic properties, both at the molecular and cellular level.

Within this frame, a fruitful collaboration with the Departments of Pharmacology and of Biochemistry has been started to study the panel of our gold compounds.

Particular attention has been paid to define the solubility profile and the behaviour in solution of the study compounds prior to biological testing; their spectral features, under physiologically relevant conditions, were monitored for 72 hours mainly through spectrophotometric analysis and some differential properties highlighted. More in detail, two gold(III) complexes –namely Auoxo<sub>6</sub> and Au<sub>2</sub>phen- manifested a clear propensity to undergo reduction to gold(I) while the organogold(III) complex Aubipic turned out to be far more resistant toward reduction. No significant oxidising character was detected for Auranofin, AuNHC, and Au(NHC)<sub>2</sub>. These observations are very important when considering the reactivity of these gold complexes with proteins. Activation of the tested gold(III) compounds - beyond through reduction- may occur through ligand replacement reactions.



Specific studies addressed protein metalation by cytotoxic gold compounds. The nature of the metallic fragments that bind proteins was straightforwardly identified; at the same time, precise information was obtained through MS analysis on the stoichiometry and kinetics of protein metalation. Localization of the metallic fragments on the protein was achieved based on crystallographic determinations. A quite exhaustive understanding of the process of protein metalation in small model proteins was thus gained.

In collaboration with the Department of Pharmacology, the antiproliferative actions of the study compounds were comparatively evaluated *in vitro* toward A2780 human ovarian carcinoma cells either sensitive (A2780/S) or resistant (A2780/R) to cisplatin. In all cases potent cytotoxic effects were disclosed with  $IC_{50}$  values typically falling in the low micromolar range; notably, the various compounds were able to overcome resistance to cisplatin. The time dependence of the cytotoxic effects was analysed in a few cases: in general, the antiproliferative effects caused by gold drugs are much faster than those induced by cisplatin.

Proteomic studies (in collaboration with the dept. of Biochemistry) represent a very powerful instrument to interpret the proteins alterations induced by gold compounds in terms of specific perturbations of the metabolic and signalling pathways of the cell. In principle, this would allow to understand which components of the cell machinery are mostly damaged, to predict the likely site and mechanism of action and –hopefully–to identify the ultimate biomolecular targets. Moreover, a direct comparison of the proteomic alterations induced by the various gold compounds would permit to assess the degree of similarity in their respective mechanisms. Proteomic results lead us to believe that a mitochondrial insult is at the basis of the cytotoxic mechanism of gold compounds was strongly supported, consistent with the view that thioredoxin reductase is a probable target.



## Acknowledgements

I would like to thank Prof. Messori, my tutor, who gave me the possibility to work in this project. Thanks for supervising me, for giving me useful advices and ideas and the freedom to work in an independent way.

Thanks to the Prof. Maria Contel, who hosted me in her research group in Brooklyn College for four months. Thanks to Jacob Fernandez-Gallardo Jimenez for teaching me chemical synthesis with patience and passion and for making my stay so enjoyable, and thanks to all the other people that I met during my stay in NYC: Gosia, Lolly, Flavia...it was very nice to meet them.

Thank to Prof. Maria A. Cinellu for providing gold complexes.

Thanks to Prof. Alessandra Modesti and Dr. Tania Gamberi for the proteomic studies.

Thanks to Prof. Enrico Mini and Dr. Ida Landini for the biological assays with gold compounds and Prof. Annarosa Arcangeli and Dr. Serena Pillozzi for the biological assays with heterometallic complexes.

Thanks to Dr. Annalisa Guerri for the crystal structures, Dr. Chiara Gabbiani and Dr. Alessandro Pratesi for collaboration and all the interesting and useful work discussion.

Thanks to Federica and Tiziano for the helpful and stimulating discussion concerning our work and thanks for the fun and laugh in our office!

Thanks to all other guys, Francesco, Riccardo, Luca... which shared with me the coffee break and their informatic knowledge.

Finally I would like to thank my family, mum and dad, my sister Manila who help me everywhere and everytime! All my friends, Michela, Giorgia, and especially Monica, who gifted me a piece of my dream, my sister-in-law Alessandra and Sara.

And the last thanks goes to Riccardo, who shared and shares with me, all trouble and all joy, who goes along with me in this adventure with his usual confidence and trust overcoming difficult times. Thanks for the wonderful moments, I spend with you my best time ever!

*Lara*